MASTER IN BIOCHEMISTRY AND MOLECULAR AND CELL BIOLOGY RESEARCH FOCUS

Study of the translational regulation of mitochondrial remodeling in a model of human Bone Marrow Mesenchymal Stem Cell hepatogenic differentiation

MEURANT, Sebastien

Award date:
2019

Awarding institution:
University of Namur

Faculté des Sciences

Study of the translational regulation of mitochondrial remodeling in a model of human Bone Marrow Mesenchymal Stem Cell hepatogenic differentiation

Mémoire présenté pour l'obtention

du grade académique de master 120 en biochimie et biologie moléculaire et cellulaire

Sébastien MEURANT

Janvier 2019

Université de Namur
FACULTE DES SCIENCES
Secrétariat du Département de Biologie
Rue de Bruxelles 61 - 5000 NAMUR
Téléphone: + 32(0)81.72.44.18 - Téléfax: + 32(0)81.72.44.20
E-mail: joelle.jonet@unamur.be - http://www.unamur.be

Study of the translational regulation of mitochondrial remodeling in a model of human Bone Marrow Mesenchymal Stem Cell hepatogenic differentiation

MEURANT Sébastien

Résumé

Les cellules souches mésenchymateuses dérivées de moelle osseuse (BM-MSCs) représentent des outils intéressants pour des applications de thérapie cellulaire et, plus particulièrement, pour la médecine régénératrice, au vu de leur capacité de différentiation. La différentiation cellulaire implique un remaniement profond de l'expression des gènes et du métabolisme, incluant un remodelage mitochondrial. Plusieurs observations faites précédemment dans notre équipe supportent une possible régulation traductionnelle, potentiellement impliquée dans le remodelage mitochondrial observé durant la différentiation hépatogénique des BM-MSCs. La régulation de l'axe eukaryotic Initiation Factor 4E (eIF4E)-Binding Protein (4E-BP1)-eIF4E est un régulateur majeur de l'assemblage du complexe eIF4F, régulant l'initiation de la traduction dépendante de la coiffe. Par ailleurs, le complexe 1 mTOR, promouvant la croissance cellulaire, est reconnu pour assurer la biogenèse mitochondriale via la régulation de l'axe eIF4E-4EBP1.

Lors de ce travail, nous avons montré une régulation de l'axe eIF4E-4EBP1, associé avec l'activité de mTOR, affectant la phosphorylation de 4EBP1 ainsi que son activité de liaison aux facteurs d'initiation de la traduction, menant à la formation du complexe eIF4F dans les cellules en différentiation. Cependant, le taux de traduction dans ces cellules n'est pas augmenté lors de l'induction de la différentiation hépatogénique, comparé aux cellules non-différenciées, tandis qu'il est faiblement augmenté dans la phase tardive de maturation du protocole de différentiation. Dans l'ensemble, ces résultats nous ont menés à proposer l'hypothèse une possible régulation traductionnelle basée sur la traduction coiffe-indépendante lors de l'étape d'induction de la différentiation hépatogénique, supportant le remodelage mitochondrial et dirigeant la différentiation hépatogénique.

Mémoire de master 120 en biochimie et biologie moléculaire et cellulaire

Janvier 2019

Promoteur: Patsy Renard & Thierry Arnould

Abstract

Bone Marrow-derived mesenchymal stem cells (BM-MSCs) represent attractive tools for cell-based therapy and more particularly for regenerative medicine, due to their differentiation capacity. Cell differentiation involves a profound rewiring of gene expression and metabolism, including a mitochondrial remodeling. Several observations previously made in our group support a possible translational regulation, potentially involved in the mitochondrial remodeling observed during the hepatogenic differentiation of BM-MSCs. Regulation of the eukaryotic Initiation Factor 4E (eIF4E)-Binding Protein (4E-BP1)-eIF4E axis is a major regulator of the eIF4F complex assembly, regulating cap-dependent translation initiation. In addition, the growth-promoting mTOR complex 1 is known to ensure mitochondria biogenesis through the regulation of the eIF4E-4EBP1 axis.
In this work we show a mTOR-associated regulation of the eIF4E-4EBP1 axis affecting 4EBP1 phosphorylation and its binding activity to initiation factors leading to formation of eIF4F complex in differentiating cells. Unexpectedly, the translational rate in those cells is not increased upon hepatogenic induction, as compared with undifferentiated cells, while it is slightly increased in the late maturation step of the differentiation protocol. Altogether these results led us to hypothesize a possible cap-independent-based translational regulation during the hepatogenic induction step, supporting the mitochondrial remodeling and driving hepatogenic differentiation.

Acknowledgements

In a first time, I obviously want to thank abundantly my promoter, the Pr. Renard, for all the time spent on my master's thesis and listening to my disordered and abundant talking each time I presented my results and for the support she bore me all along, in the coolest way possible. I also thank her for the time spent listening to my screwy projects and for nonetheless remaining enthusiastic each time I came bac with another freaky idea. I wish her lot of courage at the head of the URBC.

In addition, I want to thank my tutor Marino, which, along with my promoter, gave me all the freedom I required in order to develop my way to work both in the lab and at home, helping me to see that I was made for this life of hard, but nonetheless exiting working. I also thank Marino for all the accurate and experience-based advice he gave me while remaining objective and always open-minded, pushing me to develop my critical faculties. I also thank him to have supported me all these months and have share with me interesting discussions (concerning as well the mysteries of the human being as the passionate and beautiful science).

Moreover, I want to thank all the members of the DYSO team which were always prompt to give me advice whenever I needed it. I more particularly thank Pr. Arnould which always gave me accurate and interesting advice, always pushing me to enlarge my knowledge and be the most exhaustive possible. I also thank Damien, the main secretary of Pr. Renard, for always sharing its experience, knowledge and passion for science as well as its good mood after work. I thank Lola for being so honest and curious, always willing to discuss with me about my project's idea and so on. I also want to thank Morgane which helped me to see that everything is not always as good as it seems to be and to show so much courage and tenacity, I wish her all the good. Finally, I thank Julie for her good mood and open-mind, always open to discuss about every subject.

I thank all the other PhD and Postdoc researchers for the maintenance of the scientific environment in the lab and the available help they were always prompt to give. Of course, I thank a lot all the technicians, Antoine and Maude for the maintenance of the lab organization and for remaining available to help, always with pleasure. I particularly thank Alexis, Camille and Maude to have helped me integrate in the lab and for their continuous good-mood. I thank Guy, for its good mood and for all the job and complete involvement he shows for so long, along with Martine to whom I wish a good and deserved retirement. I also thank Marc for all the data processing and humoristic help he provided. Additionally, I thank Patricia who ensured the property in our neglected desk, always with good-mood.

I also thank all my jury members, namely, Pr. Hamer, Pr. Matroule, Pr. Van der Henst and Pr. Raes, to whom I wish a good and well-deserved retirement, for all the interesting questions they raised which made me think about and pushed me to enlarge my knowledge and scientific curiosity.

Finally, I thank all the other URBC master's thesis student to have been evening companions during the numerous hard-working days and for providing good but serious

ambiance in the lab. I thank Christoph for its passion and strong willing, showing us hard-working and pushing us to surpass ourselves. I thank Loïc for its good mood and curiosity, always willing to discuss about technical and biological questions and I thank both Karim and Tom who always ensured the good ambiance in our desk, always available to discuss of serious and less serious subjects.

I also thank my family for their great support through the less-happy periods and for their understanding of my full-involvement in the master's thesis, according few times for them, even when at home. I also thank Arthur Van Damme for his support during all the night-long sessions of writing and all along the master's thesis during the literature evening, it helped me to relax a bit and to keep the pressure and the motivation.

Table of abbreviation

4EBP	eIF4E-Binding Protein
4E-T	eIF4E-Transporter
α1AT	α-1-Antitrypsin
AFP	α-Fetoprotein
ALB	Albumin
AMPK	AMP-activated protein kinase
ATF4	Activating Transcription Factor 4
ATP	Adenosine tri-phosphate
Bcl2	B cell lymphoma 2
BMP	Bone Morphogenic Protein
BM-MSC	Bone Marrow-derived MSC
CBA	Cap Binding Assay
C/EBP	CCAAT-enhancer-binding protein
CD	Cluster of Differentiation
CDK1	Cyclin-Dependent Kinase 1
CK	Cytokeratin
CPEB	Cytoplasmic Polyadenylation Element-Binding protein
CPS1	Carbamoylphosphate Synthetase 1
CRM1	Chromosomal Maintenance 1
CYP	Cytochrome P
CoA	Coenzyme A
DAP5	Death Associated Protein 5
DDIT4	DNA Damage Inducible Transcript 4
Deptor	Death domain containing mTOR interacting protein
DNA	Deoxyribonucleic Acid
DNMT	DNA Methyl Transferase
DKO	Double KO
DMEM	Dulbecco's Modified Eagle's Medium
DYRK2	Dual pecificity tyrosine phosphorylation regulated kinase 2
eEF	Eukaryotic Elongation Factor
EGF	Epithelial Growth Factor
EGR1	Early Growth Response 1
eIF	Eukaryotic Initiation Factor

EMX2	Empty Spiracles Homeobox 2
EN2	Engrailed-2
EPS	Extended Pluripotent Stem cells
eRF	Eukaryotic Releasing Factor
ERK	Extracellular signal-Regulated Kinases
ESC	Embryonic Stem Cell
ETC	Electron Transport Chain
FGF	Fibroblast Growth Factor
FOXO	Forkhead box O
GAP	GTPase-Activating Protein
GβL	G-protein-β-subunit-like protein
GCN2	General Control Nonderepressible 2
GEF	Guanosine Exchange Factor
GAPDH	Glyceraldehyde-3-phosphate Dehydrogenase
GS	Glutamine Synthetase
GTP	Guanosine Tri-Phosphate
HAT	Histone Acetyl-Transferase
HB	Hypotonic Buffer
HDAC	Histone Deacetylase
hESC	Human Embryonic Stem Cell
HGF	Hepatocyte Growth Factor
HIF1α	Hypoxia-Inducible Factor 1α
HLA	Human Leukocyte Antigen
HMT	Histone Methyl Transferase
HNF	Hepatocyte Nuclear Factor
hnRNP C	heterogeneous nuclear RNP C
HRI	Heme Regulated Inhibitor
HSP	Heat Shock Protein
IMDM	Iscove's Modified Dulbecco Medium
IRES	Internal Ribosome Entry Sites
ITAF	IRES *trans*-acting factor
ITS	Insulin-Transferrin-Selenium
JHDM	Jumonji C Domain Demethylase
KEGG	Kyoto Encyclopedia of Genes and Genomes
KO	Knock-Out
KRT	Keratin

iPSC	induced Pluripotent Stem Cell
Klf2	Krüppel-like Factor 2
LARP1	La-Related Protein 1
LDHA	Lactate Dehydrogenase A
LRG	Leucine Rich Repeat Containing G Protein-Coupled Receptor
LRPPRC	Leucine-rich PPR motif-containing protein
MAPK	Mitogen Activated Protein Kinase
Mdm2	Mouse double minute 2
MEF	Mouse Embryonic Fibroblast
Met-tRNAi	Methionine-tRNA initiator
MNK	MAPK interacting Kinase
mRNA	messenger RNA
mSin1	mammalian Stress-activated protein kinase (SAPK) interacting protein 1
mRNP	messenger RNP
mtDNA	mitochondrial DNA
mtHSP70	mitochondrial HSP70
mTOR	mammalian Target Of Rapamycin
mTORC	mTOR Complex
MSC	Mesenchymal Stem Cell
NAD	Nicotinamide Dinucleotide
NDUFS6	NADH dehydrogenase (ubiquinone) iron-sulfur protein 6F
NPC	Neural Progenitor Cell
Oct4	Octamer-binding transcription factor 4
ODC	Ornithine Decarboxylase
ORF	Open Reading Frame
OSM	Oncostatin M
OXPHOS	Oxidative Phosphorylation
PAS	Periodic Acid Schiff
PABP	Poly-A Binding Protein
PBS	Phosphate Buffer Saline
PDC	Pyruvate Dehydrogenase Complex
PDGF2	Platelet Derived Growth Factor 2
PDK	PDC Kinase
PERK	PKR-like Endoplasmic Reticulum Kinase
PGC-1α	PPARγ Coactivator 1-α

PI3K	Phosphatidyl-3-phosphate Kinase
PIC	Pre-Initiation Complex
PKR	Protein Kinase RNA-activated
PML	Promyelocytic Leukemia protein
POLGA	Polymerase Gamma A
Post-TC	Post-termination complexes
PPARγ	Peroxisome Proliferator-Activated Receptor gamma
PRAS40	Proline-Rich AKT/PKB Substrate 40kDA
PRH	Proline Rich Homeodomain protein
Protor	Protein observed with Rictor
PSC	Pluripotent Stem Cell
PTBP1	RBP Polypyrimidine Tract Binding Protein 1
PTEN	Phosphatase and tensin homolog
PTKB2	Protein Threonin Kinase 2 B
PVDF	PolyVinyliDene Fluoride
qPCR	quantitative Polymerase Chain Reaction
Raptor	Regulatory associated protein of mTOR
RBP	RNA-binding Proteins
REDD1	Regulated in development and DNA damage responses 1
Rheb	Ras homologue enriched in brain
Rictor	Rapamycin-insensitive companion of mTOR
Rmrp	RNA component of mitochondrial RNA processing
RNA	Ribonucleic Acid
RNF43	Ring Finger Protein 43
RNP	Ribonucleoprotein
ROS	Reactive Oxygen Species
Rpl	Ribosomal protein large subunit
Rpph1	Ribonuclease P RNA component H1
Rps	Ribosomal protein small subunit
RSPO	R-spondin
rRNA	ribosomal RNA
S6K	Rps 6 Kinase
SSC	Somatic Stem Cell
SOX	SRY (sex determining region Y)-box
SUMO	Small Ubiquitin-Like Modifier

SUnSET	Surface sensing of translation
TBX3	T-box Transcription factor 3
TCA	Tricarboxylic Acid Cycle
TCF	Transcription Factor
TCF7L2	TCF 7-Like-2
TDO2	Tryptophan 2,3-dioxygenase
TET	Ten-Eleven Translocation
TGFβ	Transforming Growth Factor β
TISU	Translation Initiator of Short 5'UTR
TNFα	Tumor Necrosis Factor α
TOP	Terminal OligPyrimidine
TOS	TOR signaling
tRNA	transfer RNA
TSC	Tuberous Sclerosis Complex
uORF	upstream ORF
UTR	Untranslated Region
VEGFA	Vascular endothelial growth factor A
Wif-1	Wnt inhibitory factor-1
YY	Yin-Yang
ZNF3	Zinc and Ring Finger 3

Table of content

INTRODUCTION

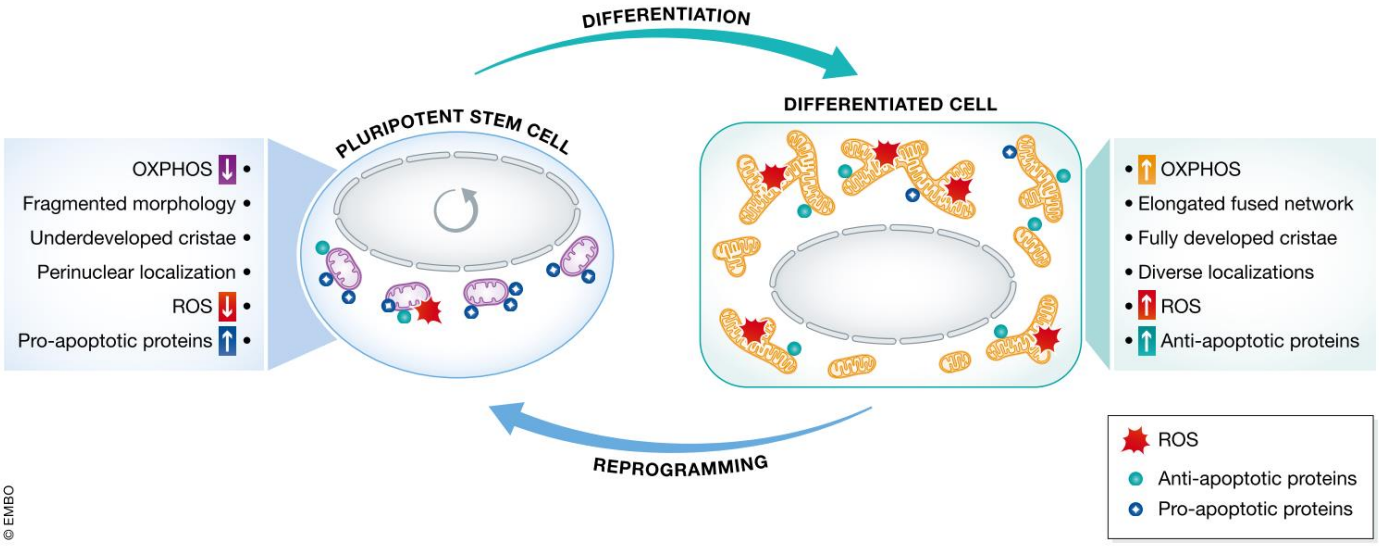

Figure 1. Mitochondrial remodeling and metabolic shift upon stem cell differentiation (Lisowski et al., 2018). Stem cells mitochondria show immature features with low OXPHOS activity, immature *cristae*, a more fragmented morphology of the mitochondrial network and perinuclear localization. Upon differentiation, mitochondria undergo remodeling with an increase in their number and OXPHOS activity with developed *cristae*, a more fused network which localization is well spread throughout the cytosol. Stem cells present low levels of ROS (but the latter are nonetheless required as signaling molecules). In case of DNA damage, stem cells are highly sensitive to mitochondria-dependent apoptosis and show increased expression of pro-apoptotic proteins of the B cell lymphoma 2 (Bcl2) family. Differentiation and oxidative-based metabolism trigger increase in endogenous ETC leaking resulting in increased ROS levels, associated with an increased susceptibility to DNA damages. Mitochondria in differentiated cells show increased expression of anti-apoptotic proteins, reducing cell-death susceptibility. During reprogramming, mitochondria return to an immature state, this process being called mitochondria rejuvenation (Lisowski et al., 2018).

I. INTRODUCTION

1. A variety of stem cells are considered for cell therapy

Differentiation is a wide-spread cellular process in the living world and is necessary for the acquisition of complexity and functional organization in pluricellular organisms. The starting point of this complex phenomenon relies on a particular set of cells called stem cells. These cells are characterized by self-renewal capacity and the ability to differentiate into one or more cell lineages, this property being called cell potency (Ullah et al., 2015; Wanet et al., 2015). Different kinds of stem cells exist with different potencies and origins: embryonic stem cells (ESCs), found in the blastocyst's inner cell mass, are pluripotent (meaning that they are capable of differentiation toward all cell lineages thus giving rise to the three primary germ layers); adult or somatic stem cells (SSCs) found in most tissues of adult organisms, are either multipotent (able to differentiate into some cell lineages derived from a sole primary germ layer) or unipotent (able to differentiate into only one cell type); and, finally, the more recently described induced pluripotent stem cells (iPSCs), correspond to somatic differentiated cells reprogrammed into a pluripotent state thanks to the overexpression of pluripotency master transcriptional regulators (Takahashi & Yamanaka, 2006; Wanet et al., 2015). This latter kind of stem cells shows great promises for cell-based therapy and also for gene therapy (reviewed in, Mikkers et al., 2012). Nonetheless, currently, the use of Yamanaka and Takahashi's OKSM cocktail of transcription factors (*Oct3/4*, *Klf2*, *SOX2* and c-*Myc*) and iPSCs for medical application is still waiting for further validation due to the tumorigenic potential and the incomplete understanding of these cells (Ghosh et al., 2011; reviewed in, Tapia & Schö Ler, 2016).

ESCs have been most deeply described in mouse but recent advances in human ESC (hESC) characterization allow for a better understanding of their biology and for the improvement of their *in vitro* culture (Sperber et al., 2015; Theunissen et al., 2014). However, these cells present ethical issues associated with their origin, show genomic instability and have tumorigenic potential compared to somatic stem cells (Ghosh et al., 2011). Recently, an enhanced type of pluripotent stem cells (PSCs: ESCs and iPSCs), called extended pluripotent stem (EPS) cells, have been developed. These cells present totipotency, meaning that they can give rise to embryonic and extraembryonic tissues while PSCs can only differentiate into embryonic tissues. In addition, EPSs show greater genomic stability than PSCs and interspecies chimerism ability which is extremely limited for PSCs (Yang et al., 2017). Actually, the other kinds of stem cells and more particularly SSCs represent, so far, a safer and more commonly accepted alternative for medical concern.

SSCs can be found in most tissues of the human body and although they present limited potency (multipotent instead of pluripotent), these stem cells remain attractive for cell-based therapy. Indeed, due to their high genomic stability and easy access with less associated ethical issues, this kind of stem cells represents a really powerful tool for regenerative medicine and cellular therapy (Iansante et al., 2018; Rodrigues et al., 2010; Ullah et al., 2015; Wanet et al., 2015). SSCs gather progenitor cells as well as Mesenchymal Stem Cells or Mesenchymal Stromal Cells (MSCs). According to the definition proposed by the International Society for Cellular Therapy, Mesenchymal Stromal Cells are heterogenous populations of cells found in many tissues and deriving from mesodermal lineage with a fibroblast-like phenotype and plastic adherence property (Dominici et al., 2006). Among this cell population, the ones presenting specific features such as the expression of specific surface markers (CD73, CD90 and CD105) and absence of other ones (CD14, CD34, CD45 and HLA-DR) with the ability to differentiate at least into osteoblasts, chondrocytes and adipocytes are called Mesenchymal Stem Cells (Horwitz et al., 2005). These stem cells have raised increasing interest for medical applications, partly due to their immunomodulatory properties, and represent models of *in vitro* differentiation (Banas et al., 2007; Iansante et al., 2018; Najar et al., 2013; Stock et al., 2014; Ullah et al., 2015). Indeed, these cells have the ability to trans-differentiate into ectodermal and

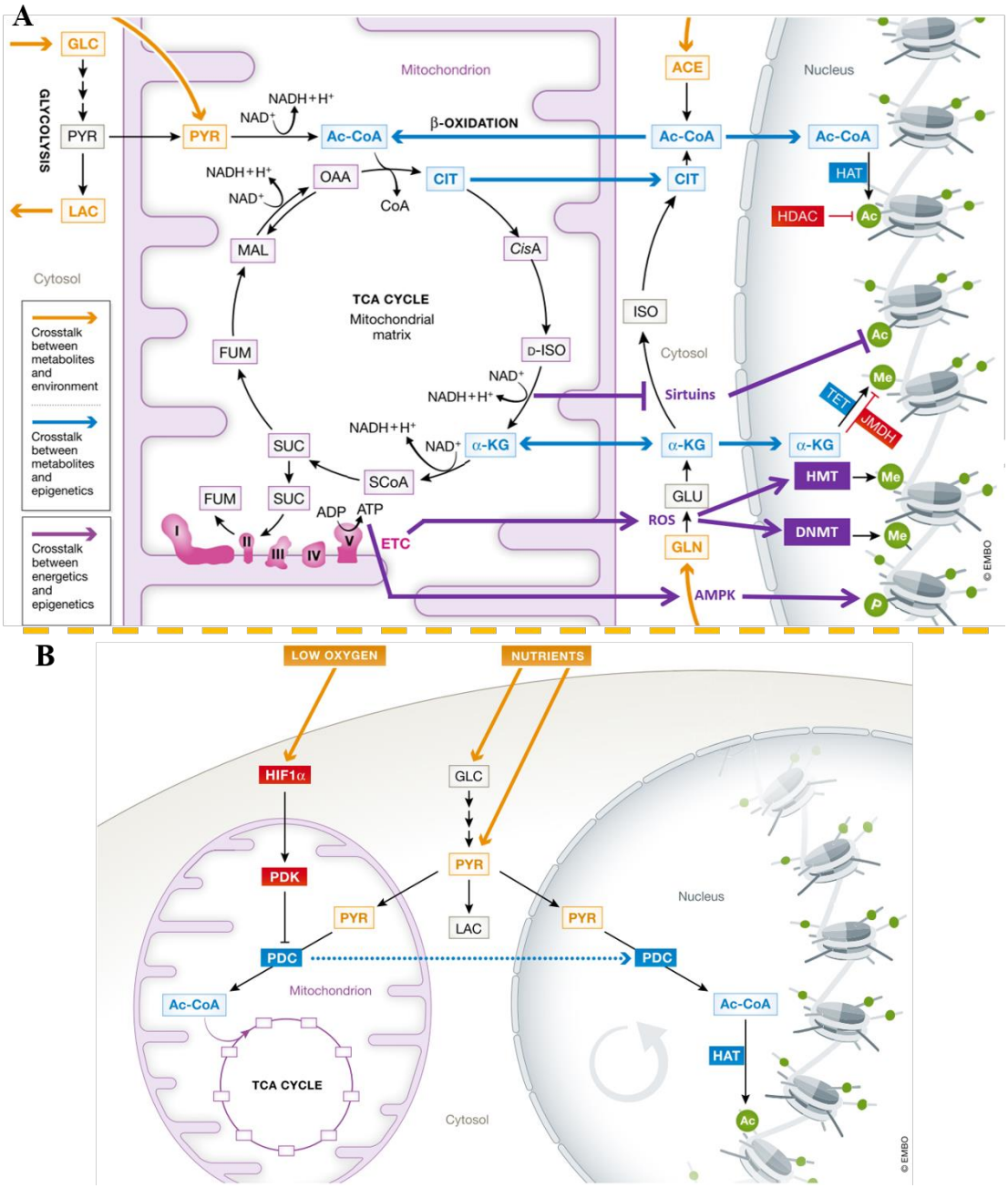

Figure 2. Mitochondria as the gatekeeper of stem cell metabolism through bioenergetic and redox regulation and ensuring metabolic regulation of the epigenetic landscape (adapted from Lisowski et al., 2018). (A) The nutrient sources influence the epigenetic landscape of stem cells and favor stemness maintenance. Among the main metabolites involved in epigenetic regulation which are mainly derived from glucose or lipids, the acetyl-CoA and citrate can translocate from mitochondria to cytoplasm and give acetyl-CoA thanks to the action of the ATP-citrate lyase enzyme. The latter metabolite is a substrate of histone acetyl-transferase (HAT) enzymes that acetylate histones, ensuring an open chromatin context which plays a role in PSC maintenance. At the opposite, histone deacetylases (HDACs) promote the removal of the acetylated marks and favor thus a more closed and repressive state of the chromatin. Another important metabolite involved in epigenetic regulation is α-ketoglutarate which can be derived from glutamate and glutamine through glutaminolysis. Glutamine is a major substrate for stem cells. α-ketoglutarate is a co-substrate for ten-eleven translocation (TET) methylase generally associated with transcription repression and Jumonji C domain demethylase (JHDMs) enzyme promoting either transcription activation or repression. Bioenergetic regulation is also involved in epigenetic regulation through AMP-activated protein kinase (AMPK) activation sensitive to the ATP/ADP ratio; AMPK is involved in the shutdown of anabolic process and stops proliferation, thus constituting a roadblock in reprogramming and impairing stemness maintenance. The reductive state of the cells also plays a role as high NADH/NAD^+ ratio, associated with higher Krebs cycle activity, leads to the inactivation of sirtuins such as Sirtuin 1, a deacetylase enzyme favoring stem cell maintenance (Lisowski et al., 2018; Rodriguez et al., 2013). Finally, ROS signaling is also involved in epigenetic regulation where those reactive species can promote histone methyl transferase (HMT) and DNA methyl transferase (DNMT) oxidation and subsequent inactivation combined with direct nucleotide oxidation. In stem cells, hypermethylation of the nuclear-encoded mitochondrial polymerase gamma A (POLGA) gene keeps the mtDNA copy number and thus mitochondrial activity at low levels. (B) An important metabolite involved in epigenetic crosstalk is pyruvate which is mainly derived from glucose utilization through glycolysis, enhanced in stem cells, and which is further converted into lactate to restore NAD^+ availability. In stem cells, pyruvate follow a metabolic shunt and is predominantly used for fermentation in the cytosol. Therefore, it is less used in mitochondria where pyruvate is normally converted into acetyl-CoA through pyruvate dehydrogenase complex (PDC) activity. However, in stem cells, strong hypoxia-induced factor 1 α signaling promotes *PDC kinase* (*PDK*) expression, whose activity inhibit PDC complex activity. Nonetheless, both pyruvate and PDC can be found in the nucleus and could therefore be preferentially targeted in there for direct histone acetylation through nuclear acetyl-CoA production (Lisowski et al., 2018).

endodermal cell lineages, making them potential candidate for regenerative medicine and for transversal studies of differentiation processes (Stock et al., 2014).

2. Pluripotency and differentiation regulation through mitochondria-related metabolic shift

A conserved feature of stem cell differentiation concerns the requirement of a metabolic shift to ensure efficient differentiation toward some cell lineages. Indeed, mouse and human ESCs priming and differentiation involve mitochondrial maturation and transition from a glycolytic-based metabolism to an oxidative one (Sperber et al., 2015; Theunissen et al., 2016). This mitochondrial remodeling involves a transition of perinuclear mitochondria with poorly developed *cristae* and low Oxidative Phosphorylation (OXPHOS) activity to an extended mitochondrial network with mature *cristae* and an oxidative phenotype (reviewed in, Rafalski et al., 2012; Wanet et al., 2015) (**Figure 1**). This phenomenon, necessary for ESCs differentiation, is also required during the differentiation of MSCs into several lineages such as the osteogenic and adipogenic lineages (reviewed in, Hsu et al., 2016) as well as for the differentiation of neural progenitors toward mature neurons (Agostini et al., 2016; Xie & Sheppard, 2018; Zheng et al., 2016). In addition, this metabolic shift and its-associated mitochondrial remodeling have also been previously described by our team in a model of hepatogenic differentiation of human BM-MSCs (hBM-MSCs). Interestingly, the reverse phenomenon is observed during the spontaneous de-differentiation of hepatocytes *in vitro* with reversal of the mitochondrial remodeling (Wanet et al., 2014). Similarly, during the reprogramming of somatic cells into iPSCs, a transition of mitochondria from a mature to an immature state is observed (**Figure 1**). This process, involving mitophagy, is called mitochondrial rejuvenation (Hawkins et al., 2016; Vazquez-Martin et al., 2016; Wanet et al., 2015; J. Zhang et al., 2012). The observed metabolic shift upon cellular differentiation is required for proper and complete differentiation process as the impairment of mitochondrial respiration prevents differentiation and favors reprograming and stemness maintenance (Wanet et al., 2015).

However, it seems puzzling that stem cells favor a poor energetic-yield glycolytic phenotype over a high ATP-yield oxidative metabolism since these cells need to maintain sufficient proliferation rate to ensure their self-renewal and tissue homeostasis. Three main raisons can be proposed to explain this unexpected metabolic behavior: first, stem cells grow *in vivo* in hypoxic niches (<5% O_2) and so a glycolytic metabolism is adapted to this cellular environment. Hypoxic conditions favor the stabilization of the Hypoxia-Inducible Factor 1α (HIF1α), a central regulator of stemness, which regulates the expression of numerous metabolic genes, ensuring the glycolytic phenotype of stem cells (Lisowski et al., 2018; Rafalski et al., 2012; Wanet et al., 2015). Secondly, limited OXPHOS activity allow for a low level of ROS produced endogenously by electron leak of the Electron Transport Chain (ETC), therefore reducing ROS-induced DNA damage. Furthermost, stem cells are highly susceptible to mitochondria-dependent apoptosis mediated in response to DNA damage. Indeed, they have high levels of pro-apoptotic proteins, as these cells must ensure tissue integrity and cannot afford genetic alterations accumulation (Lisowski et al., 2018). Finally, the increase in glycolysis and decrease of oxidative metabolism allow for the redirecting of metabolic flux toward anabolic pathways such as the pentose phosphate pathway, resulting in increased nucleotide biosynthesis (Lisowski et al., 2018; Wanet et al., 2015).

Moreover, mitochondria also ensure metabolic regulation of stem cell maintenance and differentiation through additional mechanisms: bioenergetic regulation (ATP and redox state regulation of the cell), regulation of ROS production and associated signaling and metabolic-epigenetic crosstalk thanks to the production of some metabolites such as pyruvate or acetyl-CoA (**Figure 2**) (reviewed in, Lisowski et al., 2018; Wanet et al., 2015).

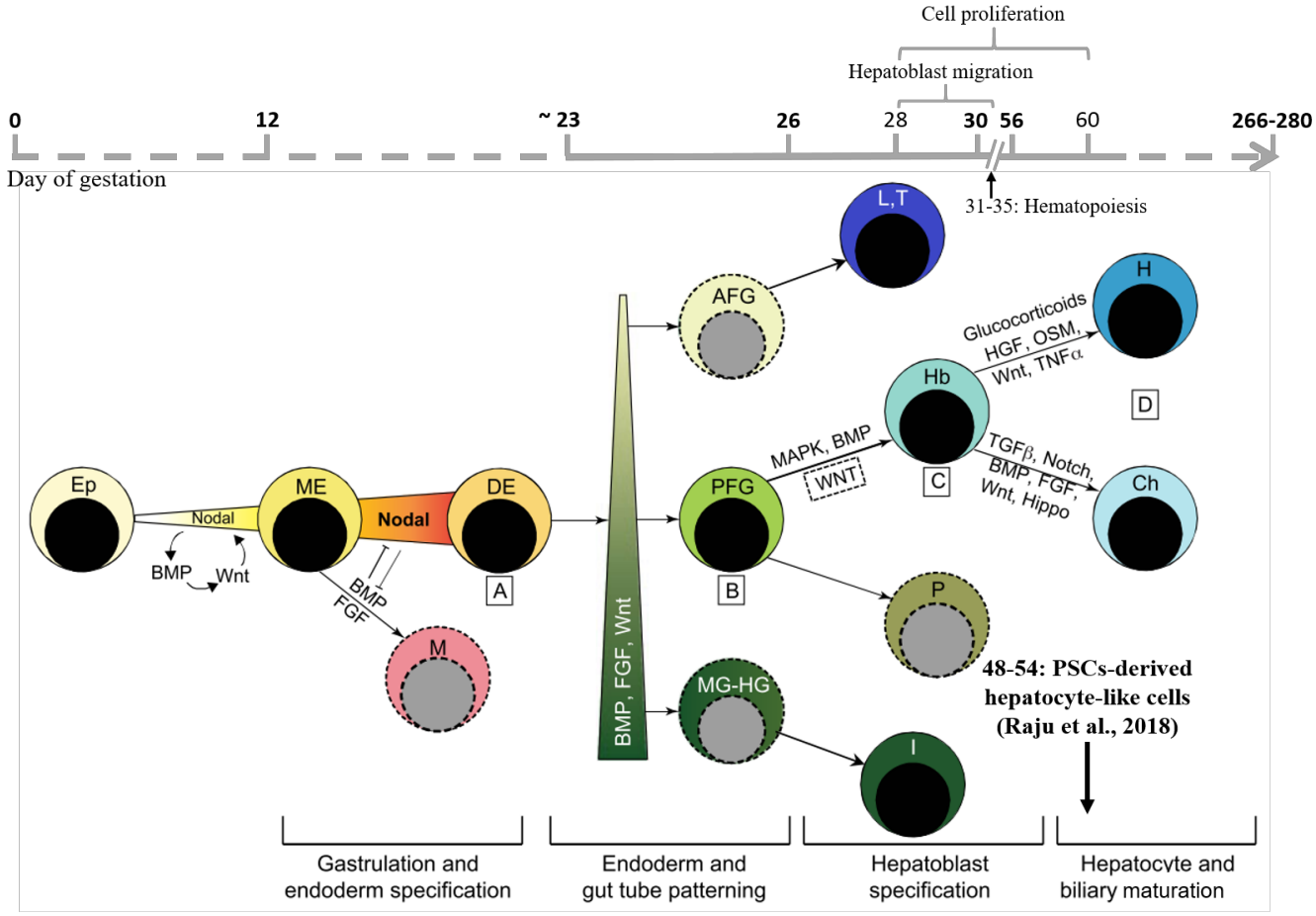

Figure 3. Signaling pathways involved in human *in vivo* liver development (adapted from Gordillo et al., 2015). (A) Nodal signaling generated from epiblast (Ep) cells is necessary and sufficient for mesendoderm (ME) specification. BMP and Wnt signaling are involved in the reinforcement of Nodal signaling in the posterior epiblast and this auto-regulatory loop leads to the formation of the primitive streak (corresponding to gastrulation at day 12) and of the mesendoderm. High levels of Nodal give rise to definitive endoderm (DE) and is antagonized by BMP and FGF signaling, promoting mesoderm (M) formation. (B) Gut tube patterning (day 23-26) is dependent on graded BMP, FGF and Wnt signaling on the anterior-posterior axis where high levels of these morphogens, in the posterior region, induce mid- and hindgut precursor (MG-HG) formation from which derive intestinal progenitors (I). The absence of BMP, FGF and Wnt signaling at the anterior extremity leads to anterior foregut precursors (AFG) formation, responsible for the formation of lungs (L) and thyroid (T) progenitors, whereas low levels of these morphogens in the anterior side of the embryo promote the formation of posterior foregut precursors (PFG). (C) The latter will give rise to both pancreatic (P) progenitors and hepatoblasts, depending on FGF and BMP signaling. (D) Hepatoblast will then give rise to hepatocytes or cholangiocytes, where the balance is determined by the presence of specific morphogens in the microenvironment (glucocorticoids, HGF, OSM, Wnt and TNFα for hepatocyte differentiation and TGFβ, Notch, BMP, FGF, Wnt and Hippo signaling for biliary differentiation). The maturation of hepatocytes and cholangiocytes then occurs from day 56-58 to the end of the gestation (Gordillo et al., 2015). A comparative transcriptomic analysis performed on human PSCs-derived hepatocyte-like cells and rodent fetal hepatocytes revealed a lack of metabolic maturity in hepatocyte-like cells which would correspond to the beginning of the hepatic maturation step (day 48-54 of human gestation) (Ravali Raju et al., 2018).

Altogether, these elements underlie the major importance of mitochondria in stem cells acting as a metabolic hub regulating both stemness maintenance and differentiation (Lisowski et al., 2018; Wanet et al., 2015). The tight interplay and inter-dependency between mitochondria dynamic and cell differentiation, underlined by the mitochondrial remodeling-dependent support of the glycolytic- to oxidative-based metabolic shift required for several differentiation processes, such as in the hepatogenic differentiation of BM-MSCs, highlights an essential role of mitochondria in stem cells homeostasis (Lisowski et al., 2018; Wanet et al., 2014, 2015).

3. Liver development and hepatogenic differentiation

The study of liver development has allowed characterization of several molecular mechanisms driving this process, allowing the development and progressive enhancement of *in vitro* hepatogenic differentiation protocol. Due to its major metabolic role in the regulation of glucose and urea metabolism and detoxification function, the liver represents one of the most complex organs. Its development is therefore extremely well controlled and is based on the combination of several signaling pathways (**Figure 3**) (Banas et al., 2007; Gordillo et al., 2015).

In the early human embryo, Nodal signaling (a member of the transforming growth factor β (TGFβ) family) generated from epiblast cells is involved in mesendoderm specification. The Nodal signaling is necessary and sufficient for this specification but bone morphogenic protein (BMP) and Wnt signaling pathways are also involved in mesendoderm formation. Indeed, both morphogens, in the posterior epiblast, ensure the reinforcement of Nodal signaling and this auto-regulatory loop leads to gastrulation with the formation of the primitive streak and of the mesendoderm. However, later on BMP and fibroblast growth factor (FGF) signaling antagonize Nodal signaling for the segregation of endoderm and mesoderm: in one hand, the expression of the key-endodermic transcription factor SOX32 is stimulated thanks to high levels of Nodal in order to give rise to definitive endoderm; in the other hand, BMP and FGF activation repress the transcriptional activity of SOX32, resulting in mesoderm formation. Endoderm is further divided and patterned in three different parts: foregut, midgut and hindgut. This patterning is dependent on graded BMP, FGF and Wnt signaling on the anterior-posterior axis where high levels of these morphogens, in the posterior region, induce mid- and hindgut formation from which derive intestinal progenitors. The absence of BMP, FGF and Wnt signaling at the anterior extremity leads to the formation of anterior foregut precursors, responsible for the formation of lungs and thyroid progenitors, whereas low levels of these morphogens in the anterior part of the embryo promote the formation of posterior foregut precursors. The latter will give rise to both pancreatic and hepatic lineages. The subsequent formation of the liver diverticulum is dependent on FGF and BMP signaling (Wnt signaling is necessary for liver specification in zebrafish but no demonstration for its dependency in mammals has been made so far), provided by the surrounding *septum transversum* cells. In addition, the presence of endothelial cells in the liver diverticulum is required for hepatoblast specification and promotes liver budding with the oncostatin M (OSM)-dependent proliferation of hepatoblast and their concomitant migration in the *septum transversum* parenchyma. Hematopoiesis then occurs with the migration of hematopoietic progenitors in the liver bud. The bipotential hepatoblasts are poised to differentiate into hepatocytes or cholangiocytes, depending on the morphogenic microenvironment where glucocorticoids, hepatocyte growth factor (HGF), OSM, Wnt and tumor necrosis factor α (TNFα) promote hepatocyte differentiation and maturation whereas TGFβ, Notch, BMP, FGF, Wnt and Hippo signaling favor biliary differentiation and maturation. The transcription factor T-box Transcription factor 3 (TBX3) helps controling the balance between Prospero homeobox protein 1 (Prox1)-Hepatocyte Nuclear Factor 4 α (HNF4α) hepatocyte specification and HNF6-HNF1β-SRY-Box 9 (SOX9) biliary specification. Liver development *per se* is achieved in 60 days in human but mature liver is only acquired after birth due to a really long maturation process (**Figure 3**) (Gordillo et al., 2015).

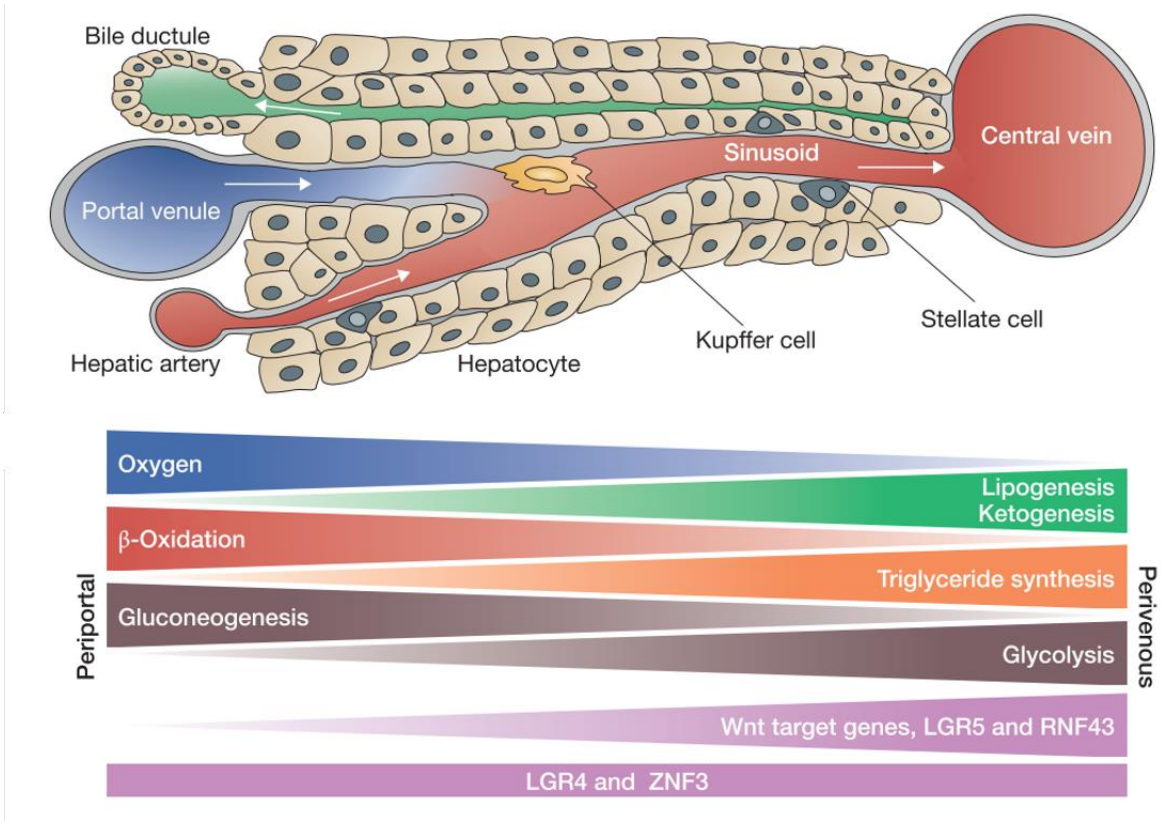

Figure 4. Metabolic zonation of the liver (adapted from Birchmeier, 2016). Nutrients coming from the intestine are transported to the liver through the portal venule and are distributed along the periportal-perivenous axis. Similarly, oxygen-enriched blood supplied from the hepatic artery follows the same distribution, and the blood from both origins leave the hepatic lobule through the central vein. Flux of bile, follows the opposite direction and leaves the lobule through the periportal system (Birchmeier, 2016). The cellular niche and environment of the hepatocytes would be essential for the acquirement of the liver zonation and the emergence of specific metabolic feature. Indeed, the identified mediators of Wnt pathway involved in the perivenous zone determination would correspond to Wnt7b and Wnt8b, secreted by hepatocytes and cholangiocytes, allowing perivenous-related metabolic activity like increase in glutamine synthesis (through the control of GS expression), citric acid cycle, lipid synthesis, and cytochrome P450 (CYP450) 1A2 metabolism capacities. At the opposite, the Wnt inhibitory factor-1 (Wif-1), secreted by cholangiocytes, would be involved in the suppression of Wnt signaling in the periportal zone, allowing for the increase in urea synthesis (through CPS1 expression), gluconeogenesis, and lipid degradation capacities (Mitani et al., 2017). In addition, the metabolic zonation is also dependent on the Frizzled co-activator receptors Leucine Rich Repeat Containing G Protein-Coupled Receptor 4 (LRG4) and 5, involved in Wnt-β-catenin activation; the presence of the extracellular ligand R-spondin (RSPO); and of the two E3 ligases: Zinc and Ring Finger 3 (ZNF3) and Ring Finger Protein 43 (RNF43). The interaction between Frizzled, LGR4/5 and RSPO is necessary to respond to Wnt signaling. At the opposite, ZNF3 and RNF43 provide the degradation of both LGR receptors and thus reduce Wnt signaling. Henceforth, the spatio-temporal control of the metabolic zonation would involve the graded expression of both activating and inhibitory signaling (Birchmeier, 2016). In addition, hepatocytes, as well as hepatocyte-like cells, show metabolic plasticity as they can rapidly adapt and change their metabolic phenotype following to exposure to perivenous or periportal cytokine environment (Mitani et al., 2017).

A last step in liver development corresponds to the acquirement of a metabolic zonation in the liver where hepatocytes located in the perivenous area show distinct metabolic features compared with hepatocytes located in the periportal area of hepatic lobules. The metabolic properties of both area depend on specific expression of metabolic enzymes as for ammonia detoxification enzymes (Birchmeier, 2016; Burke et al., 2018; Mitani et al., 2017). Indeed, *CPS1* (*Carbamoylphosphate synthetase 1*) expression, the rate-limiting enzyme involved in urea synthesis, is restricted to periportal area whereas the *GS* (*Glutamine synthetase*) expression, involved in glutamine synthesis, is found in the perivenous area. This specification seems to depend on the Wnt-β-catenin pathway as its activation, in the perivenous area, relieves of HNF4-α-dependent repression of *GS*. The patterned activation of this signaling pathway would thus be responsible for the restricted expression of *GS* and *CPS1*, as the latter is expressed in the absence of Wnt signaling, and would thus be responsible for the liver zonation occurring quickly after birth (**Figure 4**) (Burke et al., 2018).

Actually, liver diseases leading to hepatic insufficiency represent a major medical issue requiring the use of regenerative medicine, where, in some cases, the only solution is liver graft. However, the number of graft demands largely exceeds the number of available livers, making hepatic failure treatment a currently unresolved issue in our societies. Therefore, alternatives such as cellular therapy for regenerative medicine and the use of *in vitro* generated hepatocyte-like cells or stem cell-based treatments arouse growing interest (reviewed in, Iansante et al., 2018; Terryn et al., 2018).

4. *In vitro* models of hepatogenic differentiation

The study of liver development and the precise characterization of each step, using initially *in vivo* models, have allowed for the development of *in vitro* differentiation protocols modelling liver development. Further on, those cellular models allow for an even more precise study of the molecular events occurring during cell differentiation and liver development and present also therapeutic potential (Banas et al., 2007; Gordillo et al., 2015).

Several type of stem cells can be used for the generation of hepatocyte-like cells, such as PSCs or even multipotent stem cells such as MSCs. *In vitro* hepatogenic differentiation of PSCs is a common model for the study of liver development and hepatocytic differentiation. In this context, a comparative analysis of transcriptomic data from PSCs-derived hepatocyte-like cells generated with different *in vitro* protocols and from fetal rodent hepatocytes has been performed. This study showed that hepatocyte-like cells transcriptomic profiles were close to murine fetal hepatocyte at embryonic day ~E14-15 corresponding to day 48-54 of human gestation (**Figure 3**), revealing a lack of maturity of these hepatocyte-like cells. Interestingly, a genetic roadblock seems to exist during *in vitro* hepatogenic differentiation for all hepatogenic differentiation protocols, leading to early arrest in the hepatocytic maturation (Ravali Raju et al., 2018).

MSCs-based protocols are also used for hepatogenic differentiation where Bone Marrow-derived MSCs (BM-MSCs) are considered as the gold standard for MSCs differentiation capacities (reviewed in, Ullah et al., 2015). These cells can indeed be trans-differentiated (not differentiated because those cells are of mesodermal origin and thus do not naturally differentiate into endodermal lineages such as hepatocytes) in hepatocyte-like cells, which represent both a model for the study of processes occurring in the early stage of liver development and a potential therapeutic tool (Lysy et al., 2008; Wanet et al., 2014). Different protocols of *in vitro* hepatogenic differentiation exist and involve exposure to different cytokine cocktails, mimicking *in vivo* liver development. Differentiation efficiency is commonly assessed by the analysis of hepatocytic-specific markers expression (*Albumin* (*ALB*), *α-fetoprotein* (*AFP)*, *HNF3β*, *cytokeratin 18* (*CK18*), *HNF1α*, *TBX3*, *HNF4α* …) and by functional assays recording hepatocytic-specific functions (urea and albumin production, glycogen accumulation and Cytochrome P450 (CYP450) proteins activity and inducibility) (Ayatollahi et al.,

2011; Banas et al., 2007; Najar et al., 2013; Sambathkumar et al., 2018; Saulnier et al., 2009; Snykers et al., 2006; Ullah et al., 2015).

Commonly used differentiation protocols involve sequential exposure of BM-MSCs, grown on collagen-coated surfaces, to different cytokine cocktails reflecting *in vivo* liver development (Banas et al., 2007; Najar et al., 2013; Snykers et al., 2006). Generally, hepatogenic differentiation using BM-MSCs involves two-step protocol with a first step of differentiation commitment toward hepatoblast, involving different factors such as epithelial growth factor (EGF), FGF, HGF) and nicotinamide, and a second step of hepatic maturation involving OSM, dexamethasone and insulin-transferrin-selenium (ITS) (Snykers et al., 2006; Ullah et al., 2015; Wanet et al., 2014). However, other differentiation protocols involving the overexpression of liver-specific transcription factors and master regulators such as HNF4α, known to regulate liver development and inducing the expression of other hepatocytic master regulators like CCAAT-enhancer-binding protein α (C/EBPα) or HNF3β, can lead to the acquirement of hepatic functions (enhanced metabolic activity, albumin and urea production,…) (Hang et al., 2014). In addition, HNF4α represses the Wnt-β catenin signaling, involved in embryo development and osteogenic differentiation, its downregulation being necessary for the acquirement of metabolically competent hepatocytes and for liver zonation *in vivo* (**Figure 4**) (Birchmeier, 2016; Burke et al., 2018; Hang et al., 2014; Mitani et al., 2017). Other differentiation protocols using other cell types such as adult liver-derived progenitor cells with sequential overexpression of HNF4α and C/EBPα and HNF3β also exist and give functional hepatocyte-like cells showing enhanced features for medical application (Iacob et al., 2011). The differentiation protocol used in this work has been previously characterized in (Wanet et al., 2014). It involves sequential exposure to three different cytokine cocktails comprising all the above-mentioned cytokines. The differentiation efficiency has been assessed with the expression of the hepatic markers *α-1-antitrypsin* (*α1AT)* and *Tryptophan 2,3-dioxygenase* (*TDO2*), the developmental marker *TBX3* and the stemness marker *SOX9* and functionally assessed using Periodic Acid Schiff (PAS) staining (Wanet et al., 2014). In this model, a mitochondrial remodeling has been described, supporting a metabolic shift during the hepatogenic differentiation process, highlighting the importance of mitochondria in MSCs differentiation (Wanet et al., 2014).

5. Deciphering the molecular mechanisms underlying hepatogenic differentiation

A transcriptomic analysis performed in the early stage of this *in vitro* hepatogenic differentiation program allowed the identification of the tanscription factor 7-like-2 (TCF7L2)-peroxisome proliferator-activated receptor gamma (PPARγ) coactivator 1-α (PGC-1α) axis as connecting hepatogenic differentiation and mitochondrial remodeling (Wanet et al., 2017). Indeed, PGC-1α is a well-known co-activator of numerous transcription factors like PPARγ or the Nuclear Respiratory Factors (NRF 1 and 2) involved in the transcription of several nuclear-encoded mitochondrial genes, leading to mitochondrial biogenesis and increased OXPHOS activity (Fernandez-Marcos & Auwerx, 2011; Hsu et al., 2016). In addition, TCF7L2 (also called TCF4) is regulated by the Wnt-β catenin pathway which is, according to the transcriptomic analysis, shown to be downregulated during the differentiation, underlining the physiological significance and relevance of this differentiation model (Wanet et al., 2017). Interestingly, this analysis also showed modifications in the abundance of several translation-related transcripts, suggesting that translational regulation could be an additional layer of regulation in the hepatogenic differentiation. Indeed, a KEGG pathway analysis of the transcriptomic dataset showed enrichment in ribosome-related genes with upregulation of several mitochondria ribosomal genes (Wanet et al., 2017). Some pathways such as the mammalian Target of Rapamycin (mTOR) and the eukaryotic Initiation Factor 2 (eIF2) signaling pathways, both involved in translation regulation, were also shown to be upregulated during differentiation (Wanet et al., 2017). Moreover, the mRNA encoding eukaryotic Initiation Factor 4 E (eIF4E)-binding protein

	Day3: Diff/Undiff		Day3: Diff/expansion		Day5: Diff/Undiff		Day5: Diff/expansion	
	fold change	p-value	fold change	p-value	fold change	p-value	fold change	p-value
eIF4EBP1	0,53	8,38E-22	0,42	1,44E-61	0,41	5,01E-54	0,29	6,23E-127
EIF4E	1,64	1,72E-09	1,54	2,45E-10	1,1	1,86E-01	0,96	5,56E-01
EIF4G1	1	9,49E-01	1,11	3,33E-04	0,92	9,37E-03	0,74	3,61E-24
EIF4G2	1,13	3,29E-07	1,16	8,66E-14	0,91	8,26E-06	0,89	1,30E-09
HIF1A	0,87	3,95E-05	0,5	4,80E-175	0,73	2,04E-35	0,48	7,88E-230
PPARG	3,93	5,88E-14	3,22	1,26E-15	2,76	4,76E-16	3,46	6,69E-22
KRT7	0,07	5,21E-45	0,06	2,03E-82	0,04	8,75E-67	0,03	9,63E-110
ATF4	0,34	5,09E-95	0,37	3,36E-109	0,4	1,98E-136	0,49	3,08E-80

Table 1. Differentially expressed genes encoding translation-related proteins at the early stage of the hepatogenic differentiation process of hBM-MSCs. Data extracted from the transcriptomic analysis performed by Wanet et al., 2017. Cells in expansion, differentiated (diff) and undifferentiated (undiff) cells for 3 and 5 days of differentiation, derived from 5 different donors were collected and pooled and total RNA was extracted. MACE transcriptomic analysis was then performed on the different samples and data were analyzed for diff condition at days 3 and 5, either normalized to undiff or expansion condition. Data for differential gene expression are expressed in fold changes with their associated p-value, all the statistical analyses were obtained using the statistical programming language R (www.rproject.org/) with the DEGexp function of the DEGseq package (Wanet et al., 2017). Data for some genes of interest linked to translation initiation, major transcriptional regulators and differentiation marker are reported here.

1 (4EBP1), a major regulator of translation initiation (detailed hereafter), undergoes a robust downregulation in the early stages of the hepatogenic differentiation (**Table 1**). Likewise, a mitochondrial chaperone, mitochondrial heat shock protein 70 (mtHSP70), is slightly downregulated at the mRNA level but is upregulated at the protein level during the hBM-MSC hepatogenic differentiation, supporting a possible translational regulation (Wanet et al., 2017). Altogether these results support the hypothesis of a possible involvement of a translational regulation potentially involved in the mitochondrial remodeling observed during the hepatogenic differentiation.

Although transcriptional and post-transcriptional regulations have been mostly studied, translational regulation appears to be as much important and ubiquitous. Indeed, translational regulation allows faster adaptation of protein levels than transcriptional regulation and is therefore of great importance for the homeostasis maintenance in case of cellular stresses or processes requiring rapid protein level modification (Buszczak et al., 2014; Grech & von Lindern, 2012; Holcik & Sonenberg, 2005; Sonenberg & Hinnebusch, 2009). But what are the main molecular mechanisms underlying translational regulation? Translational regulation can be either global, with the inhibition or activation of initiating actors such as the eukaryotic Initiation Factors (eIF, discussed below), leading to global protein synthesis repression or enhancement respectively, or it can be specific to some mRNAs. In the latter case, it refers to a specific loading of ribosomes on these mRNAs and results in an enrichment of these mRNAs in polysome-associated fractions (Hinnebusch et al., 2016; Sonenberg & Hinnebusch, 2009). It is commonly accepted that the number of ribosomes loaded on a transcript is proportional to the intensity of its translation and thus to the level of corresponding proteins. According to this model, it is therefore the regulation of the initiation step of translation that constitutes the main mechanism of translational regulation. Different mechanisms underlie the translational regulation of specific transcripts, such as non-coding RNA, *trans*-acting RNA-binding Proteins (RBP) or the presence of *cis*-acting elements in the mRNA sequence itself such as Internal Ribosome Entry Sites (IRES) sequences, ensuring cap-independent translation (reviewed in, Holcik & Sonenberg, 2005; Komar & Hatzoglou, 2011; Sonenberg & Hinnebusch, 2009; Xue & Barna, 2012), or upstream Open Reading Frame (uORF) (Hinnebusch et al., 2016; Jackson et al., 2010; King & Gerber, 2016; Xue & Barna, 2012). Different molecular complexes and actors are involved in this ribosome selectivity for specific mRNAs that concerns mainly cap-dependent translation actors and more precisely translation initiation-related ones (Sonenberg & Hinnebusch, 2009).

Interestingly, several examples of translational regulation have been described in differentiation contexts such as hBM-MSC (Spangenberg et al., 2013) and murine 3T3-L1 cell line (Fromm-Dornieden et al., 2012) adipogenic differentiation and in the hepatogenic differentiation of HepaRG cells, an hepatic progenitor cell line (Parent et al., 2007; Parent & Beretta, 2008). In addition, neural differentiation in a model of mouse Neural Progenitor Cells (NPCs) and in the Neuro-2a murine cell line can be achieved by chemically-induced translational upregulation of specific neural transcription factors (Liao et al., 2018). Altogether, this supports the possibility of a translational regulation involved in our model of hepatogenic differentiation.

6. Coordination between the nucleus and mitochondria involves translational regulation

Mitochondrial genome encodes 13 proteins of the respiratory chain, 22 tRNAs and 2 rRNAs whereas nucleus-encoded mitochondrial genes account for more than 1000 proteins (reviewed in, Taanman, 1999). Coordination between the two genomes is therefore necessary for mitochondrial homeostasis and especially for proper OXPHOS function, as respiratory complexes are of dual origin, except for complex II (Formosa & Ryan, 2018). Therefore, genome expression synchronization must be tightly regulated and is of even greater importance in contexts of mitochondrial biogenesis and remodeling as observed in yeast upon nutrient source transition (Couvillion et al., 2016; Formosa & Ryan, 2018). In this context, the transition from a fermentable carbon source, such as glucose, to a

non-fermentable source, like glycerol, requires mitochondrial biogenesis and remodeling to support an oxidative shift. In this case, it has been demonstrated that the coordinated assembly of respiratory complexes requiring synchronization between the mitochondrial and nuclear genome expression is achieved through translation and not transcription. Indeed, upon the nutritive stress induction, the transcript levels of mitochondria- and nuclear-encoded proteins of the same respiratory chain complex do not show synchronization whereas the translational rate of these transcripts are synchronized. An unidirectional communication from cytosolic to mitochondria ribosomes seems to ensure this synchronization. For instance, nuclear-encoded mitochondrial translational activators such as Cbp6 and Cbs2 are upregulated at the translational level and thus ensure translational regulation and enhancement of mitochondria-encoded respiratory chain proteins (Couvillion et al., 2016).

In addition, modifications in ribosome composition and stoichiometry of ribosomal proteins is also involved in the regulation of translation upon nutrient source transition, both in yeast and in ESC. Indeed, following nutrient source transition, ESC ribosome composition in polysomal and monosomomal fractions is modified: the ribosomal proteins Rps14 and 29 are enriched in polysomes and Rpl11 is enriched in monosomes, suggesting a mechanism of translational regulation associated with the metabolic shift and mitochondrial remodeling. Modification of ribosomal proteins stoichiometry can also lead to ribosome imbalance and the freeing of ribosomal proteins which can ensure other functions. Indeed, extra-ribosomal functions have been described as in a case of ribosomal biogenesis defect where the sequestration of mouse double minute 2 (Mdm 2), the E3-ubiquitin ligase involved in the tumor suppressor p53 degradation, by free ribosomal proteins as (Rpl5 and Rpl11), results in p53 stabilization and increased activity. This phenomenon is also observed in case of proteotoxic stress where ribosomes stalling following an unfolded protein response contributes to p53 stabilization by free ribosomal proteins. Therefore, translational regulation, through ribosomal protein stoichiometry regulation at least, occurring in stem cell favors tissue homeostasis and prevents oncogenic transformation (reviewed in, Buszczak et al., 2014).

Paralog selectivity would also be involved in translational regulation and contribute to the coordination between mitochondria and the nucleus following external stimuli (Segev & Gerst, 2018; Xue & Barna, 2012). Indeed, in yeast, upon nutrient source transition, the ribosomal protein Rpl1b is mainly expressed over its paralog Rpl1a leading to the specific translation of mitochondrial transcripts involved in major mitochondrial pathways. The subset selectivity would depend on the presence of specific 3'UTR in the concerned mRNAs (Segev & Gerst, 2018). Moreover, ribosomal genes paralogues show tissue-specific expression in mammals and, in yeast, ~70% of all ribosomal paralogues protein are asymmetrically expressed (Xue & Barna, 2012).

Post-translational modifications of ribosomal proteins also lead to the specific regulation of mRNA translation as for Rpl13 phosphorylation, which triggers its dissociation from the 60S subunit leading to translational repression of the *Ceruloplasmin* transcript (Grech & von Lindern, 2012; Kapasi et al., 2007; Sonenberg & Hinnebusch, 2009). In yeast, the polyubiquitination of Rpl28 leads to an increase in ribosome activity, highlighting the role of post-translational modifications of ribosomal proteins in the control of translation, also found in human where at least 11 proteins of the large subunit and almost all of the small ribosomal subunit undergo post-translational modifications (Xue & Barna, 2012).

Additionally, some ribosomal proteins have been shown to be essential for ESC differentiation, potentially through translational regulation. Indeed, a genetic hemizygous loss of exit-site (site of tRNA dissociation from the ribosome occurring cyclically during translation elongation) located ribosomal proteins Rps5, Rps14 and Rps28 lead to impairment of ESC differentiation in embryoid bodies. Interestingly, Rps5 specifically interacts and favors the loading of ribosomes on two mitochondria-processing machinery-related ncRNA: RNA component of mitochondrial RNA processing (*Rmrp*) and ribonuclease P RNA component H1 (*Rpph1*), supporting a positive translational regulatory role of some ribosomal proteins for mitochondrial transcripts during the differentiation of mouse ESCs (Fortier et al., 2015). Therefore, translational regulation occurring in

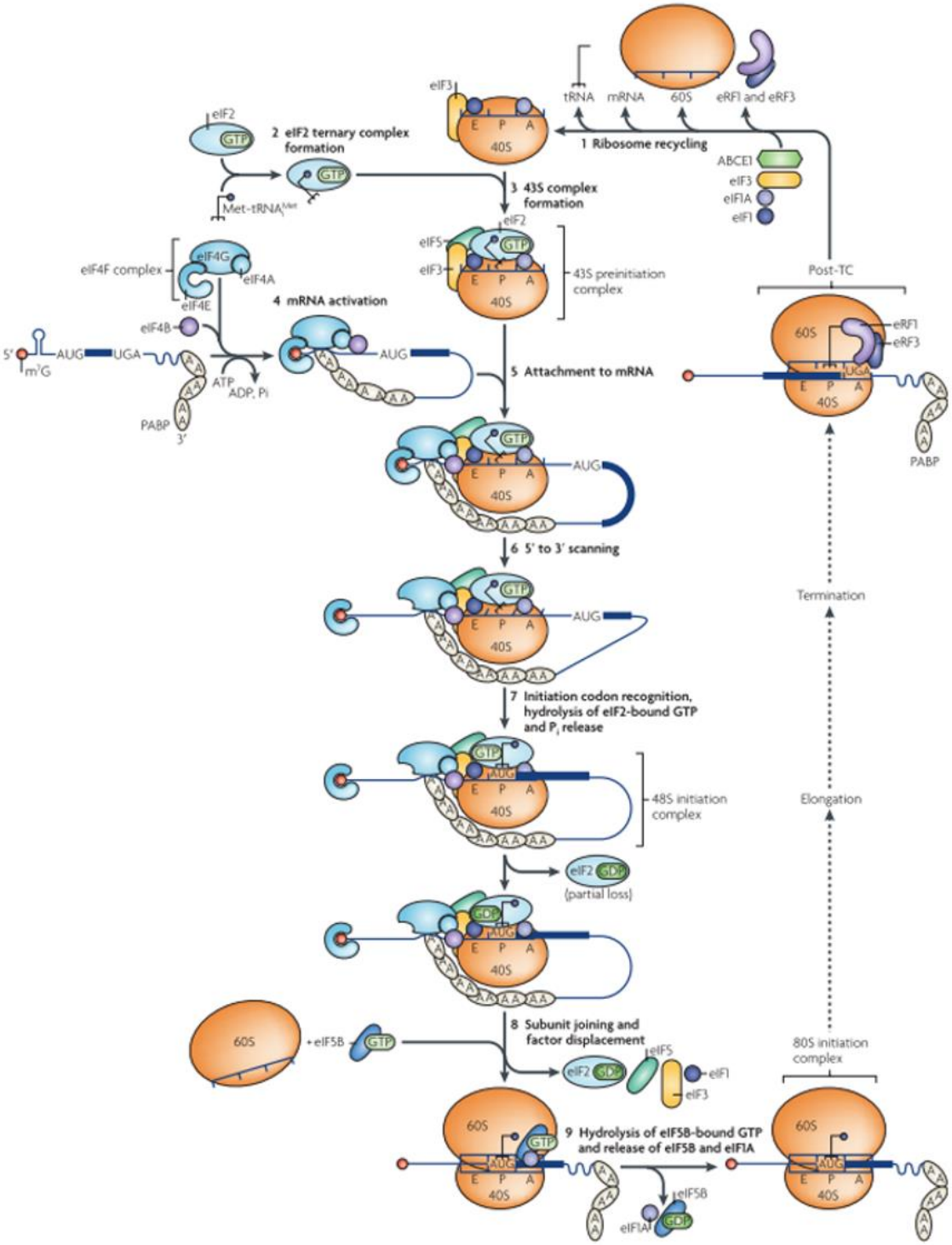

Figure 5. Mechanism of cap-dependent translation initiation (Jackson et al., 2010). After recycling from Post-termination complexes (Post-TC), 40S ribosome associates with the eIF3 complex and with the eIF2 ternary complex, allowing 43S PIC formation. After mRNA activation and unwinding, the eIF4F complex associates with the 43S Pre-Initiation Complex (PIC) leading to mRNA binding and to 48S PIC formation. Following start codon recognition after 5' to 3' scanning, eIF5-dependent GTP hydrolysis leads to ribosomal subunits joining and initiation factors displacement. The terminal hydrolysis of GTP by eIF5B allows eIF1A release from the functional 80S ribosomal which then goess to the elongation and termination step. At the end of the process, ribosomal subunits, releasing factors and PABP are recycled and available for another round of translation (Jackson et al., 2010).

stem cell allows for the control of their differentiation and adds another layer of tight control ensuring organism development and tissue homeostasis.

Protein synthesis has been further shown to be mainly regulated during different differentiation processes while protein degradation seems constant, in agreement with energy sparing (Kristensen et al., 2013). Indeed, in ESC, protein synthesis rate is maintained low despite their actively dividing state and a global increase in protein synthesis is required for their differentiation (Buszczak et al., 2014; Sampath et al., 2008). However, in those cells, protein degradation is required for the maintenance of pluripotency while reduced proteasomal activity support the differentiation process. Thus, translational regulation during differentiation is obviously a process of major importance and, indeed, all the transcriptional and epigenetic rewiring observed during differentiation are ultimately and functionally regulated at the translational level (Buszczak et al., 2014).

7. Canonical translation initiation and the eIF4E-4EBP1 axis

Protein synthesis can thus be initiated through cap-dependent or independent translation of mRNA, the latter process involving IRES, which are specific sequences found in many mRNAs. IRES-dependent translation of mRNAs has been first described in case of viral infection where global protein synthesis, and so cap-dependent translation, is repressed, allowing for the translation of specific mRNAs. The IRES sequences are complex secondary structures contained in mRNAs which interact directly with the ribosomal 40S subunit without initiation factors and so avoid the scanning required for cap-dependent translation (Holcik & Sonenberg, 2005; Komar & Hatzoglou, 2011; Sonenberg & Hinnebusch, 2009). This type of translation is less competitive for polysome recruitment than classical cap-dependent translation and represents a first layer of translational regulation because of the preferential translation of specific mRNAs. This kind of translational regulation has been described in differentiation processes. Indeed, in megakaryocyte differentiation, the preferential translation of *Platelet Derived Growth Factor 2* (*PDGF2*) transcript is involved in the differentiation process, and is dependent on the IRES *trans*-acting factor (ITAF) heterogeneous nuclear ribonucleoprotein C (hnRNP C) which recognizes the IRES sequence and enhances ribosome binding on this transcript (Grech & von Lindern, 2012).

Nonetheless, cap-dependent translation is the main and canonical mechanism of translation and takes place in four steps -initiation, elongation, termination and ribosome recycling- involving eukaryotic initiation factors (eIF), elongation factors (eEF) and releasing factors (eRF) (**Figure 5**) (Dever & Green, 2012; Jackson et al., 2010).

a) Canonical translation initiation

Translation initiation occurs in several steps and involves many actors. In a first step, 40S ribosomal subunits recycled from Post-termination complexes (Post-TC) (80S complexes following the termination step) are bound by eIF1, eIF1A and eIF3 leading to the subsequent recruitment of the eIF2-GTP-Met-tRNAi ternary complex and of eIF5 (the GTPase-Activating Protein (GAP) of eIF2), resulting in the 43S Pre-Initiation Complex (PIC) formation. Simultaneously, eIF4E binds the scaffold protein eIF4G and forms, together with eIF4A (the GTP-dependent mRNA helicase), the eIF4F complex. The eIF4F complex will then connect the mRNA with 43S PIC thanks to simultaneous binding of eIF4G to eIF3 and recognition of mRNA m7GTP cap by eIF4E. eIF4G also recruits eIF4B (an RBP, enhancer of eIF4A activity) and Poly-A Binding Protein (PABP) (a protein that binds mRNAs 3'UTR poly A sequence). Altogether, these events lead to the 48S PIC formation (constituted of 43S PIC, eIF4F complex and an mRNA in closed loop conformation) which is ready for mRNA 3' to 5' scanning. The scanning involves the unwinding of mRNA secondary structures

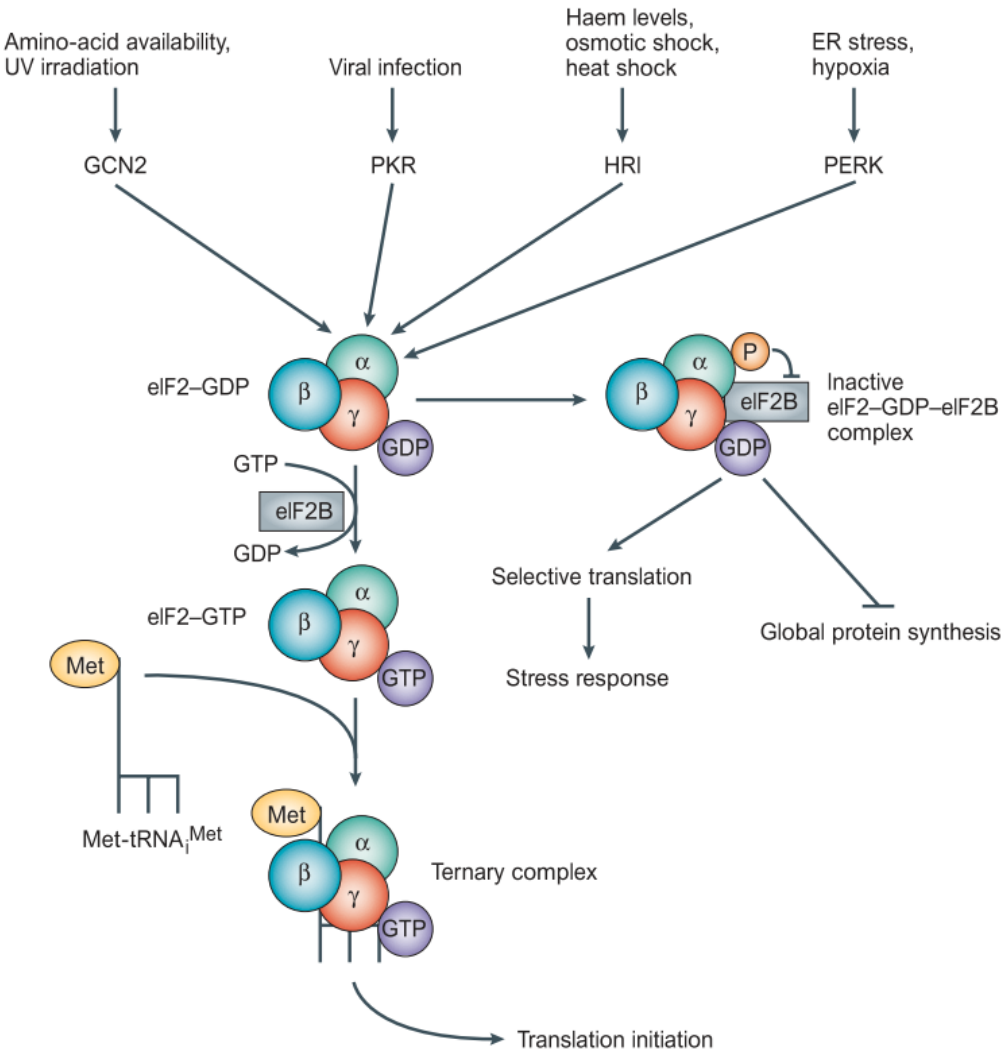

Figure 6. eIF2α-dependent regulation of translation initiation (Holcik & Sonenberg, 2005). The stress-induced phosphorylation of the α subunit of eIF2, by four different kinases activated upon either UV or nutrient stress (GCN2), viral infection (PKR), heme deficiency (HRI) or proteotoxic stress (PERK) allows global protein synthesis inhibition and targeted stress response for cell adaptation (Holcik & Sonenberg, 2005).

by eIF4A and conformational modification of 40S ribosomal subunit to a scanning-competent open conformation triggered by eIF1 and eIF1A coordinated activity. For stable codon-anticodon base-pairing, the displacement of eIF1 to the P-site is required whereas the binding of eIF1A is reinforced, allowing for a closed conformation of 40S ribosomal subunit. Upon recognition of the initiator codon, eIF5 induces the hydrolysis of eIF2-bound GTP, leading to a decreased affinity for the 40S subunit and thus to its partial release from the 48S PIC. In the final step, eIF5B binding to both 40S and 60S ribosomal subunits induces the displacement of all the initiation factors, except eIF1A, from the 40S subunit and allows 60S subunit recruitment, resulting in the 80S ribosomal complex formation. The hydrolysis of eIF5B-bound GTP leads to its dissociation and eIF1A dissociation from the newly formed 80S ribosomal complex, now functionally operational for translation elongation and then termination. Translation is a cycling process where all factors are recycled at the end of their corresponding step excepted PABP, which remains associated with the poly(A) tail of mRNA all along the translation process. PABP interacts with eRF3 during termination and would facilitate the recycling of 40S subunits from Post-TC (**Figure 5**) (Jackson et al., 2010).

The initiation step, described as the most regulated one (Caron et al., 2004; Holcik & Sonenberg, 2005; Richter & Sonenberg, 2005), is mainly regulated at the level of eIF2 and of the eIF4F complex formation (Holcik & Sonenberg, 2005; Mader et al., 1995; Qin et al., 2016; Sonenberg & Hinnebusch, 2009).

eIF2 is a small G protein needed for the recruitment of the initiator-tRNA (Met-tRNA$_i$) and for its association with the 40S subunit. In case of different cellular stresses such as viral infection, heat shock, osmotic shock, unfolded protein, or heme deficiency, the α-subunit of eIF2 is phosphorylated, thereby decreasing its interaction with eIF2B, the Guanosine Exchange Factor (GEF) of eIF2, which is necessary for eIF2 activity (**Figure 6**). eIF2α phosphorylation thus resulting in global protein synthesis repression. The kinases targeting the α-subunit phosphorylation of eIF2 correspond to at least four different kinases: Protein Kinase RNA-activated (PKR), PKR-like Endoplasmic Reticulum Kinase (PERK), Heme Regulated Inhibitor (HRI) and General Control Nonderepressible 2 (GCN2)) (reviewed in, Holcik & Sonenberg, 2005). The subsequent shutdown of cap-dependent translation allows cell adaptation through, for example, cap-independent translation of specific transcripts such as IRES-containing one in case of viral infection.

Another mechanism of cap-dependent translation initiation regulation involves the regulation of the eIF4F complex formation, responsible for the assembly of the mRNA with the 43S PIC leading to 48S PIC formation (**Figure 5**). The assembly of the complex is ensured by the cap-binding protein eIF4E which binds m7GTP of all capped mRNA and recruits the scaffold protein eIF4G (Jackson et al., 2010; Sonenberg & Hinnebusch, 2009). Structurally, eIF4E is a glove-shaped protein composed of 8 anti-parallel β-strands and 3 α-helixes. The cavity formed by the 8 β-strands corresponds to the cap binding site, while the 3 α-helixes located on the dorsal surface of the protein act as a binding domain for regulatory proteins and for eIF4G binding. eIF4E binds the conserved YXXXXLΦ eIF4E binding motif (where X is any residue and Φ any hydrophobic residue) on eIF4G and this binding has a positive allosteric effect to increase eIF4E affinity for the cap (Mader et al., 1995; Siddiqui et al., 2012). This involves a conformational modification of the eIF4E-cap complex which propagates from the dorsal binding site to the cap-binding site (Siddiqui et al., 2012). eIF4G will then recruit the other components of the eIF4F complex: the helicase eIF4A, responsible for the unwinding of mRNA secondary structures, and its activator eIF4B and PABP, allowing the circularization of the mRNA associated with translation (Jackson et al., 2010). Additionally, several actors of this complex are specifically regulated by post-translational modifications, isoform-specific expression and/or by regulatory interacting proteins (Richter & Sonenberg, 2005; C. Schmidt et al., 2016).

b) Regulation of eIF4F complex by post-translational modifications

A first example involves eIF4G phosphorylation, associated with the translation of specific mRNAs during the cell cycle where the translation is globally reduced to 75-80%, underlining translational regulation of common cellular processes (Dobrikov et al., 2014). eIF4E is also phosphorylated on two different residues: Ser53 and Ser209 (Hinnebusch et al., 2016; Jackson et al., 2010; Koromilas et al., 1992; C. Schmidt et al., 2016). The first phosphorylation is associated with an interesting feature of eIF4E which concerns its stronger affinity for specific mRNAs such as *ornithine decarboxylase* (*ODC*) or *Myc* mRNAs, leading to their specific translation (Culjkovic et al., 2006, 2007; Osborne & Borden, 2015). This eIF4E-translational specificity for some mRNAs seems dependent of the structure and complexity of 5'UTR. Indeed, mRNAs bearing abundant secondary structures are more sensitive to eIF4E translational activity and this feature would require the Ser53 phosphorylation of eIF4E as a S53A mutant shows decreased translation of these specific mRNAs (Hinnebusch et al., 2016; Koromilas et al., 1992).

Although controversial, eIF4E Ser209 phosphorylation is generally associated with increased translation (Jackson et al., 2010; C. Schmidt et al., 2016). This phosphorylation is achieved by mitogen activated protein kinase (MAPK) interacting kinase 1 (MNK1) and MNK2, two kinases associated with the eIF4F complex through their binding with eIF4G (Jackson et al., 2010). Nonetheless, Ser209 phosphorylation seems necessary for the sumoylation of eIF4E by the small ubiquitin-like modifier (SUMO)-conjugating enzyme UBC9, which results in eIF4E translational activity enhancement. Indeed, SUMO-1 conjugation to eIF4E would result in an increase in eIF4G association and decrease binding of its inhibitory protein eIF4E-binding protein 1 (4EBP1), whose function is detailed hereafter. Altogether this would ensure the pro-oncogenic and anti-apoptotic function of eIF4E due to increased translation of growth-promoting and anti-apoptotic transcripts harboring a complex 5'UTR (Xu et al., 2010).

c) Regulation of eIF4F complex by isoform specificity

Another layer of eIF4F complex regulation corresponds to the presence of different isoforms of eIF4E. Indeed, several isoforms of eIF4E exist with tissue-specific expression, eIF4E1 being the main isoform reported to be ubiquitous (Kubacka et al., 2015). This isoform, is present in two others isoforms, presenting opposite functions: eIF4E1a and b. These isoforms provide an example of isoform-specific regulation of translation initiation. The first of these two isoforms is the translationally active form and canonical isoform, whereas eIF4E1b would act as a translational repressor thanks to its association with eIF4E-Transporter (4E-T) and the cytoplasmic polyadenylation element-binding protein (CPEB) mRNP repressor complex, known to bind the 3'UTR of specific mRNAs (Kubacka et al., 2015; Richter, 2007). The association of eIF4E1b with the CPEB complex and 4E-T would lead to the formation of a "closed-loop" structure with the concerned mRNAs leading to their translational repression (Jackson et al., 2010; Minshall et al., 2007; Sonenberg & Hinnebusch, 2009).

d) Regulation of eIF4F complex by interacting proteins and eIF4E-4EBP1 axis

Finally, the formation of eIF4F complex is mainly modulated at the level of eIF4E as different families of negative regulators recognize and bind the initiation factor, preventing its association with eIF4G and thus eIF4F complex assembly, leading to global protein synthesis repression. Four different families of negative regulators can be described: (i) the RING domain-containing family with the Promyelocytic Leukemia protein (PML), (ii) HHARI and the arenavirus Z protein, using their RING domain for eIF4E binding and inhibition, associated with a 100 fold decrease in eIF4E cap affinity (Cohen et al., 2001); (iii) the homeodomain protein family with Proline Rich

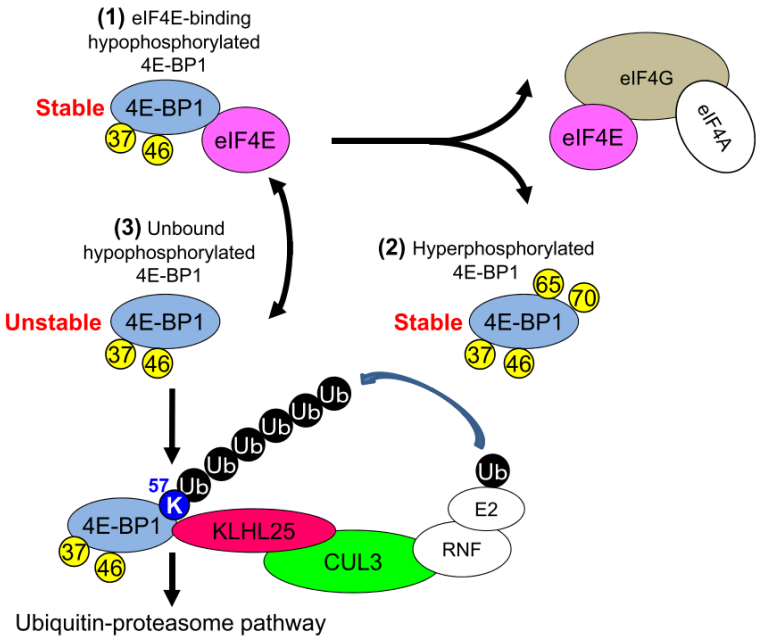

Figure 7. Phosphorylation-dependent control of 4EBP1 stability through ubiquitin-dependent proteasomal degradation (Yanagiya et al., 2012). The phosphorylation status of 4EBP1 influences its stability as the hypophosphorylated eIF4E-bound 4EBP1 and hyperphosphorylated unbound forms are more stable than the hypophosphorylated unbound 4EBP1. The KLHL25-CUL3 complex presents higher affinity for hypophosphorylated 4EBP1 and targets the unbound hypophosphorylated form of 4EBP1 to the ubiquitin-dependent proteasomal degradation. The complex would bind the protein at another site than eIF4E although the ubiquitination site identified is in the eIF4E binding site (Yanagiya et al., 2012).

Homeodomain Protein (PRH), Hox11, HoxA9, bicoid, Engrailed-2 (EN2) and Empty Spiracles Homeobox 2 (EMX2), which bind eIF4E using the same conserved site than eIF4G; and (iv) VpG proteins, that use amphipathic helix strategy to form a ternary complex with eIF4E and eIF4G (Osborne & Borden, 2015). However, among the regulatory proteins, the most important family remains the fourth one which corresponds to the eIF4E-binding proteins or 4EBPs, composed of three members in mammals: 4EBP1, the most studied and abundant isoform, 4EBP2, which shows similar properties than 4EBP1, and 4EBP3, a shortened isoform with distinct features. Those regulators share with eIF4G the conserved eIF4E binding motif and enhance eIF4E cap affinity. However, they prevent eIF4G recruitment since they bind the dorsal surface of eIF4E on the same site than eIF4G, which results in the inhibition of eIF4F complex formation and translation initiation (Mader et al., 1995; Richter & Sonenberg, 2005). Interestingly, 4EBP1 expression is shown to be downregulated in the early steps of the hepatogenic differentiation of BM-MSCs, supporting a potential role of a translational regulation during this process (**Table 1**).

An example of translational regulation involving the eIF4E-4EBP1 axis concerns the transcription factor Yin-Yang 2 (YY2), whose translation is specifically enhanced by eIF4E which shows enhanced affinity for the transcript. This transcription factor promotes the transcription of nuclear-encoded mitochondrial genes such as mitochondrial ribosomal genes and is involved in stemness regulation. Indeed, YY2 is a negative regulator of pluripotency markers such as Myc or Oct4. The enhanced affinity of eIF4E for YY2 transcript is regulated by alternative splicing: the RBP polypyrimidine tract binding protein 1 (PTBP1) protects YY2 mRNA against splicing, leading to intron retention and thus resulting in a transcript with a longer 5'UTR. Such long 5'UTR transcript is more sensitive to eIF4E specific translational activity and thus to 4EBP1 or 2 repression. Therefore, the loss of 4EBPs by double knock-out (DKO) performed in mouse ESCs, favors mesodermal differentiation with cardiac lineage specification thanks to the increased level of YY2 and subsequent downregulation of pluripotency markers (Tahmasebi et al., 2016). Thus, reduced abundance of 4EBPs favors differentiation, thanks to the increased abundance of YY2.

The eIF4E-4EBP1 complex is further regulated by phosphorylation of 4EBP1, leading to its dissociation from eIF4E due to conformational changes. Moreover, 4EBP1 phosphorylation seems to be hierarchical and involves multiple sites phosphorylation. The canonical model for 4EBP1 phosphorylation involves the successive phosphorylation of T37 and T46 required for T70 phosphorylation which would lead to 4EBP1 dissociation from eIF4E (Gingras et al., 2001). However, as 4EBPs-eIF4E complexes have been detected even after T70 phosphorylation, it suggests that other post-translational modifications are needed (Gingras et al., 2001; X. Wang et al., 2003). It seems that a fourth successive phosphorylation on S65 is necessary (Gingras et al., 2001) for eIF4E release, both with constitutive and remote phosphorylation upon S101 and S112, potentiating the p-S65 effect over 4EBP1 loss of binding activity (X. Wang et al., 2003). One of the main signaling pathway involved in 4EBP1 phosphorylation on T37/46, and which will be discussed hereafter, is the mTOR pathway and more precisely the mTOR Complex 1 (mTORC1), sensing amino acid availability (Morita et al., 2013; Schalm et al., 2003; Showkat et al., 2014). However mTORC1 is not the only kinase responsible for 4EBPs phosphorylation as other kinases could also act as negative regulators for 4EBP binding activity, such as dual specificity tyrosine phosphorylation regulated kinase 2 (DYRK2), extracellular signal-regulated kinases (ERK), AKT or other downstream actors of mitogen or insulin signaling pathways (Esnault et al., 2017; Qin et al., 2016; X. Wang et al., 2003).

Another important feature of 4EBP1 regulation is the protein stability and its ubiquitin-dependent degradation. Indeed, the unphosphorylated 4EBP1 free form is endogenously ubiquitinated and thus targeted for degradation by the proteasome, a process influenced by the phosphorylation status of 4EBP1. Indeed, the specific E3 ligase of 4EBP1 would be the KLHL25-CUL3 complex which would have a higher affinity for the hypophosphorylated 4EBP1 form (**Figure 7**) (Yanagiya et al., 2012).

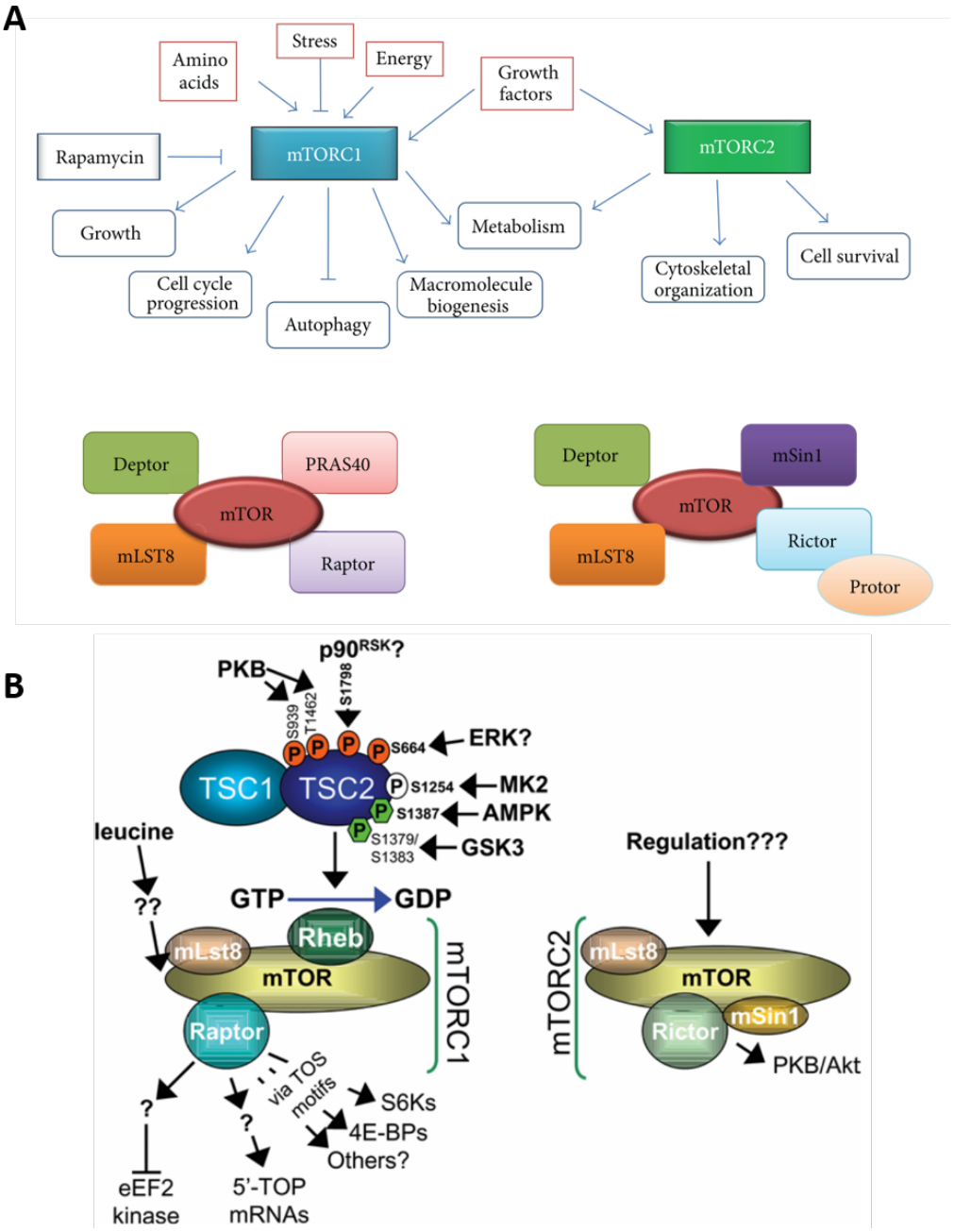

Figure 8. mTORC1 and 2 composition, cellular functions and regulation (adapted from, Proud, 2007; Showkat et al., 2014). (A) The mTORC1 and 2 complexes involve different actors and target different proteins for their phosphorylation but also differ in their sensitivity to rapamycin (an inhibitor of mTORC1 but not mTORC2) and upstream signals (reviewed in, Showkat et al., 2014; Roux & Topisirovic, 2012). The mTORC1 complex is composed of the adaptor protein Raptor (Regulatory associated protein of mTOR), mLST8 (also called G-protein-β-subunit-like protein, GβL), PRAS40 (proline-rich AKT/PKB substrate 40kDA), and Deptor (death domain containing mTOR interacting protein). mTORC1 mainly stimulates mRNA translation and other anabolic pathways in response to environmental stimuli such as hormonal or nutritive ones (Morita et al., 2013; Showkat et al., 2014). Concerning mTORC2, it is composed of the adaptor protein Rictor (Rapamycin-insensitive companion of mTOR), mSin1 (mammalian stress-activated protein kinase (SAPK) interacting protein 1), Protor (protein observed with Rictor), mLST8, Deptor, and PRAS40 and this complex is involved in the phosphorylation of AKT, itself involved in the activation of both mTOR complexes (Showkat et al., 2014). mTORC2 can also activate other kinases of the protein kinase A, G, and C families (AGC kinases) and is thus involved in the control of cell survival, cytoskeleton organization, lipogenesis, and gluconeogenesis (Morita et al., 2013; Showkat et al., 2014). (B) Activation of mTORC1 following the phosphorylation-dependent inhibition of TSC1-TSC2 complex acting as the GTPase negatively regulating Rheb, the small protein activator of mTOR found in mTORC1.Among the positive regulators of mTOR activity are found AKT, ERK, AMPK and GSK3. Interestingly a cross-talk exists between mTORC1 and mTORC2 as the latter one activates AKT, a positive regulator of mTORC1 activity. mTORC1 phosphorylates two main targets: 4EBP1 and S6K1 through the recognition of their TOR signaling motif (TOS) and thus enhances translation. In addition, mTORC1 promotes the translation of a specific pool of transcripts containing 5'Terminal OligoPyrimidine (5'TOP) motifs in their 5'UTR (Proud, 2007).

8. mTOR regulation of eIF4E-4EBP1 axis

mTOR is a conserved Ser/Thr kinase of the Phosphatidyl-3-phosphate Kinase (PI3K) family which can be found in association with different proteins therefore forming two different complexes (see detail in **Figure 8A**). The activation of mTOR is ensured by a small G protein, Ras homologue enriched in brain (Rheb) which activity is inhibited by the complex formed of Tuberous Sclerosis Complex 1 (TSC1)-TSC2 acting as its GTPase-Activating Protein (GAP). The phosphorylation of TSC2 on several residues by AKT results in the dissociation of the inhibitory complex and thus in mTOR activation (**Figure 8B**) (Inoki et al., 2002; Proud, 2007; Showkat et al., 2014). Indeed, TSC2 and TSC1 are bound to the lysosomal membrane where they interact together as well as with Rheb. Upon AKT-dependent phosphorylation, TSC2 is bound and sequestrated by 14-3-3 protein in the cytosol leading to the destabilization of the TSC1-TSC2 complex (Cai et al., 2006; Inoki et al., 2002). However, regulated in development and DNA damage responses 1 (REDD1, also known as DNA damage inducible transcript 4 or DDIT4), a negative regulator of mTOR signaling pathway compete with TSC2 to bind 14-3-3 protein. Upon release, TSC2 is free to interact with TSC1, leading to Rheb inhibition resulting in mTOR inhibition independently of AKT activation or TSC2 phosphorylation (DeYoung et al., 2008).

The canonical and main targets of mTORC1 are the 4EBP1 and 2 and the ribosomal protein S6 (RPS6) kinase 1 (S6K1) which phosphorylation induces the repression and activation of their activity respectively. Upon phosphorylation, 4EBP1 and 2 isoforms lose their affinity for eIF4E making eIF4E available for eIF4F complex formation, thereby resulting in translation initiation (Magnuson et al., 2012; Schalm et al., 2003; Showkat et al., 2014). The phosphorylation of S6K1 promotes its activity, leading to the phosphorylation of its numerous targets, the main one being RPS6. RPS6 phosphorylation is necessary for the 80S ribosomal complex assembly, therefore supporting a role for the mTORC1-S6K1 axis in cell growth (reviewed in, Magnuson et al., 2012).

In addition, mTOR and principally mTORC1 complex specifically promotes the translation of nuclear-encoded mitochondrial proteins, especially proteins of the ATP synthase (complex V). mTORC1 also promotes mitochondrial biogenesis as shown by a decrease in mtDNA abundance and respiratory capacity following Raptor depletion or mTOR inhibition. This specific regulation of mTOR translational activity is achieved through 4EBP1 phosphorylation as its depletion reduces the negative effects of mTOR inhibition on mitochondrial function following inhibitory treatment of mTOR (Morita et al., 2013). In addition, mTORC1 also regulates mitochondrial biogenesis through transcriptional mechanisms and has indeed been described to be involved in the direct transcriptional regulation of estrogen-related receptor α (ERRα) target genes involved in metabolic processes related to mitochondria, such as gene encoding proteins of the tricarboxylic acid cycle or involved in lipogenesis (Morita et al., 2015). Moreover, mTORC1 is known to control mitochondria respiratory capacity through the YY1- PGC-1α axis. The transcription factor YY1 is a known regulator of mitochondrial respiration through its inducible action on several mitochondrial genes and on *PGC1α* and acts in coordination with PGC1α itself. The association between the two transcriptional regulators requires mTORC1 activity, while rapamycin treatment disrupts their association and provokes a downregulation of the mitochondrial target genes (Cunningham et al., 2007). In a *PTEN*$^{-/-}$ (Phosphatase and tensin homolog) model of mouse embryonic fibroblast (MEF), an increase in mitochondria activity is observed, supporting the role of mTORC1 in the promotion of mitochondrial biogenesis through the eIF4E-4EBP1 axis regulation. Indeed, the consequent upregulation of the PI3K-AKT pathway leads to increased mTORC1-containing mTOR activity and thus to the phosphorylation of 4EBP1, whose expression is additionally decreased, leading to an increase in translation of transcripts encoding mitochondrial proteins (Goo et al., 2012). Altogether, mTORC1 represent a major actor in the control of mitochondria biogenesis and metabolic and respiratory activity since the complex coordinates the transcription, through the control of mitochondria-related transcription factors, and translation, through the eIF4E-4EBP1 axis, of nuclear-encoded

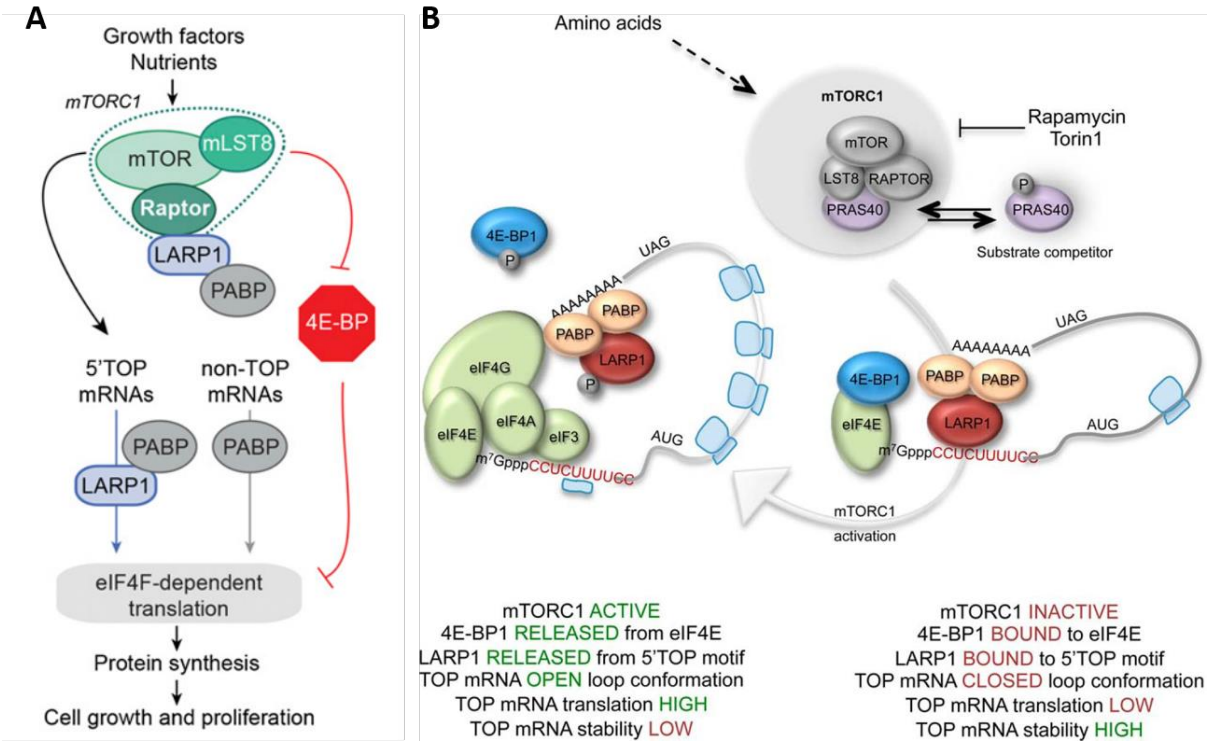

Figure 9. Two models for LARP1-dependent recognition and enhancement of TOP-containing mRNAs (adapted from, Fonseca et al., 2015; Tcherkezian et al., 2014). (A) The first model of LARP1-dependent TOP-mRNA specific translation through mTORC1 recruitment proposes that LARP1 would recognize and bind the TOP motifs in the target mRNAs and recruit mTORC1 which would spatially relieve the 4EBP1-dependent inhibition of eIF4F complex assembly through phosphorylation of the surrounding 4EBP1 (Hong et al., 2017; Tcherkezian et al., 2014). (B) Further studies suggested an inhibitory role of LARP1 on the TOP mRNA: LARP1 would bind both the 3'and 5'UTR of these mRNAs leading to an inhibitory closed-loop conformation. Upon mTORC1 phosphorylation, LARP1 would dissociate from the 5'UTR, leading to high translation of these mRNA with always the spatially-restricted effect of 4EBP1 inhibition by mTORC1 (Fonseca et al., 2015; Lahr et al., 2017).

mitochondrial genes (reviewed in, Morita et al., 2015). mTORC1 represents thus an interesting candidate linking translational regulation with mitochondrial remodeling.

Interestingly, mTORC1 has been shown to play a capital role in adipogenesis in MEFs and in the adipogenic differentiation of the murine 3T3-L1 cell line through induction of PPARγ (Magnuson et al., 2012; H. H. Zhang et al., 2009). In mouse, mTOR-dependent S6K1 activation participates to the commitment stage of adipogenic differentiation, while 4EBP1 and 2 are more specifically involved in the terminal differentiation of adipocytes. Indeed, 4EBP1 and 2 DKO mice show increased adipogenesis while S6K1 KO mouse shows impaired adipogenesis as for the triple KO mouse, suggesting that S6K1 acts earlier than 4EBPs in the adipogenesis process (Carnevalli et al., 2010).

4EBP1 and 2 are thus mainly regulated by mTORC1-dependent phosphorylation, contrary to the third 4EBP isoform which escapes all negative regulations described so far. Indeed, these mTORC1-mediated phosphorylation depend on the presence of two conserved motifs: a TOR signaling (TOS) motif and a RAIP (referring the amino acid sequence) motif, that are not found in 4EBP3 sequence (Chen et al., 2012). The TOS motif, also found in other mTORC1 targets such as S6K1 (**Figure 8B**) (Proud, 2007; Schalm & Blenis, 2002), allows for the binding of Raptor (Schalm et al., 2003; X. Wang et al., 2003) whereas the RAIP motif is also involved in Raptor binding and together with the TOS motif, allows the mTOR-dependent multiple-site phosphorylation of 4EBP1, in response to insulin (V. H. Y. Lee et al., 2008). mTORC1 is also involved in the preferential translation of 5'Terminal OligoPyrimidine (5'TOP) motif-containing mRNAs, in which the cap moiety is followed by a cytosine followed by 4-15 consecutives pyrimidines (Gandin et al., 2016; Masvidal et al., 2017). This mTORC1-specific binding to TOP-containing mRNAs leads to the specific translation of these mRNAs (mainly mRNA encoding translation-related proteins such as PABP or ribosomal proteins) upon mTORC1 activation (Gandin et al., 2016; Masvidal et al., 2017; Thoreen et al., 2012). Mechanistically, this specific recognition of these mRNAs would depend on the mRNA binding protein La-Related Protein 1 (LARP1) as identified by a proteomic analysis of cap-associated proteins (**Figure 9A**) (Tcherkezian et al., 2014). Indeed, LARP1 would act as an adaptor for mTORC1-sensitive TOP-mRNAs translation where it would recruit Raptor and thus mTORC1 to the specific mRNAs and lead to a spatially restricted phosphorylation of 4EBP1 and 2 and of S6K1, increasing the polysomal loading of these mRNAs and thus their translation (Hong et al., 2017). However, another study proposed another role of LARP1 which would act predominantly as a cap-binding protein showing an increased affinity for the TOP sequence and would compete with and displace eIF4E, disrupting the eIF4F complex. In this model, mTORC1 phosphorylation of LARP1 would therefore have an inhibitory effect on LARP1 (**Figure 9B**) (Fonseca et al., 2015; Lahr et al., 2017). In addition, mTORC1 would also promote the specific translation of mRNAs containing TOP-like motif, which consist of a minimum 5 pryrimidines located within four nucleotides of the main transcriptional start site. This more permissive definition of TOP motif thus enlarge the repertory of TOP mRNAs with additional translation-related proteins such as all ribosomal proteins but for RPS27A which presents extra-ribosomal functions (Thoreen et al., 2012).

Several non-TOP containing mRNAs have also been described to be sensitive to mTORC1 inhibition by rapamycin (Gandin et al., 2016; Masvidal et al., 2017). Among non-TOP mRNA two types of transcripts are found: either long-5'UTR transcripts, mainly pro-survival and cell-cycle associated transcripts (*cyclins*, *Bcl-2*, *Myc*, …), sensitive to eIF4E and eIF4A inhibition; or short-5'UTR transcripts, mainly mitochondrial transcripts enriched for TISU (Translation Initiator of Short 5'UTR) elements (*ATP5O*, *ATP5G1*, *UQCC2*, …), sensitive to eIF4E inhibition but not to eIF4A inhibition (Gandin et al., 2016; Masvidal et al., 2017). Indeed, eIF4A has been described to promote the translation of a subset of mRNAs (mainly pro-survival and cell cycle-associated transcripts like *Myc* or *Bcl-2*) containing particular structures in their 5'UTR, called G-quadruplexes and consisting in a minimal four repetition of CGG (Wolfe et al., 2014). The targeted mRNAs are thus sensitive to eIF4A inhibition and present long and complex 5'UTR as described above (Gandin et al., 2016; Wolfe et al., 2014).

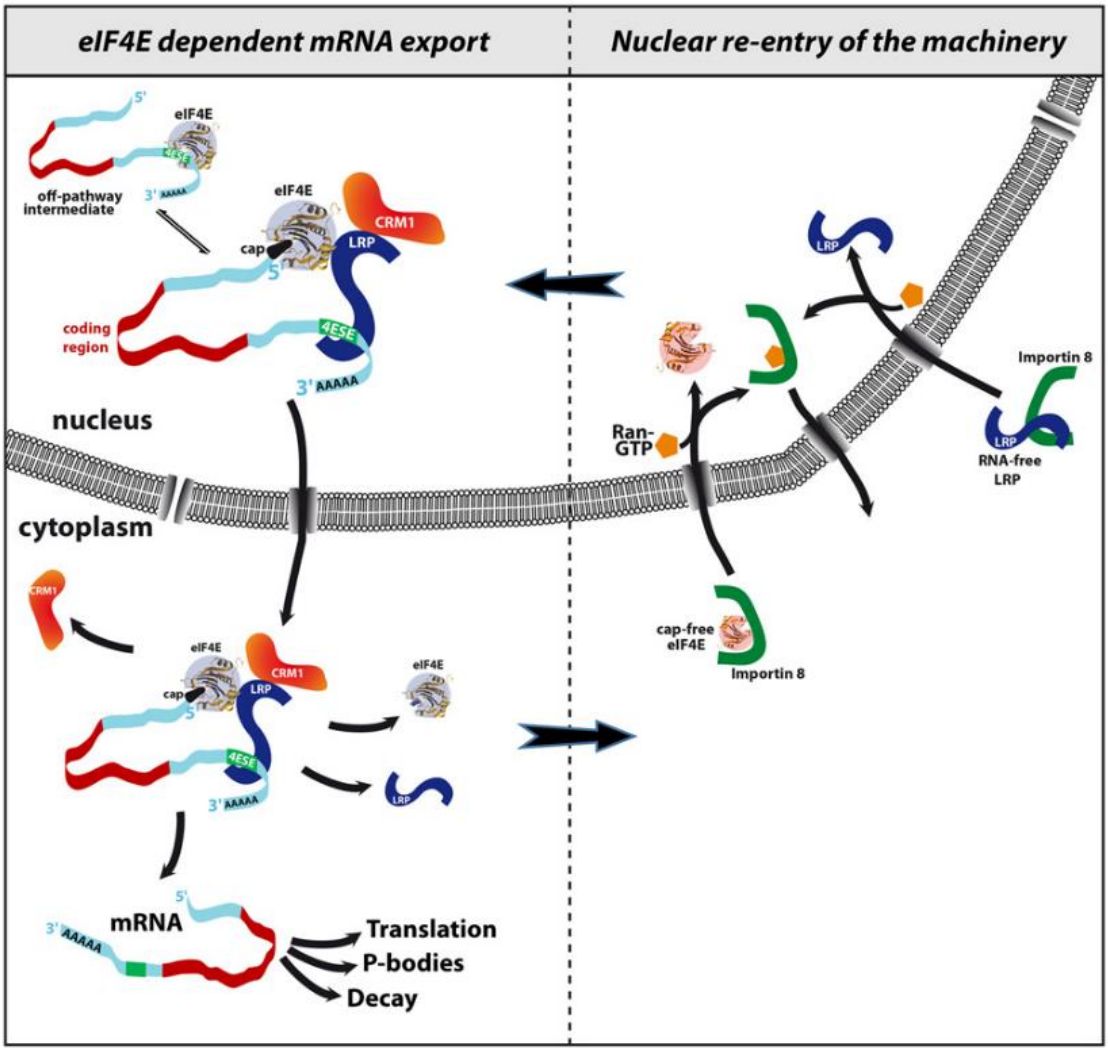

Figure 10. eIF4E export function model of growth promoting mRNAs (Volpon et al., 2017). eIF4E and its adaptor protein LRPPRC enter the nucleus with the importin 8 entry pathway and upon 4E-SE recognition, LRPPRC binds the target mRNAs and associates with eIF4E, binds to the cap of target mRNAs. Additionally, LRPPRC binds the nuclear export protein CRM1 and allows the export of the whole complex to the cytosol. In the cytosol, the specifically exported mRNAs can undergo different fates (Volpon et al., 2017).

Mechanistically, the activity of mTOR depends on its phosphorylation. The serine residues S2448 and S2481 are associated with active mTORC1 and mTORC2, respectively, and can be used as mTORC1 and 2 activity markers. The phosphorylated S2448 is part of a feed-forward loop and is targeted by S6K or AKT while the second one, less specific, would result from autophosphorylation (Copp et al., 2009; Inoki et al., 2002). Another specificity concerns Raptor phosphorylation on serine 863 and 859, necessary for mTORC1-associated mTOR activity. Indeed, both phosphorylations are insulin-dependent and are achieved by mTOR in a way similar to 4EBP1 and S6K1 phosphorylation, while the p-S863 would allow the stabilization of Rheb-mTOR activating interaction and allow the closeness of TOS-containing mTORC1 specific targets, increasing their mTOR directed phosphorylation (L. Wang et al., 2009).

9. Another branch of eIF4E-4EBP1 axis: eIF4E mRNA export function

In addition to its specific cap-dependent translation activity, eIF4E has been described to ensure a second activity: the export activity of specific mRNAs out of the nucleus. This specific activity has been first described for the specific export of the cyclin D1 mRNA in NIH3T3, U2OS and HEK293T cell lines (Culjkovic et al., 2005). This specific export is achieved thanks to the presence of a 50 nucleotides sequence in the 3'UTR of this mRNA, called the 4E-Sensitive Element (4E-SE) sequence, that additionally requires eIF4E cap binding. It is principally the secondary structure (adjacent Stem Loop Pairs) formed by this sequence which is important for eIF4E specific recognition. 4E-SE is found in several transcripts which mainly encode for proteins involved in cell growth. The biological effect of the increased export of specific mRNAs is correlated with increased protein level of the corresponding mRNAs (Culjkovic et al., 2006). Some mRNAs are also both specifically transported and translated such as the ODC which possesses both the 3' and 5' UTRs structures sensitives to the nuclear and cytoplasmic functions of eIF4E, respectively (Culjkovic et al., 2007).

Nijmegen Breakage Syndrome 1 (NBS1) mRNA is also specifically exported thanks to its 4E-SE. NBS1 is involved in AKT pathway since increase in its protein expression leads to an increased AKT activation. This mechanism leads notably to an increased phosphorylation of 4EBP1, leading to an upregulation of eIF4E translational activity (Culjkovic et al., 2008). The transcription factor Myc, a positive transcriptional regulator of eIF4E (Raught & Gingras, 1999), is also specifically exported, thereby providing a positive feedforward loop for eIF4E expression and activity, possibly involved in the oncogenic potential of eIF4E (Osborne & Borden, 2015).

Therefore, due to this export function, eIF4E presents both a cytoplasmic and nuclear localization. In the nucleus, eIF4E has been described to form nuclear bodies, as well as PML (Lallemand-Breitenbach & de Thé, 2018). In addition, to its transcriptional regulator function, PML would sequestrate eIF4E in these nuclear bodies, thus acting as a potent inhibitor of eIF4E export activity of specific mRNAs. Indeed, PML can associate with eIF4E and inhibits its mRNA export activity due to the 100-fold decreased eIF4E cap affinity, the cap binding being necessary for the mRNA export (Culjkovic et al., 2006; Osborne & Borden, 2015; Volpon et al., 2017). PML interacts with eIF4E using its RING domain, which usually binds zinc residues, and binds eIF4E nearby the common eIF4E binding motif in the dorsal part of the protein (Cohen et al., 2001).

To complete this model, the Leucine-rich PPR motif-containing protein (LRPPRC), a mitochondrial and nuclear protein, is the adaptor protein required for eIF4E export activity (**Figure 10**) (Osborne & Borden, 2015; Topisirovic et al., 2009). Indeed, LRPPRC contributes to localize eIF4E to the nucleus and competes with PML for the nuclear form of eIF4E, leading to the loss of its PML-dependent inhibition. LRPPRC binds eIF4E thanks to two consensus eIF4E binding sites and binds an overlapping region of the common binding site over eIF4E (Topisirovic et al., 2009). Moreover, LRPPRC binds the 4E-SE element on one hand and eIF4E on the other hand and additionally interacts with chromosomal maintenance 1 (CRM1) to exit the nucleus. Finally, the

recycling pathway of eIF4E and its associated protein LRPPRC allowing for their nuclear entry corresponds to the importin 8 pathway (**Figure 10**) (Volpon et al., 2017).

eIF4E would also be involved in the recognition and direct binding of particular 4E-SE element found in the coding sequence of histone H3 and H4 mRNA and not in their 3'UTR. Indeed, the amino-terminal domain of eIF4E would be involved in this binding, necessary for the particular translation initiation mechanism of these mRNAs. Mechanistically, eIF4E recognizes the internal secondary structure of the mRNA and allows the assembly of the ribosome. The folding of the mRNA ensures eIF4E binding to the cap and thus eIF4A recruitment, required for the inhibitory three-way helix-unwinding of the mRNA leading to its translation (Martin et al., 2011).

Another important feature is that 4EBPs themselves are also able to induce the nuclear localization of eIF4E in response to cellular stresses. Indeed, an increase in the nuclear form of eIF4E, bound to 4EBP1, has been observed in response to heat shock (Sukarieh et al., 2009) or starvation (Rong et al., 2008). The 4EBP3 isoform has also been described as a potent inhibitor of the specific mRNA export activity of eIF4E since at least 40% of 4EBP3 are found in the nucleus (compared with maximum 30% for 4EBP1) (Kleijn et al., 2002). This 4EBP3 function has been described for different mRNAs such as *CyclinD1*, resulting in decreased cell-growth (Chen et al., 2012; Cohen et al., 2001).

II. OBJECTIVES

The overall objective of this work was to characterize the potential translational regulation involved in the mitochondrial remodeling occurring during the hepatogenic differentiation of BM-MSCs. In a first step, we have focused on the eIF4F complex, as preliminary data indicate a downregulation of 4ENP1 abundance during BM-MSC hepatogenic differentiation (see Introduction, point I.5). We began to evaluate the protein abundance of the cap binding protein eIF4E and of its partners eIF4G and 4EBP1 during the differentiation process. In addition, the functional activity of the eIF4F complex has been assessed.

In a second step, 4EBP1 upstream regulators have been explored, and more precisely the mTOR regulatory pathway. The phosphorylation status of 4EBP1 during the differentiation process, in addition with the assessment of S6K1 phosphorylation during the hepatogenic differentiation have been assessed, giving functional information about the activity of mTORC1 pathway during the process. In addition, to further evaluate the translational level during the differentiation, global protein synthesis measurement has been done.

Finally, a potential nuclear function of the eIF4E-4EBP1 axis has been explored by the characterization of the subcellular localization of both eIF4E and 4EBP1. Altogether these results contributed to complete the characterization and understanding of the hepatogenic differentiation process.

MATERIAL AND METHOD

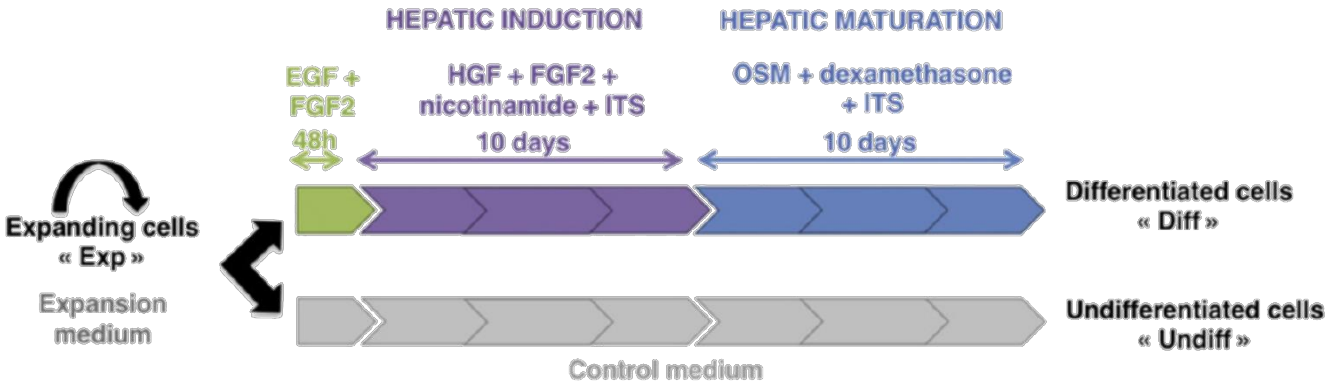

Figure 11. Differentiation protocol and workflow for hepatogenic differentiation of hBM-MSCs (Wanet et al., 2014). The differentiation process takes place in 22 days with sequential exposure of the cells to three cytokine cocktails, allowing respectively differentiation induction, hepatic induction and hepatic maturation. Upon confluency, expanding cells ("Exp") are either exposed to cytokine-containing differentiation medium ("Diff" condition) or to cytokine-less medium ("Undiff" condition).

III. MATERIALS AND METHODS

1. Cell culture and differentiation

Human bone marrow-derived mesenchymal stem cells (hBM-MSC) were obtained from healthy and consenting donor and were isolated in Jules Bordet institute (thanks to a collaboration with D^r M. Najar laboratory of Clinical Cell Therapy, Jules Bordet Institute). The donors are represented here with the "BM" notation followed by a number, the passage is indicated with the "P" notation after the donor identification. Expanding hBM-MSCs (referred to as "Exp" in the present manuscript) were cultivated at 37°C and 5% CO_2 in DMEM (Dulbecco's Modified Eagle's Medium) 1g/L glucose (Gibco, Thermo Fisher Scientific, Waltham, MA, USA) supplemented with 10% Fetal Bovine Serum (FBS) (Gibco), 100 U/mL penicillin and 100 µg/L streptomycin (Gibco). Expanding cells were seeded at ~4000 cells/cm^2 and passaged every 3-7 days depending on the donor (to avoid reaching confluency). Cells used for differentiation were from passages 3-7 and were seeded on surfaces previously coated by incubation of 0,02M filtered acetic acid containing 50 µg/mL rat tail collagen type 1 (354236, VWR International, Radnor, PA, USA) during 2h at 37°C.

The differentiation process was performed as previously described in (Najar et al., 2013) and illustrated in **Figure 11**. Briefly, cells were seeded on collagen-coated surfaces at a density of 10 000 cells/cm^2. When confluent, this corresponds to the experimental condition called "Day 0". The differentiation was then started when cells (Diff condition) were cultivated in IMDM containing (Iscove's Modified Dulbecco Medium, Gibco) 100 U/mL penicillin and 100 µg/mL streptomycin supplemented with 20 ng/mL EGF (PeproTech, Rocky Hill, NJ, USA) and 10 ng/mL fibroblast growth factor-2 (FGF-2) (PeproTech) for the first two days (differentiation initiation). For the 10 following days (hepatic induction), the medium was supplemented with 10 ng/mL FGF-2, 20 ng/mL hepatocyte growth factor (HGF) (PeproTech), 0,61 mg/mL Nicotinamide (Sigma-Aldrich, Saint-Louis, MO, USA) and 1X insulin-transferrin-selenium (ITS) (Thermo Fisher Scientific). The medium was renewed at days 5 and 9. For the last 10 days (hepatic maturation), the medium was supplemented with 20 ng/mL OSM (PeproTech), 1 µM Dexamethasone (Sigma-Aldrich) and 1X ITS. The medium was renewed at days 15 and 19. The undifferentiated hBM-MSC (Undiff condition) were seeded at the same density and followed the same kinetics as the Diff condition but were cultivated in IMDM supplemented with 1% FBS, 100 U/mL penicillin and 100 µg/mL streptomycin.

2. Western Blot analyses

Cells cultured in T25 and T75 flasks were washed once with Phosphate Buffer Saline (PBS) (pH 7,4), trypsinized and centrifuged at 300xg for 5 minutes. The cell pellets were stored at -80°C or directly lysed in DLA-MITO lysis buffer (7M Urea; 2M Thiourea; 1% CHAPS; 1% ASB-14; 30 mM Tris HCl pH 7,6 and 1% Sodium Dodecyl Sulfate) complemented with Complete Protease Inhibitor Cocktail (#04693116001; Roche, Basel Switzerland) and homemade phosphatase inhibitor cocktail (25 mM Na_3VO_4 [S-6508, Sigma-Aldrich]; 250 mM 4-nitrophenylphosphate [N-3254, Sigma-Aldrich]; 250 mM di-Sodium β-glycerophosphate pentahydrate [27874295, VWR] and 125 mM NaF [6449/106441, Merck Millipore]). Cell lysates were incubated 15 minutes on a thermomixer at 12°C with 500RPM followed by 3x 10 seconds sonication at 50% amplitude-Pulse 1. Afterwards the lysates were centrifuged at 14000xg at 12°C for 15 minutes, the supernatants were collected and protein concentration was assessed with the Pierce protein assay reagent (Thermo Fisher Scientific) (supplemented with 1 g/20 mL Ionic Detergent Compatibility Reagent) as specified by the manufacturer.

8 or 10 µg of proteins were resuspended in equal volumes of Western Blot loading buffer (0,5 M Tris pH 6,8, SDS, β-mercaptoethanol, glycerol) prior to loading on home-made SDS-polyacrylamide gels composed of a layer of 6% acrylamide gel on top of a layer of 15% acrylamide gel. Color Prestained Protein Standard, Broad Range (11–245 kDa) was used as protein ladder (New England Biolabs, Ipswich, MA, USA). Protein migration was performed at 120-150V during approximately 1h (until frontline reaches the bottom of the gel) into Mini-PROTEAN Tetra Cell (BioRad, Hercules, CA, USA). Proteins were transferred on PolyVinyliDene Fluoride (PVDF) (Immobilon-P, Merck Millipore) membranes using either Trans-Blot Turbo Transfer System (BioRad) (25V, 1,3A, 10 minutes) or liquid transfer (100V, 2h30). Membranes were blocked by incubation in 50% Odyssey Blocking Buffer (LI-COR Biosciences, Lincoln, NE, USA)-PBS during at least 1h at Room Temperature (RT) on rocker prior probing with primary antibodies overnight at 4°C or 1h at RT on rocker. Secondary fluorescent antibodies were incubated 1h at RT. Primary and secondary antibodies, listed in **Table 2,** were diluted in Odyssey Blocking Buffer (LI-COR Biosciences) 0,1% Tween-20 (BioRad, USA). Membrane fluorescence was detected using Odyssey Licor Scanner (LI-COR Biosciences) and fluorescent signals were quantified using the Odyssey Application Software Version 3.0 of LI-COR Biosciences. All quantifications are expressed in relative protein abundance after normalization of the fluorescence intensity of each protein of interest over its corresponding loading control fluorescence. The ratio was then reported to day 0 condition signal.

Western-Blot-Primary antibodies				
Target	**Manufacturer**	**Reference**	**Specie**	**Dilution**
eIF4E (P-2)	Santa Cruz Biotechnology, Inc. (Dallas, TX, USA)	sc-9976	Mouse monoclonal	1:1000
eIF4G (A-10)	Santa Cruz Biotechnology, Inc. (Dallas, TX, USA)	sc-133155	Mouse monoclonal	1:1000
ATP synthase β (3D5AB1)	Thermo Fisher Scientific (Waltham, MA, USA)	A-21351	Mouse monoclonal	1:1000
ATP synthase α (7H10BD4F9)	Thermo Fisher Scientific (Waltham, MA, USA)	459240	Mouse monoclonal	1:1000
Lamin A/C	BD Biosciences (Franklin Lakes, NJ, USA)	612162	Mouse monoclonal	1:1000
Puromycin (12D10)	Merck Millipore (Burlington, MA, USA)	MABE343	Mouse monoclonal	1:5000
4EBP1 (53H11)	Cell Signaling Technology, Inc. (Danvers, MA, USA)	9644	Rabbit monoclonal	1:2000
Histone H3 (D1H2)	Cell Signaling Technology, Inc. (Danvers, MA, USA)	4499	Rabbit monoclonal	1:4000
GAPDH (EPR6256)	Abcam (Cambridge, UK)	128915	Rabbit monoclonal	1:1000
LDHA	Cell Signaling Technology, Inc. (Danvers, MA, USA)	2012	Rabbit monoclonal	1:1000
Phospho-p70 S6 Kinase (Thr389)	Cell Signaling Technology, Inc. (Danvers, MA, USA)	9205	Rabbit monoclonal	1:1000
Phospho-eIF4E (Ser209)	Cell Signaling Technology, Inc. (Danvers, MA, USA)	9741	Rabbit monoclonal	1:1000
Phospho-mTOR (Ser2448)	Cell Signaling Technology, Inc. (Danvers, MA, USA)	2971	Rabbit monoclonal	1:1000
Phospho-4EBP1 (Thr37/46) (236B4)	Cell Signaling Technology, Inc. (Danvers, MA, USA)	2855	Rabbit monoclonal	1:2000
p70 S6 Kinase	Cell Signaling Technology, Inc. (Danvers, MA, USA)	9202	Rabbit monoclonal	1:1000
Phospho-eIF2α (Ser51)	Cell Signaling Technology, Inc. (Danvers, MA, USA)	9721	Rabbit monoclonal	1:1000
NDUFS6	Abcam (Cambridge, UK)	195807	Rabbit monoclonal	1:1000
Western-Blot-Secondary antibodies				
Targeted specie	**Manufacturer**	**Reference**	**Specie**	**Dilution**
Mouse (IR Dye 800CW)	LI-COR Biosciences (Lincoln, NE, USA)	926-32210	Goat polyclonal	1:10000
Rabbit (IR Dye 800CW)	LI-COR Biosciences (Lincoln, NE, USA)	926-32211	Goat polyclonal	1:10000
Mouse (IR Dye 680RD)	LI-COR Biosciences (Lincoln, NE, USA)	926-68070	Goat polyclonal	1:10000
Rabbit (IR Dye 680RD)	LI-COR Biosciences (Lincoln, NE, USA)	926-68071	Goat polyclonal	1:10000
Immunofluorescence-Primary antibodies				
Targeted protein	**Manufacturer**	**Reference**	**Specie**	**Dilution**
4EBP1 (53H11)	Cell Signaling Technology, Inc. (Danvers, MA, USA)	9644	Rabbit monoclonal	1:1500
eIF4E (P-2)	Santa Cruz Biotechnology, Inc. (Dallas, TX, USA)	sc-9976	Mouse monoclonal	1:100
TOM20 (FL-145)	Santa Cruz Biotechnology, Inc. (Dallas, TX, USA)	sc-11415	Rabbit polyclonal	1:100
Immunofluorescence-Secondary antibodies				
Targeted specie	**Manufacturer**	**Reference**	**Specie**	**Dilution**
Mouse (Alexa fluor 488 nm)	Thermo Fisher Scientific (Waltham, MA, USA)	A-11001	Goat polyclonal	1:1000
Rabbit (Alexa fluor 488 nm)	Thermo Fisher Scientific (Waltham, MA, USA)	A-11008	Goat polyclonal	1:1000
Rabbit (Alexa fluor 647 nm)	Thermo Fisher Scientific (Waltham, MA, USA)	A-21244	Goat polyclonal	1:1000

Table 2. Antibodies used for Western-Blot and immunofluorescence analyses.

3. Immunofluorescence

Exp, differentiated and undifferentiated hBM-MSCs were trypsinized prior to seeding on sterilized coverslips (coated with collagen for differentiated and undifferentiated cells) at 20 000 cells/cm^2 in 24-wells plates. On the next day, cells were washed 3x with PBS, fixed by a 10 minutes incubation with 4% paraformaldehyde and permeabilized 5 minutes with 1% Triton X-100 in PBS. Cells were then washed 3x with PBS containing 2% Bovine Serum Albumin (BSA) Protease Free (422361V, VWR) (hereafter called PBS-2% BSA) and incubated overnight at 4°C with primary antibodies diluted in PBS-2% BSA. After 3 additional PBS-2% BSA washes, cells were incubated 1h at RT with secondary antibodies diluted in PBS-2% BSA and then washed twice with PBS-2% BSA and once with PBS. Afterwards, cells were incubated 20 minutes in PBS supplemented with 1 µg/mL 4′,6-diamidino-2-phenylindole (DAPI) (1023627001, Sigma-Aldrich) to stain nuclei, and then washed thrice with PBS. Primary and secondary antibodies are listed in **Table 2**. Coverslips were then mounted on slides using Mowiol (4-88, Sigma-Aldrich) and left to harden overnight at 4°C. Confocal microscopy analyses were performed using Leica Confocal Microscope (Leica microsystem, Wetzlar, Germany).

4. Periodic Acid Schiff (PAS) Staining

PAS staining was performed using the Sigma-Aldrich PAS Kit (395B-1KT). Cells at the end of the differentiation process (Day 22) were trypsinised and seeded on collagen-coated sterilized coverslips at 45 000 cells/cm^2 in 24-wells plates. Cells were then washed 3x using PBS and fixed with 4% paraformaldehyde for 20 minutes, incubated with 1% periodic acid for 10 minutes, washed 3x with ddH_2O and then incubated for 15 minutes with Schiff reagent. Coloration was then developed by 10x tap water washes for 10 minutes with 1 wash/minute. Coverslips were mounted on slides using Mowiol and left to harden overnight at 4°C in the dark, before observation with phase contrast microscope.

Genes	Forward Primers (5' ⟶ 3')	Reverse Primers (3' ⟶ 5')
SOX9 (SRY-Box 9)	CACACAGCTCACTCGACCTTG	TTCTTCGGTTATTTTTAGGATCATCTC
TDO2 (Tryptophan 2,3-dioxygenase)	GAGGAACAGGTGGCTGAATTT	GCTCCCTGAAGTGCTCTGTA
α1AT (Alpha-1 Antitrypsin)	GGGTCAACTGGGCATCACTAA	CCCTTTCTCGTCGATGGTCA
TBX3 (T-box transcription factor 3)	GTCGGGAAGGCGAATGTTTC	ACGACAGTCATCAGCAGCTA
PPIE (Peptidyl-prolyl cis-trans isomerase E)	CCGCTCTTGACCCTGCATAT	TCCAAGCAGACCCTGAGGAA
DDIT4 (DNA Damage Inducible Transcript 4)	CTAGCCTTTGGGACCGCTTC	CCAGGTAAGCCGTGTCTTC
GAPDH (Glycéraldéhyde-3-phosphate déshydrogénase)	CGGAGTCAACGGATTTGGTC	TGGAATTTGCCATGGGTGGA
ND2 (NADH dehydrogenase subunit 2)	TGTTGGTTATACCCTTCCCGTACTA	CCTGCAAAGATGGTAGAGTAGATGA
TBP (TATA box binding protein)	TCCCGCCTGGTGCCCTACTC	CGCCCAGCCAGCCAGTAGTA
EIF4EBP1 (eIF4E-binding protein 1)	CAAGGGATCTGCCCACCATT	AACTGTGACTCTTCACCGCC
CCND1 (cyclin D1)	CCATGAACTACCTGGACCGC	TGAAATCGTGCGGGGTCATT
ODC1 (Ornithine decarboxylase 1)	TGATGCCCGCTGTGTTTTTG	AACTGCAAGCGTGAAAGCTG
VEGFA (Vascular endothelial growth factor A)	CCATCCAATCGAGACCCTGG	TCTCTCCTATGTGCTGGCCT
HSPA9 (mitochondrial Heat Shock Protein 70)	CTGAAGAAGACCGGCGAAAGA	AGCTTGTTGCACTCATCAGCA
EGR1 (Early growth response 1)	TGACCGCAGAGTCTTTTCCT	GTTTGGCTGGGGTAACTGGT
ATF4 (Activating Transcription Factor 4)	GCCAAGCACTTCAAACCTCA	GCATCCTCCTTGCTGTTGTT

Table 3. Primers used for RT-qPCR.

5. Cellular fractionation, RNA and protein extraction

Nuclear and cytosolic fractions were prepared according to (Tacheny et al., 2012). All steps for cellular fractionation were performed at 4°C. Briefly, hBM-MSCs cultured in T150 flasks were rinsed

and then incubated 20 minutes with Hypotonic Buffer (HB) (5 mM NaF, 1 mM Na_2MoO_4, 20 mM HEPES [pH 7,9] and 0,1 mM EDTA) prior to lysis by addition of lysis buffer (HB supplemented with 0,5% Nonidet P-40 and 100 U/mL RNAINH-RO [Roche]) and scraping for 5 minutes. One-fifth of the cell homogenate was saved as the total fraction. The cell homogenate was centrifuged at 14000xg at 4°C for 30 seconds and the supernatant was collected as cytoplasmic fractions. The nuclear pellets, corresponding to nuclear fractions, were resuspended in a defined volume of lysis buffer (e.g. 400 µL for 1x T150 flask). The same volume of supernatant fractions (in excess) and total fractions (that needed completion with lysis buffer to reach the volume) were used for protein and RNA extraction. Three volumes of TRI Reagent Solution (AM9738, Thermo Fisher Scientific) were added to each fraction (total, nuclear and cytoplasmic) which were left for 5 minutes incubation at RT. One-fifth volume of chloroform was then added to each fraction, mixed by inversion, and left for 5 minutes incubation at RT prior to centrifugation at 12 000xg at 4°C for 15 minutes, allowing for the formation of three phases. For RNA extraction, the upper phase was collected and transferred in a new tube. One volume of isopropanol was added, the two remaining phases were saved for protein extraction (see below).

For the RNA extraction, the three fractions were let to incubate 10 minutes at RT with the isopropanol and were then centrifuged at 12 000xg at 4°C for 10 minutes. The RNA pellets were then washed with 100% and 75% ethanol sequentially, then left to air dry prior resuspension in nuclease-free water. RT-qPCR was then performed on each sample as described below (the used primers are listed in **Table 3**).

For protein extraction, 100% ethanol was added to the remaining phases for each fraction, left incubate 3 minutes at 4°C and centrifuged at 2000xg at 4°C for 5 minutes. The supernatant was then saved and isopropanol was added, let incubate 10 minutes at 4°C and centrifuged at 12 000xg at 4°C for 10 minutes. Protein pellets were then washed thrice with 0,3 M guanidinium chloride (1.04219.0100/104220, Merck Millipore) in 95% ethanol and once with 100% ethanol. Protein pellets were then let to air dry and then resuspended in DLA-MITO buffer (see Western Blot analyses). Fractionation efficiency was assessed by Western-blot detection of Lamin A/C and Lactate Dehydrogenase A (LDHA) as nuclear and cytoplasmic markers, respectively.

6. RNA extraction and RT-qPCR

RNA was extracted using the RNeasy Mini kit and QIACube device (Qiagen, Venlo, The Netherlands). Reverse transcription was performed using the Promega GoScript Reverse Transcriptase kit (A2791, Promega, Fitchburg, WI, USA) (250-1000 ng of extracted RNA was engaged, depending on the available material and extraction yield) and quantitative Real-Time PCR (Rt-qPCR) was then achieved using the Gotaq qPCR Master Mix (A6002, Promega) with ViiA 7 Real-Time PCR System (Thermo Fisher Scientific). The used primers are listed in **Table 3**. Results were normalized with the ddCT method using PPIE (Peptidyl-prolyl cis-trans isomerase E) mRNA abundance as housekeeping gene and reported to Day 0 condition mRNA abundance.

7. Cap binding assay

Cap binding assay protocol was adapted from (Tahmasebi et al., 2016). This method consists in the specific pull-down of eIF4E and bound partners using mRNA cap analogous-coated beads (Bradley et al., 2002). At indicated timepoints, hBM-MSCs were washed once with PBS, trypsinized and centrifuged at 300xg for 5 minutes. Cell pellet was then resuspended in buffer A (lysis buffer) (50 mM MOPS-KOH pH 7,4; 100 mM KCl; 0,02 mM NaN_3; 0,5 mM EDTA; 1% Nonidet P-40; 1%

sodium deoxycholate supplemented with cOmplete™, EDTA-free Protease Inhibitor Cocktail [#11873580001, Roche]) and incubated 10 minutes on ice. The lysate was then centrifuged at 16 000xg for 10 minutes and the supernatant was transferred in a new tube, on ice. 2% of total lysate was saved as the "Input" sample for Western Blot analysis. A fraction corresponding to 500 µg of protein lysate was added to x µL of buffer B in order to reach a final volume of 1 mL (MOPS-KOH pH 7,4 50 mM; KCl 100 mM; NaN_3 0,02 mM; EDTA 0,5 mM, and EDTA-free Complete Protease Inhibitor Cocktail) prior incubation with immobilized γ-aminophenyl-m^7GTP (C_{10} spacer) beads (AC-155S, Jena Bioscience, Germany) for 2h on rotating wheel at 4°C. Beads were then washed 5x with buffer B and bound proteins were then eluted with 0,2 mM m^7GTP (NU-1122S, Jena Bioscience) for 15 minutes at 4°C on thermocycler at 500 RPM. Beads were centrifuged at 4500xg for 30 seconds at 4°C. The supernatant corresponding to eluate was collected and analyzed by Western Blot to assess the abundance of eIF4E, eIF4G and 4EBP1. Detection of Glyceraldehyde-3-phosphate Dehydrogenase (GAPDH) was used as a negative control.

8. mtDNA content evaluation

Total DNA was extracted using the Wizard Genomic DNA Purification Kit (A1120/ A1125/ A1620, Promega). Mitochondrial DNA content was assessed by qPCR using primers targeted against the mitochondria-encoded gene *NADH dehydrogenase subunit 2* (*ND-2*) and was normalized to genomic DNA by using primers targeted against the genomic gene *TATA-Binding Protein* (*TBP*) (**Table 3**). qPCR was performed using the Gotaq qPCR Master Mix with ViiA 7 Real-Time PCR System. Relative mtDNA content was normalized over Day 0 condition.

9. Global translation measurement

Global translation was assessed by surface sensing of translation (SUnSET) as described in (E. K. Schmidt et al., 2009). hBM-MSCs were incubated for 10 minutes in medium supplemented with 5 µg/mL puromycin dihydrochloride from *Streptomyces alboniger* (P88-33, Sigma-Aldrich). The puromycin is a well-known analog of amino-acyl-tRNA which is incorporated in the nascent chain during translation. However, once incorporated, puromycin prevents translation elongation, thereby triggering premature translation termination (Blanco & Blanco, 2017). For negative controls, cells were previously incubated 30 minutes in the presence of 20 µg/mL cycloheximide (C7698-1G, Sigma-Aldrich) or underwent a medium replacement without puromycin. Cells were then lysed in DLA-MITO (see Western Blot analyses) and global protein synthesis was assessed by western-blot (as previously described in E. K. Schmidt et al., 2009). 10 µg of proteins were resolved on 10% acrylamide gel and puromycin was detected with monoclonal anti-puromycin antibody (**Table 2**). For each condition, signal intensity was normalized over histone H3 signal.

10. Statistical analyses

All the statistical analyses were performed using the statistical programming language R (www.rproject.org/) with the "ggplot2" and "ggpubr" packages. Assuming normal distribution of the data, unpaired two-tailed t-tests were performed for the comparison between Diff and Undiff conditions for each time point but for *SOX9* expression in **Figure 12D** where day 22 Diff and Undiff conditions were also compared to EXP and Day 0 condition. Bonferroni correction was applied for the multiple comparison. Significance symbols used correspond to: **: $p < 0,01$; *: $p < 0,05$.

RESULTS

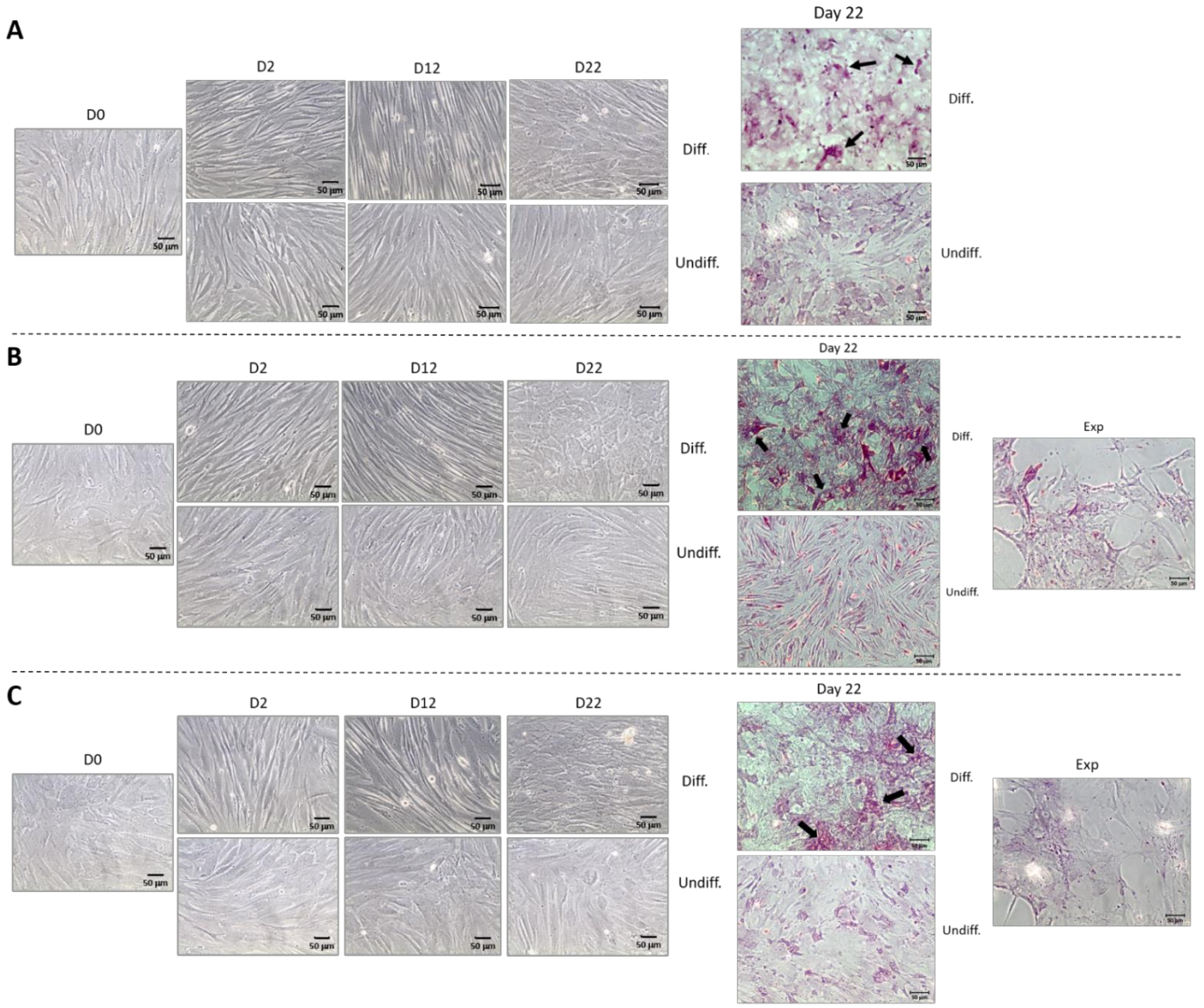

Figure 12. Assessment of differentiation efficiency based on cell morphology, PAS staining and gene expression on three different donors. The differentiation was performed on three different donors namely: (A) BM18P6, (B) BM2P7 and (C) BM22P7, cited hereafter donor 1, donor 2 and donor 3 respectively. Cells were seeded at 10 000 cells/cm2 following the differentiation protocol described in (Najar et al., 2013) with sequential exposure of the cells to three different cytokine cocktails: EGF and FGF-2 for the first two days; FGF-2, HGF, Nicotinamide and ITS for the next ten days; OSM, dexamethasone and ITS for the last ten days, responsible for differentiation initiation, hepatic induction and maturation steps respectively (**Figure 11**). Cell micrographs were taken when medium was replaced and the cytokine cocktail changed, at Day 2, 12 and 22. For each donor, Periodic Acid Schiff staining was performed on cells in expansion (Exp.) (for donors 2 and 3) and at the end of the process on differentiated (Diff.) and undifferentiated (Undiff.) cells. Cells were seeded on coverslips at a density of 45 000 cells/cm^2 and underwent PAS staining, highlighting glycogen accumulation with granule-like staining, indicated by the black arrows. Scale bar = 50 µm. (D) RNA extraction was performed on cells in expansion and on differentiating and undifferentiated cells collected at day 0, 2, 3, 5, 9, 12, 15 and 22 of differentiation. Expression of hepatic (*α-1-antitrypsine* (*α1AT*), *tryptophan 2,3-dioxygenase* (*TDO2*)), developmental (*T-box Transcription factor 3* (*TBX3*)) and stemness markers (*SRY-Box 9* (*SOX9*)) was assessed using Real-time PCR. mRNA abundance of each gene is normalized to *PPIE* (*Peptidyl-prolyl cis-trans isomerase E*) and then expressed relatively to day 0 ratio. The profile of *α1AT* corresponds to the one of the first donor represented in A (n=1), *TDO2* values are represented as mean of donors 1 and 2 (n=2) and data for *TBX3* and *SOX9* are presented for the three donors as mean ± SEM (n = 3). Unpaired two-tailed t-test were performed for each timepoint, comparing Diff with Undiff conditions and comparing EXP and Day 0 with Day 22 Diff and Undiff conditions for *SOX9* expression.

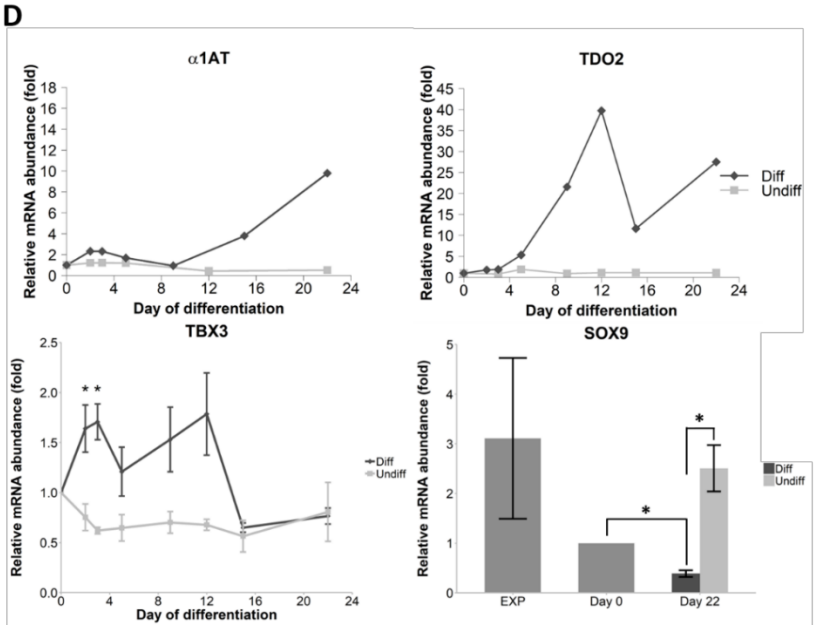

Figure 12. (following). Assessment of differentiation efficiency based on cell morphology, PAS staining and gene expression on three different donors. (D) RNA extraction was performed on cells in expansion and on differentiating and undifferentiated cells collected at day 0, 2, 3, 5, 9, 12, 15 and 22 of differentiation. Expression of hepatic (*α-1-antitrypsine* (*α1AT*), *tryptophan 2,3-dioxygenase* (*TDO2*)), developmental (*T-box Transcription factor 3* (*TBX3*)) and stemness markers (*SRY-Box 9* (*SOX9*)) was assessed using Real-time PCR. mRNA abundance of each gene is normalized to *PPIE* (*Peptidyl-prolyl cis-trans isomerase E*) and then expressed relatively to day 0 ratio. The profile of *α1AT* corresponds to the one of the first donor represented in A (n=1), *TDO2* values are represented as mean of donors 1 and 2 (n=2) and data for *TBX3* and *SOX9* are presented for the three donors as mean ± SEM (n = 3). Unpaired two-tailed t-test were performed for each timepoint, comparing Diff with Undiff conditions and comparing EXP and Day 0 with Day 22 Diff and Undiff conditions for *SOX9* expression.

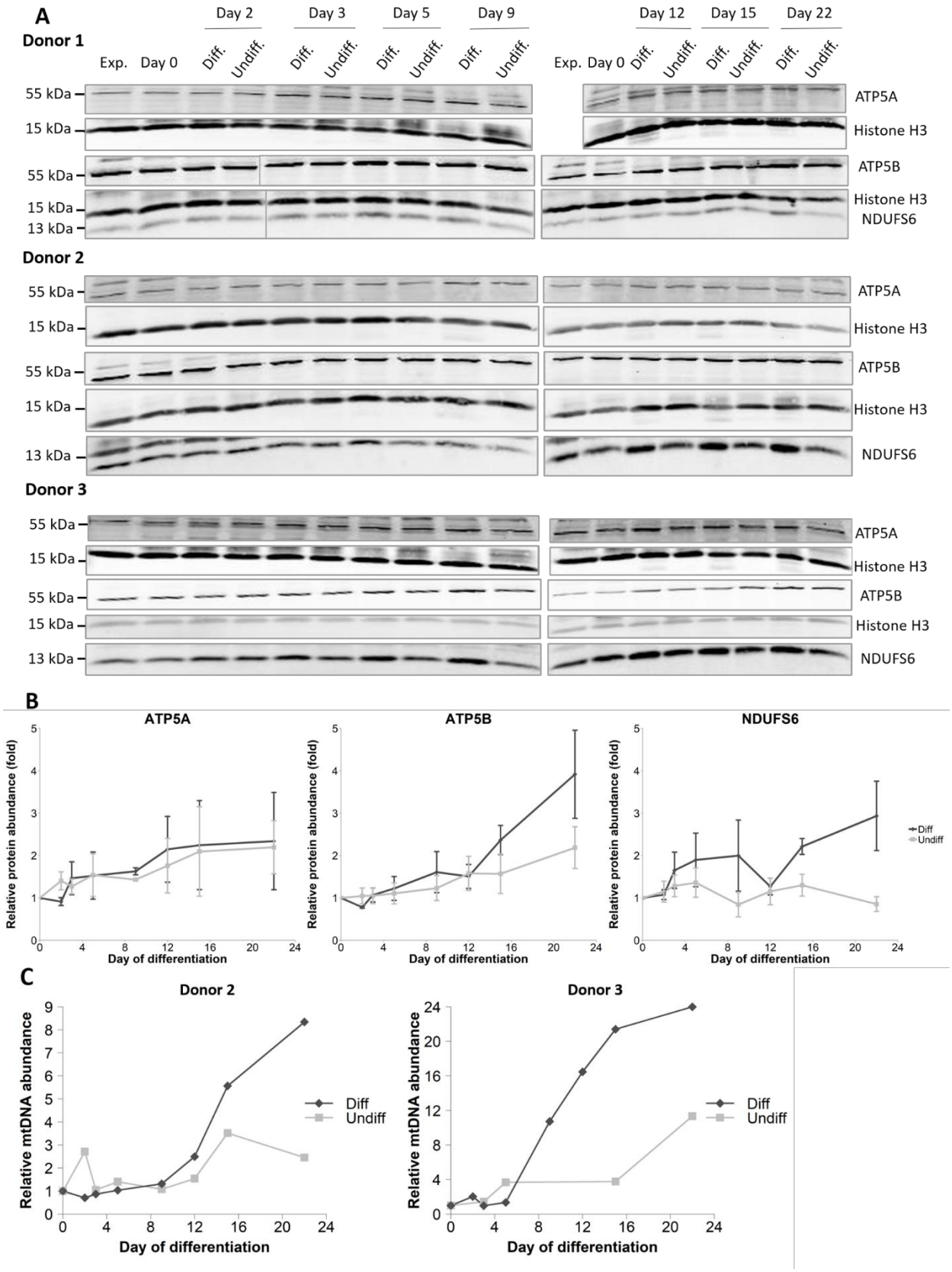

Figure 13. Assessment of mitochondrial remodeling at the protein level. (A) Cells corresponding to the three different donors presented in **Figure 12** followed a complete differentiation program. Exp, Diff and Undiff cells were collected at the indicated time-points for proteins extraction. 8 µg of proteins were loaded on four 6-15% polyacrylamide gels, where for each gel, Exp and Day 0 samples were loaded as control. ATP5B, ATP5A, NDUFS6 and histone H3, the loading control, were detected. (B) Quantification of the signal intensity of the different proteins was normalized with the histone H3 signal and then with the ratio calculated for day 0 to obtain relative protein abundance. Data are presented as mean ± SEM (n = 3). Unpaired two-tailed t-test were performed for each timepoint, comparing Diff with Undiff conditions. (C) Exp, Diff and Undiff cells of donor 2 and 3 were collected at the indicated time-points and DNA extraction was performed to assess *TATA-Binding Protein* (*TBP*) and *ND2* (*NADH dehydrogenase subunit 2*) gene abundance, as nuclear and mitochondrial genomic markers, respectively. *ND2* gene abundance is normalized to *TBP* abundance and the relative mtDNA content is then normalized over day 0 condition.

IV. RESULTS

1. Hepatogenic differentiation efficiency assessment

Although the hepatogenic differentiation model of hBM_MSC has been previously described (Wanet et al., 2014), three different read-outs were selected to assess the efficiency of cell differentiation: the cell morphology, the glycogen storage ability (assessed at the end of the process), and the evolution of mRNA markers during the process. Results for three independent differentiation processes performed on independent donors, further referred as donors 1, 2 and 3, are presented on **Figure 12**. Morphologically, expanding BM-MSCs show fibroblast-like phenotype which is maintained upon confluency and in undifferentiated cells all along the differentiation process. On the other hand, upon differentiation induction, cells acquire a more elongated phenotype following exposure to the first and second cytokine cocktails, corresponding to the differentiation induction and hepatic induction steps, respectively (**Figure 11**). Hepatic maturation then occurs, following the exposure to the third cytokine cocktail, where cells shrink and become more cuboid with polygonal-like shapes at the end of the process, typical of hepatocyte-like cells.

For the functional assessment of the differentiation efficiency, Periodic Acid Schiff (PAS) staining was performed at the end of the process, highlighting glycogen accumulation. PAS reaction leads to the non-discriminate staining of carbohydrates and thus only granule-like staining is informative. Such staining is only observed in differentiated cells and corresponds to glycogen granules accumulated in the cytosol, as indicated by the arrows on **Figure 12**. Notably, only few cells, in the differentiated condition, are positives for the PAS staining, underlining a limited differentiation efficiency and confirming previous observations concerning the limitations of this *in vitro* differentiation model (Wanet et al., 2014). In addition, the number of PAS positive cells is also different between the three donors, suggesting donor-dependent responsivity to the differentiation protocol.

Concerning the evaluation of mRNA markers, the four target genes selected correspond to two hepatic markers: the *α-1-antitrypsine* (*α1AT)*, encoding the major circulating serine protease inhibitor produced by the liver, and the *tryptophan 2,3-dioxygenase* (*TDO2*)), encoding an enzyme involved in tryptophan catabolism, more particularly in the early steps of the Kynurenine pathway and which is essentially produced in the liver (Jones et al., 2013); the developmental marker *T-box Transcription factor 3* (*TBX3*) involved in liver development (**Figure 3**); and the stemness marker *SRY-Box 9* (*SOX9*) maintaining cells in an undifferentiated state (Kawaguchi, 2013).

α1AT expression increases from day 12 to day 22 only in differentiating cells. However, *α1AT* expression profile could only be obtained for donor 1 due to technical issues for its assessment for donor 2 and 3. *TDO2* expression profile shows similar feature with a continuous increase from day 2 to day 12 as previously described (A. Wanet, PhD thesis). However, an unexpected decrease is observed with a consecutive increase from day 15 to day 22, where the expression of *TDO2* in differentiated hepatocyte-like cells is still 25-fold higher than its expression in undifferentiated cells. The data for *TDO2* represents results obtained for the two first donors as no amplification could be obtained for donor 3, in undifferentiated cells. Regarding *TBX3* expression profile, an early significant increase is observed from day 0 to day 2, with a ~2-fold higher expression maintained in differentiating cells until day 12. *TBX3* expression then decreases to reach similar levels than observed in undifferentiated cells. Finally, the stemness marker *SOX9* shows higher expression in expanding cells compared with hepatocyte-like cells at day 22, while the expression level in undifferentiated cells remain similar (**Figure 12D**).

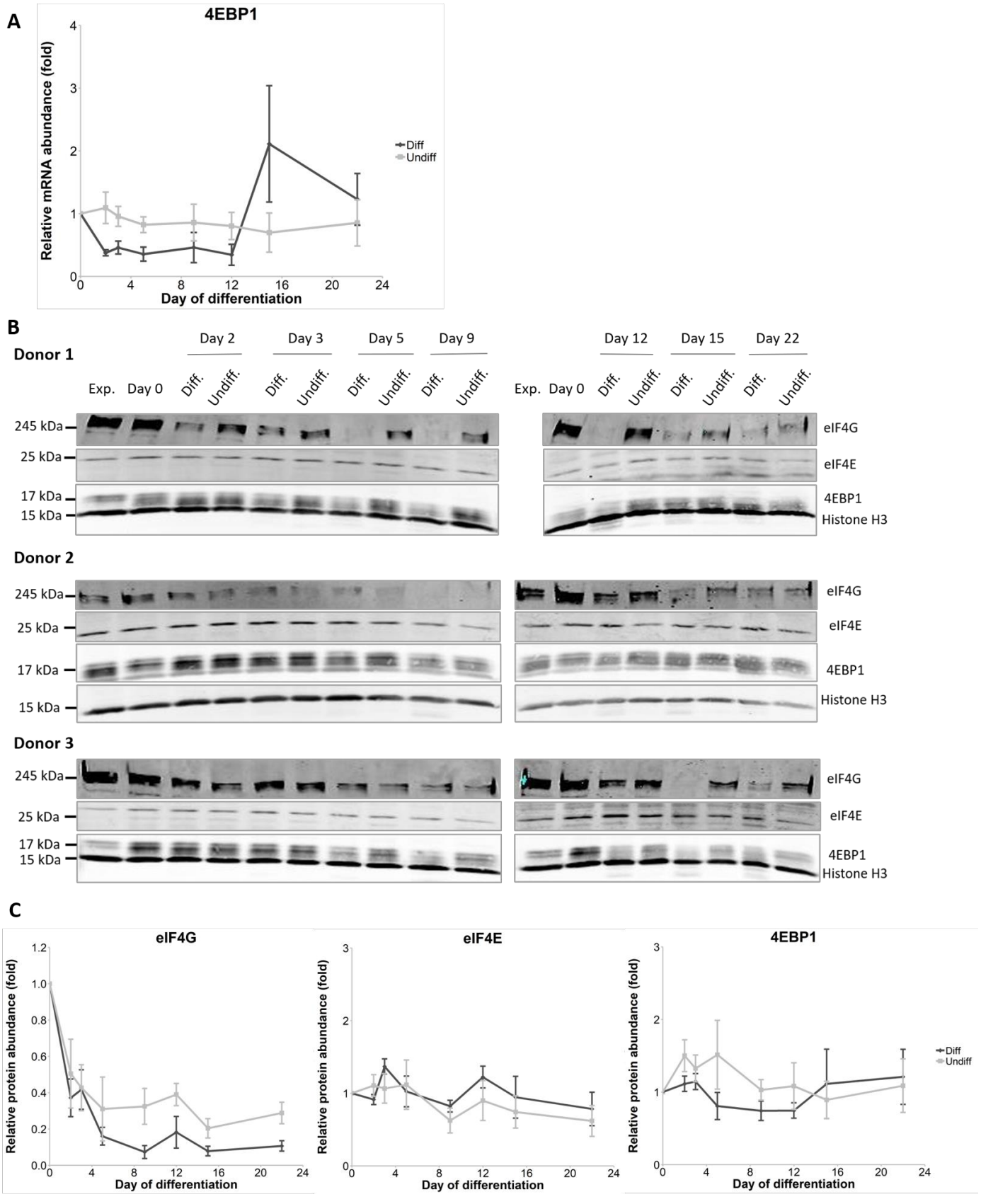

Figure 14. Evolution of the eIF4F complex members abundance along the hepatogenic differentiation process. (A) Diff and Undiff cells from the previously mentioned three donors were collected at different time points and the expression of *4EBP1* was assessed by Real-Time PCR. (B) The protein abundance of 4EBP1 was also assessed, during the differentiation process for the three donors, using western blot, as for the other main components of the eIF4F complex: eIF4G and eIF4E. (C) Averaged quantification associated with the three blots in B. Quantification of the signal for each protein is normalized to the signal of its respective loading control (histone H3 signal) and is then expressed relatively to day 0 condition. Data are presented as mean ± SEM (n = 3). Unpaired two-tailed t-test were performed for each timepoint, comparing Diff with Undiff conditions.

2. Mitochondrial remodeling assessment

In order to confirm the mitochondrial remodeling occurring during the hepatogenic differentiation of BM-MSC, the abundance of several mitochondrial proteins was analyzed (**Figure 13**). Despite variability between donors, displayed on the blots presented in **Figure 13A**, no straight abundance differences between differentiating and undifferentiated cells can be observed for the α subunit of the ATPase (ATP5A) while only a late but not significant difference can be observed for the β subunit (ATP5B) from day 15 to day 22. However, the NADH dehydrogenase (ubiquinone) iron-sulfur protein 6F (NDUFS6), an assembly factor of the mitochondrial respiratory complex I, shows a clear, although not significant, increased abundance in differentiating cells compared with undifferentiated ones in the three donors from day 3 to the end of the process, with a small drop at day 12. Despite the absence of significant differences, a consistent trend to increased abundance is observed regarding the signal intensities of the proteins on the blots (**Figure 13A**) and their associated individual quantifications per donor (**Supplementary figure 1**). Indeed, regarding the donors independently (**Figure 13A**, **Supplementary figure 1A**), a 2-3 fold difference is observed at day 22. Thus, due to different intensities in the differences between conditions, pooled information result in the disappearance of the biological effect which seems to exist regarding the consistency between the independent replicates. Two levels of variabilities are involved in this case: the variability linked to the donor and thus heterogenous cell population and the variability linked to the differentiation efficiency which shows inter-individual variability, meeting the first point, but also intra-individual variability. Therefore, three replicates are probably not enough to allow detection of a significant effect but describing general tendencies and looking at the data independently (**Supplementary figure 1**) can help to draw observations and conclusions. In addition, the method used here is only a semiquantitative method whereas a quantitative and more sensitive method would give supplemental information.

Another mitochondrial parameter has been further assessed to strengthen these results (**Figure 13C**). Mitochondrial DNA (mtDNA) content was addressed during the differentiation process for donors 2 and 3 (**Figure 13C**). Once again variability between donors is observed as the increase in mitochondrial content in differentiating cells occurs earlier (around day 9) for donor 3, compared with donor 2 (around day 15). Interestingly, the protein abundance of NDFUS6 show the similar profile while regarding individually donor 2 and 3 (**Supplementary figure 1A**).

3. Characterization of the eIF4F complex assembly during the differentiation process

Preliminary results obtained from the transcriptomic analysis performed after 5 days of differentiation suggest that 4EBP1 expression is downregulated in differentiating cells (see Introduction, point I.5). In order to validate *4EBP1* downregulation, its expression was analyzed all along the differentiation process (**Figure 14A**). Although no significant differences could be detected, due to the high inter-individual variability, a consistent profile for *4EBP1* can be observed with a downregulation from day 2 to day 12 and a subsequent upregulation till day 22 in differentiated cells compared with undifferentiated ones. This *4EBP1* expression profile is also observed at the protein level with the same variability between donors (**Figure 14B**), suggesting an increase in global protein synthesis followed by a decrease. However, this interpretation is not supported by the protein abundance of the eIF4F complex components, directly impacted by 4EBP1 activity. The eIF4G abundance profile is so different between donors that it can hardly by interpreted. Indeed, opposite effects are even observed for eIF4G expression at day 2 between donors 1 and 3 for example as its abundance is clearly downregulated in differentiating cells for donor 1 but slightly upregulated for donor 3 (**Figure 14B**). Importantly, the used antibody does only detect eIF4G1, the major isoform of eIF4G while the information concerning the other isoforms is not provided. In addition, the signal for

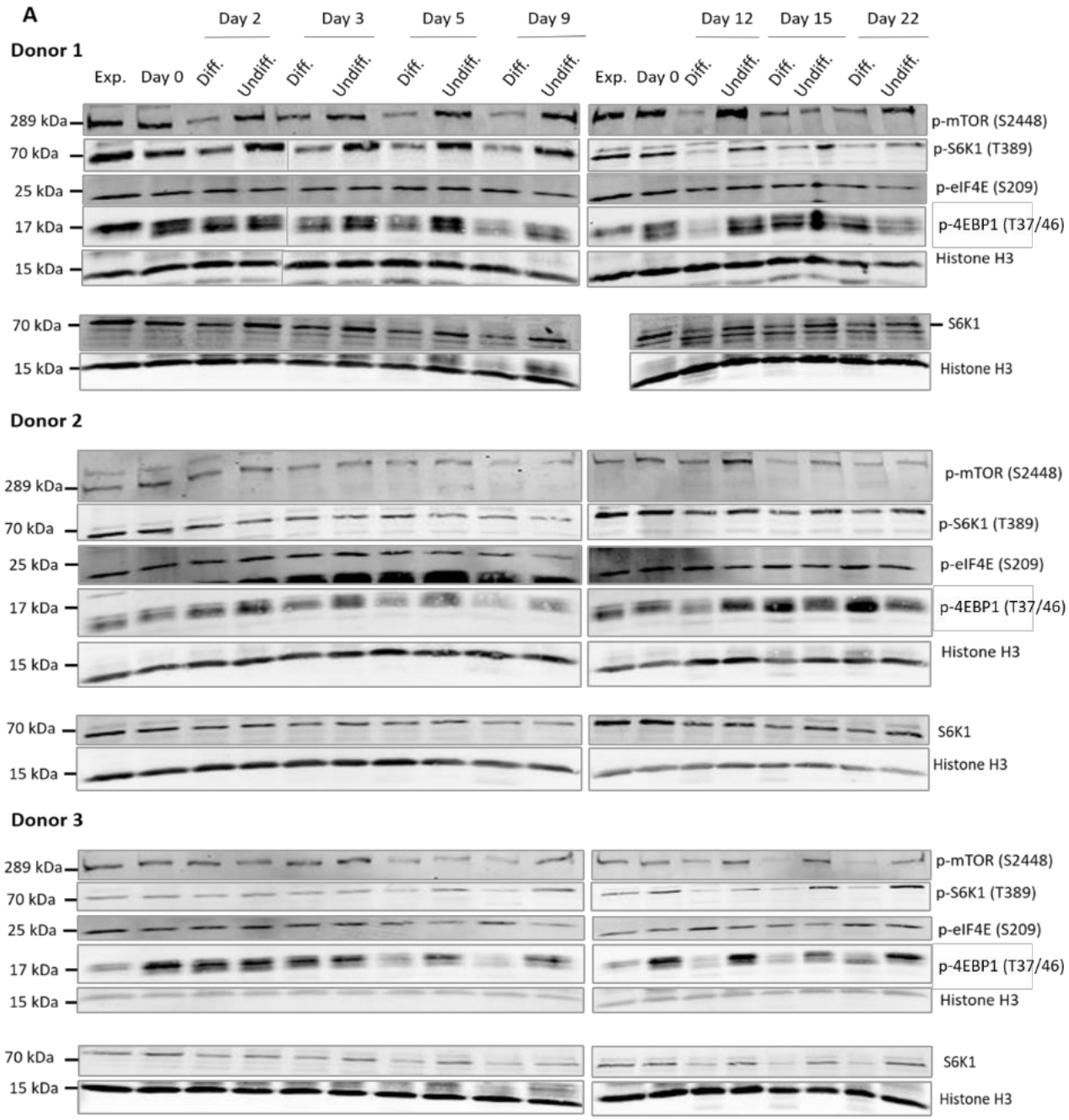

Figure 15. Regulation of the eIF4F complex and mTORC1 activity assessment. (A) Diff and Undiff cells from the previously mentioned three donors were collected at the indicated time points and the protein abundance of mTORC1-related proteins and targets was assessed by western blot. Revelation of p-mTOR (S2448), p-S6K1 (T389), p-4EBP1 (T37/46), p-eIF4E (S209), S6K1 and histone H3, the loading control, was performed.

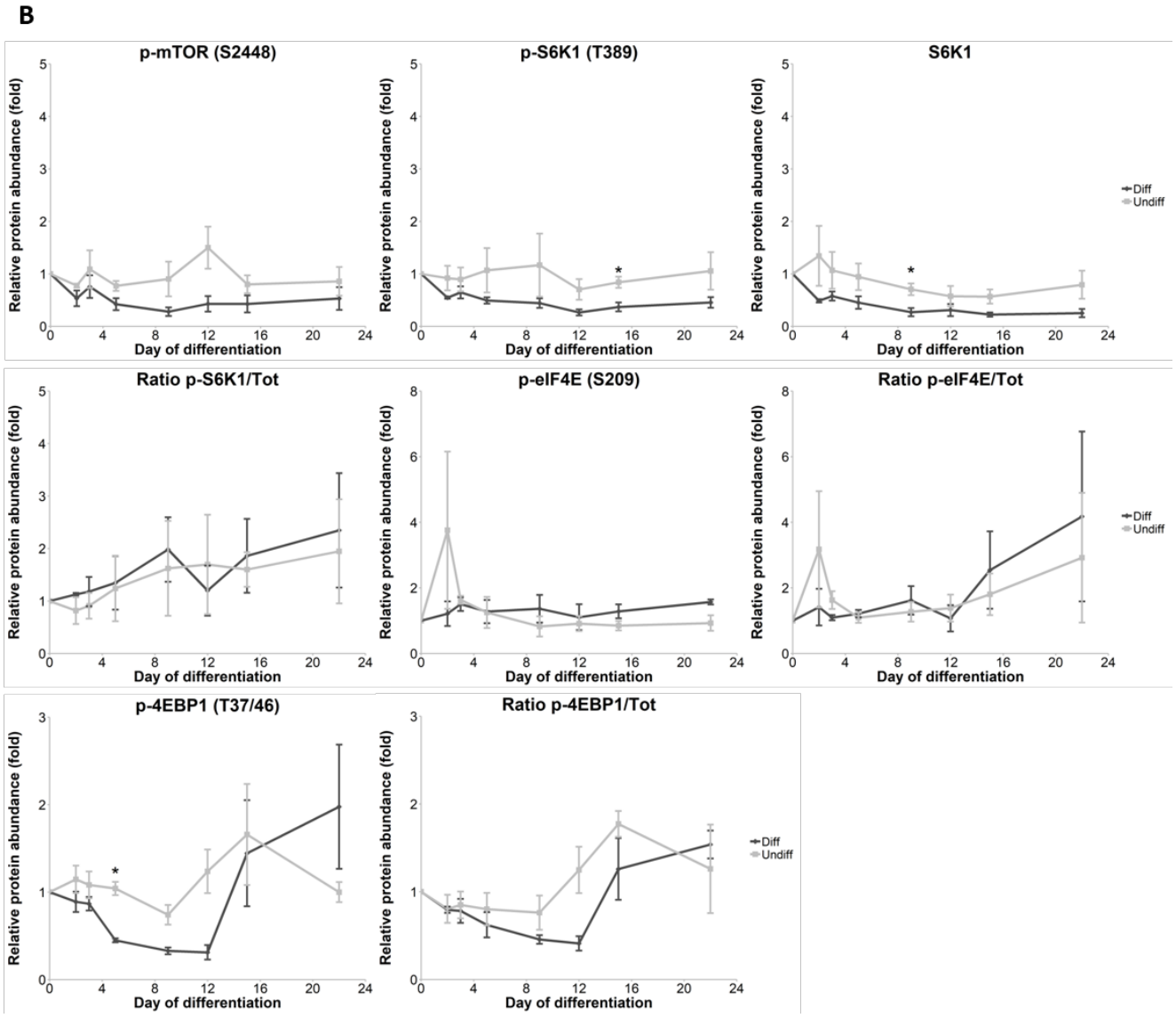

Figure 15 (following). Regulation of the eIF4F complex and mTORC1 activity assessment. (B) Averaged quantification associated with the three blots in A. Quantification of the signal for each protein is normalized to the signal of its respective loading control (histone H3 signal) and is then expressed relatively to day 0 condition. Data are presented as mean ± SEM (n = 3). Unpaired two-tailed t-tests were performed for each timepoint, comparing Diff with Undiff conditions.

this protein is really faint for some conditions and barely detectable, related to the poor sensitivity and quality of the used antibody. However, for the end of the differentiation process, a consistent profile is observed between the three different replicates, with a reduced abundance of the protein in differentiating cells compared with undifferentiated ones, suggesting a decrease in eIF4F complex assembly and thus of protein synthesis. Finally, the protein abundance of eIF4E remains globally unchanged all along the differentiation, in the two conditions (**Figure 14C**) with the sole exception of donor 2 where an upregulation is observed from day 12 to day 22 in differentiating cells, once again underlining the variability between donors (**Figure 14B**).

To get closer to functional characterization of eIF4F complex, the phosphorylation status of both eIF4E and 4EBP1 have been addressed, as well as the involvement of mTORC1 in the regulation of the eIF4E-4EBP1 axis (**Figure 15**). As for the total abundance of eIF4E, the abundance of phospho-eIF4E (p-eIF4E) remains unchanged in both conditions during the differentiation process even if quantification of the donor 1 blot detects a peak in p-eIF4E abundance for undifferentiated cells at day 2, probably due to technical bias in the quantification of this condition (**Figure 15B**, **Supplementary figure 1C**). Similarly, the profile of p-4EBP1 abundance is parallel to the total form abundance profile with a decreased expression in differentiating cells compared with undifferentiated ones and, this time, a significantly reduced abundance at day 5, which is maintained till day 12, followed by an increase of p-4EBP1 in differentiated cells compared with undifferentiated one at day 22. However, the decrease in the phosphorylation of 4EBP1 seems to be more pronounced than the decrease observed for the total form abundance, resulting in a lower fraction of phosphorylated 4EBP1 in differentiating cells, highlighted by the p-4EBP1/4EBP1 ratio (**Figure 15B**). The reverse phenomenon is observed at the end of the process with the concomitant increase of the p-4EBP1/4EBP1 ratio.

These results support the possible involvement of mTORC1 in the regulation of the eIF4E-4EBP1 axis. This hypothesis has been next tested with the characterization of the S2448 phosphorylation of mTOR, associated with mTORC1 activity (Copp et al., 2009), along the process as well as the phosphorylated status of the other canonical target of mTORC1, S6K1. The S2448 phosphorylation of mTOR is reduced in differentiating cells compared with undifferentiated ones all along the differentiation process, with the difference between the two conditions begin more marked for donors 1 and 3 (**Figure 15A**). This seemingly slightly reduced activation of mTORC1 is further confirmed following the phosphorylated status of S6K1. Indeed, a ~2-fold lower abundance of p-S6K1 is observed all along the differentiation process in differentiating cells, significantly validated at day 15. The total form of S6K1 follows the same profile. Therefore, the phosphorylated fraction of S6K1 is maintained identical between differentiating and undifferentiated cells all along the process (**Figure 15B**). Altogether these results do not support our working hypothesis of an increase in mTORC1 activity during the differentiation process. Additionally, variability is observed between donors with a more pronounced downregulation of the mTORC1 axis observed for donor 3 (**Figure 15A**), more particularly regarding the part of phosphorylated 4EBP1 which is more reduced than in the two other donors (**Supplementary figure 1C**). What's surprising is that this donor showed the strongest increase in NDUFS6 abundance, suggesting a putative mTORC1-dependent regulation of 4EBP1 activity, which is apparently not the case.

The sequential decreased abundance but reduced phosphorylation of 4EBP1, followed by increased abundance and phosphorylation, observed in the differentiating cells, might suggest an unchanged global activity with a similar abundance of active 4EBP1 in these cells. Indeed, the relevant information regarding eIF4F activity is actually the abundance of the unphosphorylated 4EBP1, which is the active form of the protein (associated with eIF4E and thereby inhibiting translation initiation). The higher abundance of p-4EBP1 observed in undifferentiated cells in the early time points thus cannot be interpreted as an indicator of high translational activity as the 4EBP1 abundance is clearly higher in this experimental condition, leaving many unphosphorylated 4EBP1 molecules available for eIF4E sequestration. This, together with the unchanged levels of eIF4E,

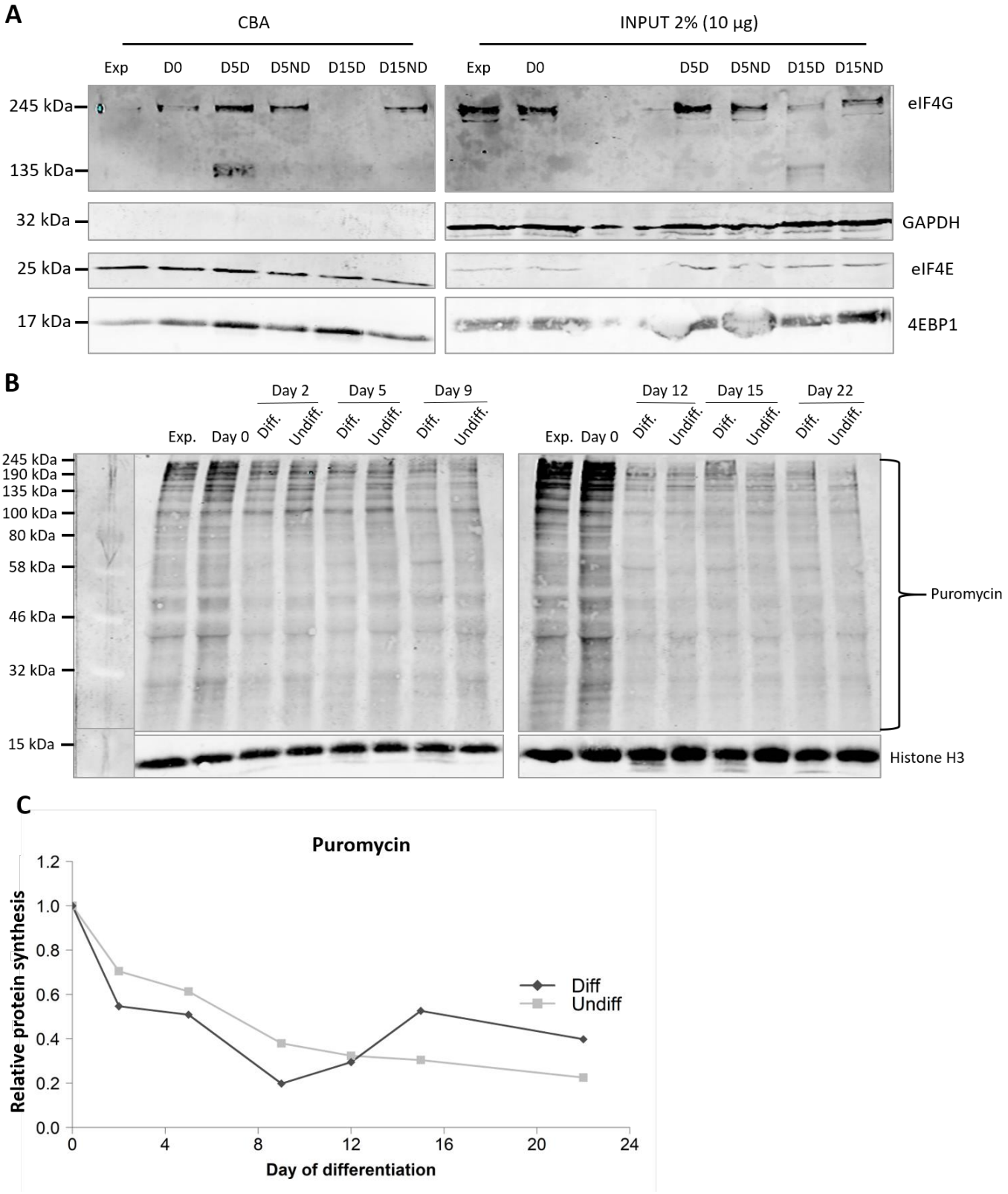

Figure 16. Functional assessment of eIF4F complex activity and general protein synthesis rate determination. (A) Donor 1 cells were collected and cap-binding assay (CBA) was performed on cells in expansion (Exp), cells at day 0 (D0) and differentiating (D) and undifferentiated (ND) cells at day 5 (D5) and 15 (D15). 500 µg of proteins were used for the cap binding assay (CBA) and loaded on 6-15% acrylamide gel along with 2% of total protein lysates (10 µg), previously saved. eIF4G, eIF4E, GAPDH and 4EBP1 were revealed. (B) SUnSET experiment was performed on Exp, Day 0, Diff and Undiff donor 1 cells which underwent a 10-minutes exposure to 5 µg/mL puromycin and were then harvested. 10 µg of proteins were loaded on 10% acrylamide gel and puromycin and histone H3, the loading control, were revealed. (n=1). (C) Relative protein synthesis is given by quantification of the puromycin signal for the whole lane, normalized to histone H3 signal and reported to the Day 0 ratio. (n=1).

would suggest no strong differences in eIF4F complex assembly all along the differentiation process. In another hand, the reduction in eIF4G abundance in the late time-points would suggest decreased eIF4F complex assembly during the differentiation, although it may be that another isoform of the scaffold protein ensures translation initiation, the isoform detected here corresponding to eIF4G1. The lower abundance of phosphorylated status of 4EBP1 (at least in the early time-points) is associated with reduced activation of mTORC1 all along the differentiation complex as supported by the reduction in the abundance of p-S6K1 and reduced phosphorylated state of mTOR on S2448. Nonetheless, the increased phosphorylation of 4EBP1 at the end of the process in differentiating cells, paralleling the increase in its abundance, suggests an increased activity of mTORC1 toward 4EBP1 at the end of the process, although no increase of mTOR and S6K1 phosphorylation is observed. To further assess the functional effect on eIF4F complex assembly of the combined regulation by phosphorylation and abundance of 4EBP1, the measurement of eIF4E-4EBP1 binding is necessary and this can be measured by a cap binding assay (CBA). This method is based on the specific pull-down of eIF4E using m7GTP-coated beads, mimicking mRNA cap structure, and subsequent detection of its binding partners (Bradley et al., 2002).

The CBA was performed on expanding cells and differentiating and undifferentiated cells at day 0, 5 and 15 (**Figure 16A**). These time-points were selected to screen the impact of the different abundance and phosphorylated state of 4EBP1 on eIF4F complex assembly. First of all, glyceraldehyde-3-phosphate dehydrogenase (GAPDH), used as a negative control, is not pulled down in the CBA, despite its presence in the input (corresponding to total lysate), as expected. In expanding cells and cells at day 0, eIF4G binds weakly to eIF4E, as revealed by the weak signal in the pull-down condition compared with input signal. Further on, eIF4G binding in differentiating cells at day 5 is stronger than observed in undifferentiated cells whereas eIF4G would be more abundant in differentiating cells than in undifferentiated cells, showing opposite results to what was previously observed in **Figure 14**. This discrepancy highlights the previously mentioned high variability between donors but also between differentiation processes, as the donor used here corresponds to donor 1, for whom a decreased abundance of eIF4G is observed in differentiating cells compared with undifferentiated ones (**Figure 14A**). Secondly, as illustrated in **Figure 14**, a constant abundance of eIF4G is observed in the input for undifferentiated cells, as in the CBA condition (**Figure 16A**), suggesting that eIF4G remains bound to eIF4E with constant abundance in undifferentiated cells. However, in the differentiating cells at day 15, eIF4G is even not detected in the CBA, suggesting that no functional eIF4F complex is formed in this experimental condition.

As observed in **Figure 14**, the total abundance of eIF4E remains constant during the differentiation process with similar levels between both conditions. Similarly, constant pull down of eIF4E underlines that no modifications of its binding activity occurs during the differentiation process between both conditions. Concerning 4EBP1 total abundance, the previously observed downregulation and subsequent upregulation in differentiating cells cannot be observed due to lack of resolution and technical problem occurring during the migration in the input gel. Nonetheless, for day 15, no upregulation seems to occur in the differentiating condition compared with undifferentiated one but no signal for the loading control could be detected, due to technical issues, to verify that the differences observed are not due to loading differences. However, regarding its association with eIF4E, increased binding of 4EBP1 to eIF4E seems to occur in differentiating cells at day 5 and 15 while constant and lower binding occurs in undifferentiated cells. Unexpectedly, at day 5 both eIF4G and 4EBP1 are bound to eIF4E in differentiating cells although they normally should antagonize each other for eIF4E binding. Comparatively, the fraction of 4EBP1 bound to eIF4E, in undifferentiated cells, is reduced at the advantage of eIF4G binding to eIF4E. Importantly, as explained for the **Figure 14**, the only isoform detected by the eIF4G antibody used here is eIF4G1 and thus no information concerning the other isoforms is provided. Interestingly, a 135 kDa band is detected by the antibody only in the differentiating conditions (**Figure 16A**) and, although the different forms of eIF4G1 can be detected by this antibody, even the shortest one is too large to correspond to this isolated band (Byrd et al., 2002). Even though the differentiation process performed during this

particular experiment was efficient, as shown in **Supplementary figure 2**, additional replicates are required to validate these results.

Altogether, these results suggest a decrease in eIF4F complex assembly with increased association of 4EBP1 with eIF4E at the expense of eIF4G binding, at least at the end of the differentiation process in differentiating cells. At day 5, the picture is much less clear as the increased 4EBP1-eIF4E interaction observed in differentiating cells is not compatible with the abundant eIF4G pulled-down with m7-GTP-interacting eIF4E. Thus, at least at day 15, this could suggest a reduced global protein synthesis in differentiating cells while a maintained assembly of eIF4F complex is observed in undifferentiated cells which would thus present constant protein synthesis rate. In order to confirm this hypothesis, global protein synthesis rate has been assessed, using the surface sensing of translation method (SUnSET) consisting in the exposure of the cells to puromycin, an analogous of amino-acyl tRNA which is incorporated in the peptide nascent-chain leading to elongation arrest. Afterward, newly synthetized peptides are detected by Western Blott analysis of cell lysates and blotting with anti-puromycin antibody.

SUnSET experiment was thus conducted all along the differentiation process to further characterize precisely relative protein synthesis during 10 minutes (**Figure 16B**). Negative controls of the experiments are shown in **Supplementary figure 4**, validating the method where no signal can be observed in the absence of puromycin treatment and almost no puromycin integration is observed upon cycloheximide treatment. Relative protein synthesis in expanding cells and in cells at day 0 is higher than in both differentiating and undifferentiated cells. Unexpectedly, quite similar total signal is observed for differentiating and undifferentiated cells with a slightly lower signal for differentiating cells in the beginning of the process till day 12, while the opposite is observed with a slightly increased signal in differentiating cells as compared with undifferentiated counterpart (**Figure 16C**). In addition, protein synthesis seems to slowly decrease in undifferentiated cells with the time. However, these results correspond to a single replicate and thus need to be reproduced, also to determine if the slight difference observed between differentiating and undifferentiated cells is significant or not. The differentiation controls are presented in **Supplementary figure 3** and show valid differentiation process.

These results were unexpected regarding the result of the cap-binding assay. Indeed, the increased binding of eIF4G to eIF4E in differentiating cells at day 5 and the following loss of eIF4G abundance and binding to eIF4E at the end of the process would suggest higher protein synthesis rate at day 5 which would then decrease at day 15. However, regarding the SUnSET results, the opposite is observed. Nonetheless, only eIF4G1 isoform has been addressed and it may be that another one is involved in eIF4E binding in differentiating cells. In addition, one element remains unclear: the dual binding of both eIF4G and 4EBP1 to eIF4E at day 5 which is unexpected and unexplained along with the presence of a 135 kDa band which cannot correspond to another eIF4G1 isoform.

Surprisingly, the globally reduced activation of the mTORC1 complex in differentiating cells along the differentiation process, underlined by the reduced phosphorylation of mTOR on S2448 and of S6K1 phosphorylation, is not corroborated regarding the phosphorylated state of 4EBP1. Indeed, although the phosphorylated state of the protein is well reduced in the beginning of the process, confirming a reduced mTORC1 activity in the early steps of the process, the increased phosphorylation in the end of the differentiation process suggests an increased activity of mTORC1 toward 4EBP1. Therefore, it appears that mTORC1, which seemed to be the best candidate linking translational regulation and mitochondrial remodeling, may not regulate the eIF4E-4EBP1 axis in the same way than currently observed as it would maintain a constant pool of active 4EBP1 all along the differentiation process. However, this still does not help to explain the discrepancy between the CBA and SUnSET results discussed above.

Nevertheless, in order to complete the characterization of the eIF4E-4EBP1 axis regulation a last point had to be addressed: the subcellular localization of both eIF4E and 4EBP1 and eIF4E-specific export activity of mRNAs.

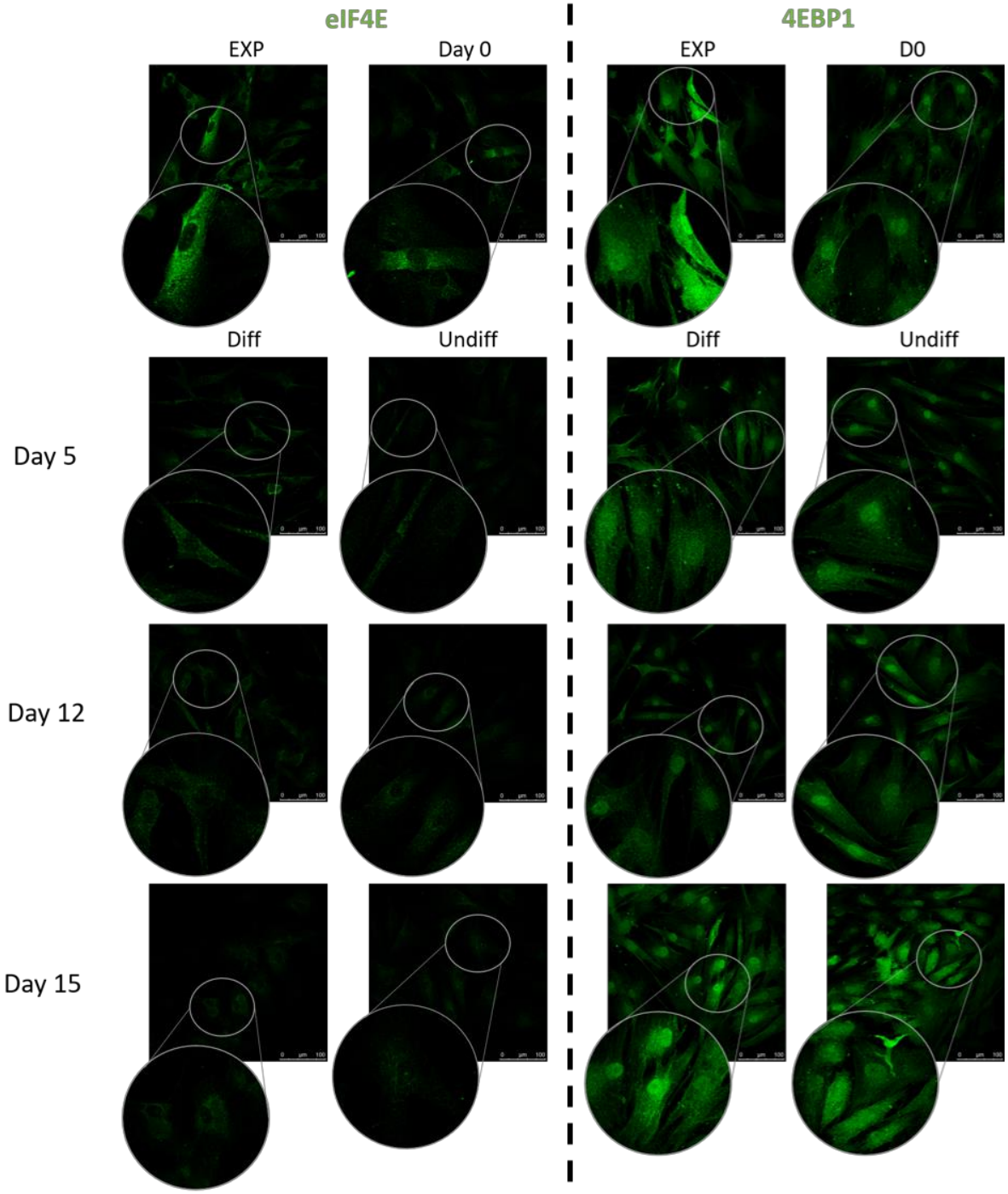

Figure 17. Subcellular localization of eIF4E and 4EBP1 during the differentiation process. Donor 1 cells underwent a differentiation process and Exp cells and Diff and Undiff cells at day 0, 5, 12 and 15 were collected, seeded on coverslips and fixed. A green immunofluorescence labelling was then performed on the different samples for eIF4E and 4EBP1. Scale bar = 100 µm. (n=1).

4. Subcellular localization of eIF4E and 4EBP1 and functional characterization of eIF4E export function

In order to address the question of a possible regulation of the eIF4E-4EBP1 axis with differential subcellular localizations of the two main actors, immunofluorescence analyses and cell fractionation followed by protein and RNA analyses were performed. The immunofluorescence experiment was performed on expanding cells and undifferentiated and differentiated cells at day 0, 5, 12 and 15. Concerning eIF4E localization, the protein was found both in the nucleus and in the cytosol, as previously described in other cellular models (**Figure 17**) (Culjkovic et al., 2005). The signal intensity for eIF4E in the differentiating and undifferentiated cells is really faint and does not allow to see any differences in the subcellular localization of the protein. In expanding cells, the strong signal for eIF4E is diffuse inside the cytosol whereas a similar but weaker signal is observed in cells at day 0. Regarding 4EBP1 distribution, the protein is also both found in the nucleus, to a larger extent than eIF4E, and in the cytosol in all conditions. A first observation is that the downregulation of 4EBP1 abundance in differentiating cells seems not clear at day 5 but is more visible at day 12. In addition, stronger overall signal of 4EBP1 in differentiating cells compared with their undifferentiated counterpart is observed at day 15, confirming the upregulation of 4EBP1 observed by Western Blot (**Figure 14**). The nuclear to cytoplasm ratio of 4EBP1 observed in expanding cells increases upon confluency (day 0) as more 4EBP1 seems to locate in the nucleus. Upon differentiation induction, 4EBP1 distribution is more diffuse in differentiating cells at day 5 while the nucleus to cytoplasm ratio observed in cells at day 0 is maintained in undifferentiated cells till day 15 where a more diffuse distribution is observed. At the opposite, the nuclear localization of 4EBP1 increases in cells at day 12 and this higher nucleus to cytoplasm ratio is maintained at day 15 with stronger overall signal of 4EBP1 (**Figure 17**). The negative control antibodies did not reveal any signal, validating these observations (**Supplementary figure 5**). The differentiation process occurred well as shown in **Supplementary figure 2**.

In order to biochemically confirm the cell distribution of eIF4E and 4EBP1 observed by immunofluorescence, nuclear and cytoplasmic fractionation was performed on expanding cells, differentiating and undifferentiated cells at day 0, 5 and 15. The day 12 could not be addressed due to lack of cells at this experiment time-point. First, the nuclear marker lamin A/C is predominantly detected in total fractions and nuclear fractions, where the abundance is enriched, and is detected to a lesser extent in the cytoplasmic fraction of differentiating cells at day 5 and 15, underlining nuclear to cytoplasmic contamination. This contamination may be due to an increased fragility and sensitivity of the differentiating cells to the hypotonic and thereafter lysis buffers used (associated with the typical elongated morphology of differentiating cells at these time-points), resulting in increased nuclei lysis. However, for the cytoplasmic marker, LDHA is only detected in the total and cytoplasmic fractions of all conditions and is barely detectable in nuclear fractions, indicating that the cytoplasmic to nuclear contamination is negligible (**Figure 18A**).

eIF4E distribution is also both nuclear and cytoplasmic, confirming the immunofluorescence results. In expanding cells, eIF4E signal appears to be weak in all fractions with a little enrichment in the cytoplasmic fraction while, in day 0, the protein seems equally enriched in both nuclear and cytoplasmic fractions. The difference in the nuclear localization of eIF4E in differentiating cells compared with undifferentiated ones is not that clear. Indeed, even if eIF4E seems more enriched in the cytoplasmic fraction in differentiating cells, the contamination of the cytoplasmic fraction by nuclear proteins makes this result difficult to interpret. In undifferentiated cells however, a slight enrichment of the nuclear form of eIF4E is observed at day 5 whereas equal distribution is observed at day 15.

Concerning 4EBP1 distribution, the protein is mostly found in cytoplasmic fractions, although some signal is also detected in the nuclear fractions, except for expanding cells (**Figure 18A**). Let's notice that this latter result is in contradiction with immunofluorescence data where the protein is

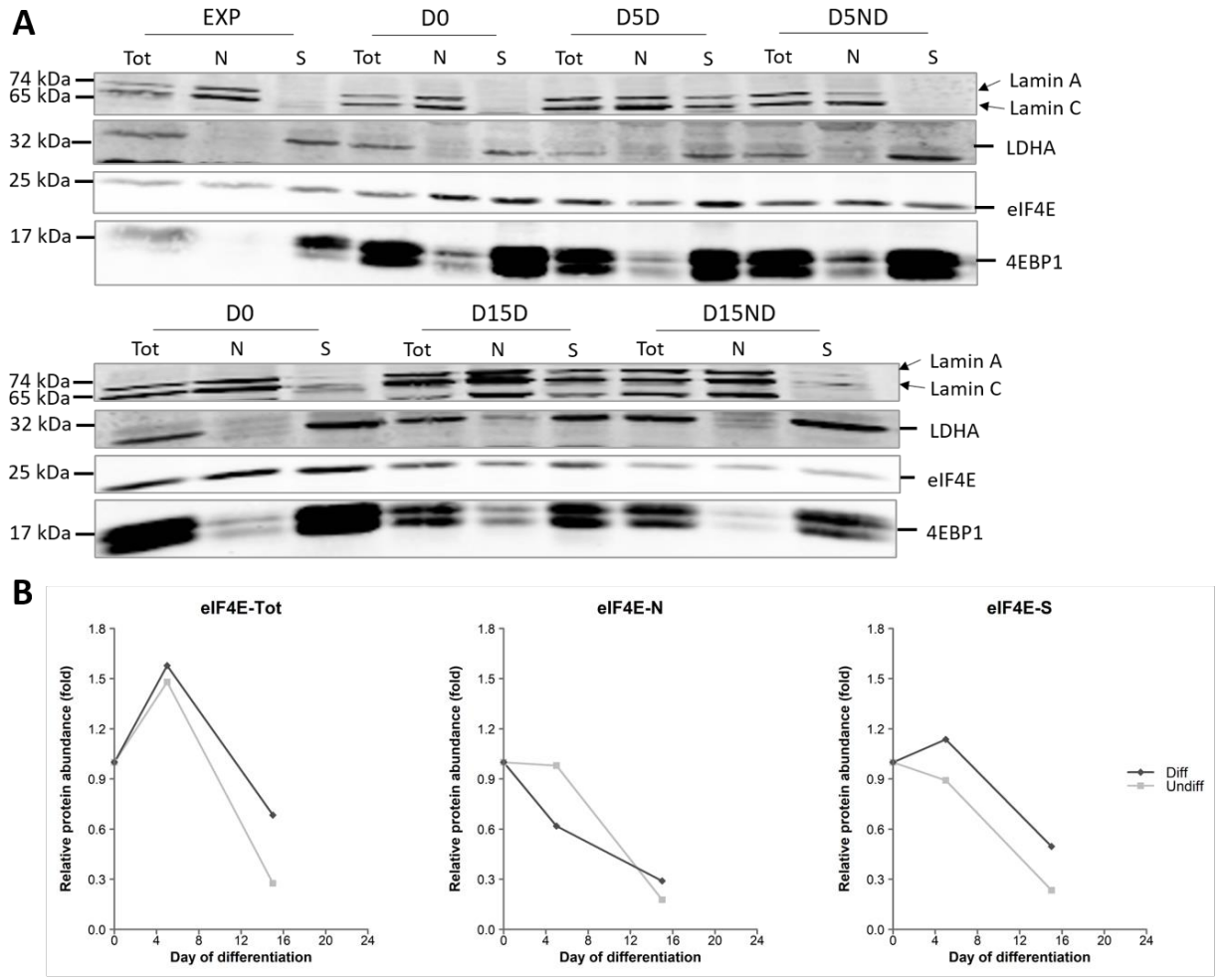

Figure 18. eIF4E and 4EBP1 distribution in subcellular fractions and functional assessment of eIF4E export activity. (A) Donor 3 cells in expansion and differentiating and undifferentiated cells at day 0 (D0), 5 (D5) and 15 (D15) of differentiation were fractionated and total (Tot), nuclear (N) and cytoplasmic (S) fractions were analyzed. After protein extraction on each sample, 10 µg of proteins were loaded on two 6-15% polyacrylamide gels. Lamin A/C, LDHA, eIF4E and 4E-BP1 were revealed. Lamin A/C corresponds to a nuclear marker and LDHA to a cytoplasmic marker, to assess fractionation quality. (B) Quantification of eIF4E signal intensity in the different fractions, presented in A, and expressed relatively to Day 0 signal. (n=1).

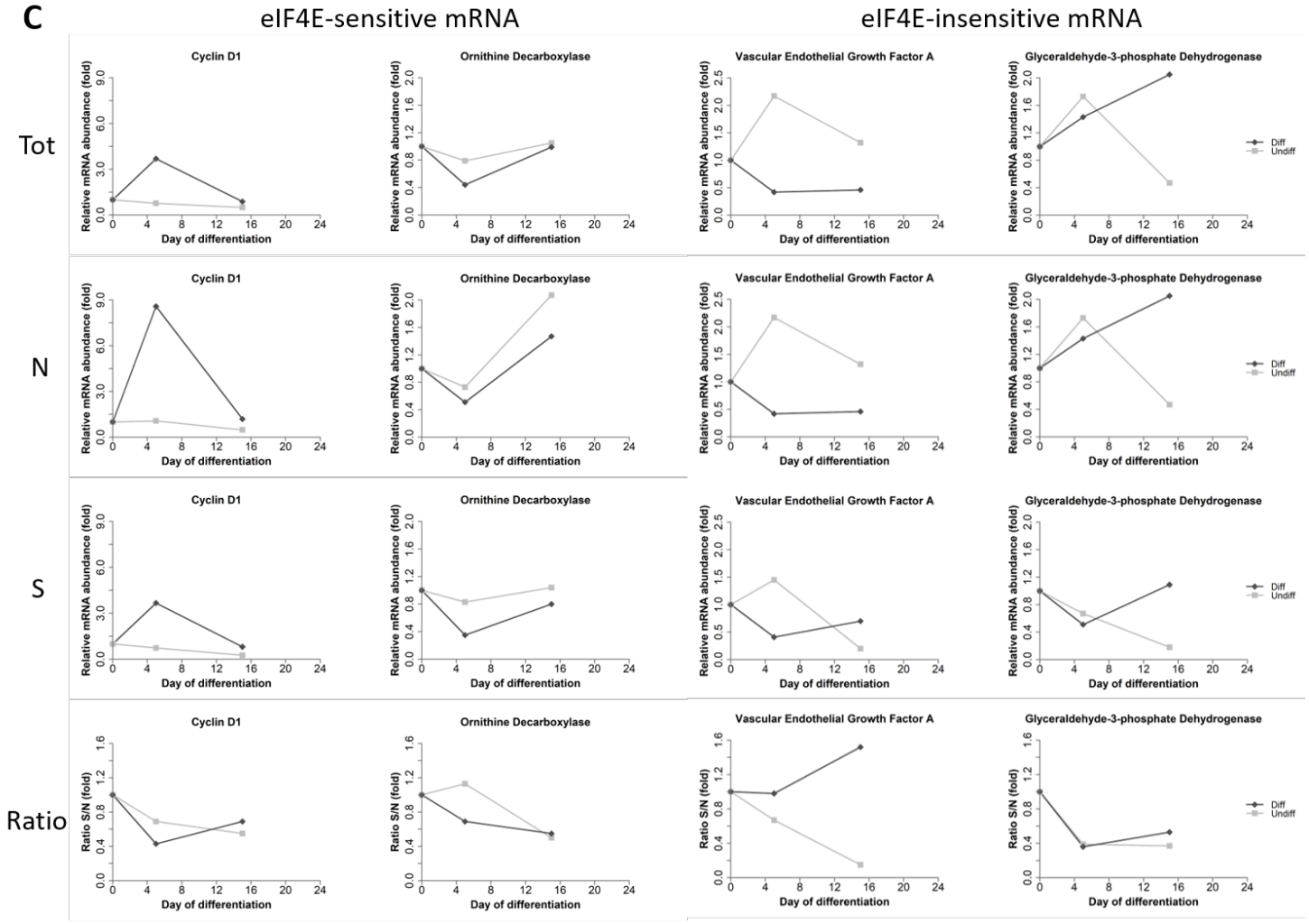

Figure 18 (following). eIF4E and 4EBP1 distribution in subcellular fractions and functional assessment of eIF4E export activity. (C) RNA extraction on each fraction was performed and the relative mRNA abundance of two eIF4E-export function-sensitive (*Cyclin D1* and *ODC*) and insensitive (*VEGFA* and *GAPDH*) transcripts was assessed using Real-Time PCR. mRNA abundance of each gene is normalized to *PPIE* (*Peptidyl-prolyl cis-trans isomerase E*) and then expressed relatively to day 0 ratio, for the Tot and N and S fractions. For the S/N ratio the normalized expression of each gene in S fraction is expressed relatively to its expression in N fraction.

found in the nucleus too (**Figure 17**). In day 0 cells, a stronger signal of nuclear 4EBP1 can be detected compared with expanding cells. Once again, due to cross-contamination, the difference in differentiating cells cannot be taken into account as most of the 4EBP1 signal is found in the cytoplasm fraction at both day 5 and 15 but where an unknown part of the signal probably accounts for the nuclear form of 4EBP1 (**Figure 18A**). Altogether these results globally corroborate with the immunofluorescence results.

In order to functionally characterize eIF4E export function, the abundance of two eIF4E target mRNAs (*Cyclin D1* and *ODC*) and of two negative controls (*Vascular endothelial growth factor A* (*VEGFA*) and *GAPDH*) in the different fractions was assessed and their cytoplasmic to nuclear ratio was obtained (**Figure 18B**). In addition, the eIF4E signal detected by Western Blot in the different fractions of all conditions has been quantified and represented in **Figure 18C**, in order to check if the eIF4E profile follows the subcellular profile of its target mRNAs. Globally, the general profile of eIF4E abundance, with an increase in total abundance at day 5 during the differentiation process, is similar between both conditions with nonetheless a stronger decrease in differentiating cells at day 5 in the nuclear fraction. The reverse profile is observed for *Cyclin D1* mRNA which is more abundant in the nucleus in differentiating cells at day 5 and yet another scenario is observed for *ODC* transcript distribution which is increasing from day 0 to day 15 in both differentiating and undifferentiated cells. Globally, all addressed mRNAs seem to be equally distributed between the two compartments with no specific enrichment of eIF4E-sensitive mRNAs in the cytoplasmic fraction compared with the nuclear fraction, suggesting an absence of modified eIF4E export function during the differentiation process. However, these results do only represent one experiment for both the immunofluorescence and the fractionation and thus need replication. In addition, the nuclear to cytoplasmic cross contamination issue observed in differentiating cells needs to be fixed and the experiment redone before drawing conclusions.

Altogether these results do not suggest a modification in the export activity of eIF4E during the differentiation nor a specific subcellular localization of 4EBP1 and eIF4E in differentiating compared to undifferentiated cells. Thus, the regulation of the eIF4E-4EBP1 axis does not seem to be the main driver of the putative translational regulation.

5. Undermining 4EBP1 transcriptional regulation

In order to understand and link external stimuli corresponding to the different cytokine cocktails used and 4EBP1 transcriptional profile, which is correlated at the protein level, the expression of several transcription factors was assessed. A first hypothetical model explaining 4EBP1 profile is presented in **Figure 19**. The initial downregulation of *4EBP1* could be associated with the FGF/HGF-dependent expression of the *early growth response 1* (*EGR1*) transcription factor, a known negative regulator of *4EBP1* expression (K. H. Lee et al., 2003; Raucci et al., 2004; Rolli-Derkinderen et al., 2003), and with the insulin-dependent degradation and cytosolic sequestration of forkhead box O1 (FOXO1) and FOXO3A, both known to induce *4EBP1* expression (**Figure 19A**) (Daitoku et al., 2011; Puig et al., 2003; Tzivion et al., 2011). Following exposure to the third cytokine cocktail where an upregulation of *4EBP1* expression and increased protein abundance is observed, the dexamethasone-induced expression of *REDD1* ensures the restoration of FOXO1/FOXO3A transcriptional activity leading to increased *4EBP1* expression (**Figure 19B**) (Dennis et al., 2014; DeYoung et al., 2008; Tzivion et al., 2011; H. Wang et al., 2006).

Therefore, in order to test this first hypothesis, the transcriptional profile of both *EGR1* and *REDD1* was assessed during the differentiation process (**Figure 19C**). *EGR1* expression appears to be extremely fluctuant during the differentiation process without any differences between differentiating and undifferentiated cells. Regarding *REDD1* expression, a significant increase in undifferentiated

cells is observed in the beginning of the process compared with differentiating cells which maintain lower level of expression till day 12 where a strong (6-fold) induction is observed following dexamethasone exposure, as expected. *REDD1* expression remains unchanged in undifferentiated cells after the 3-fold increase at day 2, with significantly reduced levels compared to differentiating cells at day 15, for which *REDD1* expression remains higher at day 22. Altogether, these two results do not support the potential involvement of EGR1 in *4EBP1* downregulation but they are consistent with a REDD1 potential role in the differentiation process, functional assessment of REDD1 activity being necessary for complete validation. Always in order to characterize the potential actor involved in *4EBP1* downregulation, the expression of the *Activating Transcription Factor 4* (*ATF4*), another inducer of *4EBP1* was assessed (**Figure 19C**) (Yamaguchi et al., 2008). A decrease in *ATF4* expression is observed in differentiating cells where significantly lower (at least at day 3) expression remains from day 3 to day 12. *ATF4* expression level then increases to reach similar levels than observed in undifferentiated cells. The transcriptional profile of *ATF4* thus somehow follows *4EBP1* profile with weaker amplitude and could therefore be involved in *4EBP1* down- and subsequent upregulation.

DISCUSSION

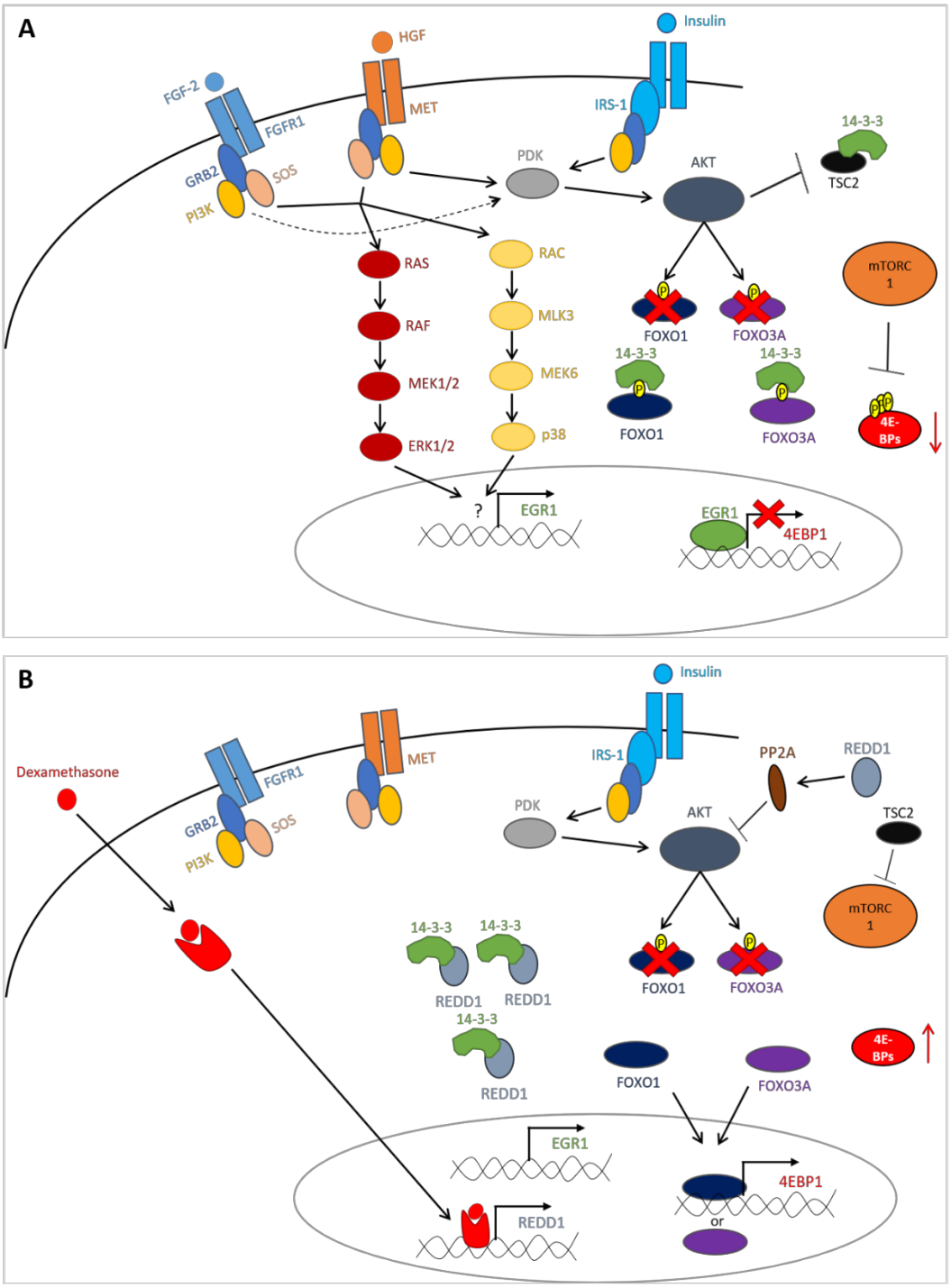

Figure 19. Proposed mechanistic hypothesis for 4EBP1 expression profile during the hepatogenic differentiation. (A) The second cytokine cocktail is composed of FGF-2, HGF, nicotinamide and ITS. Upon exposure to this cocktail, several signaling pathways can be activated. Indeed, both FGF2 and HGF are known to stimulate the ERK and p38 MAPK pathways (K. H. Lee et al., 2003; Raucci et al., 2004) leading to the expression of *EGR1* (the transcriptional factor inducing its expression being not known and thus represented by the "?" symbol). EGR1 was demonstrated to be a repressor of *4EBP1* expression, which could explain the observed downregulation from day 3 to day 12 (Rolli-Derkinderen et al., 2003). In the same time, the insulin induces PI3K pathway and thus AKT activation which is involved in TSC2 inhibition and consequent mTORC1 activation. Upon activation mTORC1 phosphorylates and inhibit 4EBP1 (Magner et al., 2013; Showkat et al., 2014). In addition, AKT can phosphorylate FOXO transcription factors, mainly FOXO1 and FOXO3A, promoting their ubiquitin-dependent degradation and additional sequestration by 14-3-3 proteins preventing their nuclear translocation and transcriptional activity (Daitoku et al., 2011; Tzivion et al., 2011). However, FOXO are known to induce *4EBP1* expression (Puig et al., 2003). (B) The third cytokine cocktail is composed of OSM, dexamethasone and ITS. The loss of MAPK stimulation would lead to the loss of EGR1-dependent *4EBP1* repression, restoring normal levels of 4EBP1. Dexamethasone is known to induce *REDD1* expression (H. Wang et al., 2006), which is involved in mTORC1 signaling repression thanks to the binding and subsequent sequestration of 14-3-3 proteins (DeYoung et al., 2008). Consequently to the 14-3-3 proteins sequestration, the FOXO, transcription factors are free to translocate into the nucleus and to induce *4EBP1* expression. In addition, REDD1 is known to promote PP2A activity and thus AKT partial inactivation, relieving mTORC1 inhibition and FOXO degradation (Dennis et al., 2014).

V.DISCUSSION

1. Hepatogenic differentiation model characterization

Differentiation efficiency is important to address and control each time a differentiation process is achieved because of the great variability existing between donor cells, even more important while using MSCs which represent highly heterogenous cell populations (Horwitz et al., 2005; Ullah et al., 2015). Indeed, it was described that in addition to the intra-individual heterogeneity of BM-MSCs population, inter-individual differences are observed concerning differentiation potential and growth kinetic with donor-dependent features where the sex, age and gender influence several features of BM-MSCs. For example, BM-MSCs derived from women are significantly smaller than man-derived BM-MSCs and show higher proliferative potential (Siegel et al., 2013). Regarding the variability in differentiation efficiency, it becomes clear that individual assessment of differentiation efficiency is necessary each time a differentiation process is achieved. Through visualization of the three independent differentiation processes presented in **Figure 12**, heterogeneity between donors is clearly apparent where the second donor (**Figure 12B**) shows, phenotypically and functionally, a higher differentiation efficiency with more polygonal-shaped cells at the end of the process associated with numerous PAS-positive cells.

The morphological changes observed during the differentiation process are the result of the action of cytokines found in the differentiation media. HGF, found in the second cytokine cocktail ensuring hepatic differentiation, is known to induce actin cytoskeleton rearrangement, in part through the regulation of Asef-IQGAP1 complex regulating the Cdc42-Rac1 complex controlling actin polymerization (Rodrigues et al., 2010; Tian et al., 2015). Similarly, hepatic maturation, ensured by the third cytokine cocktail, involves OSM, known to reorganize actin cytoskeleton through Protein Threonin Kinase 2 B (PTKB2)-Paxillin activity. In addition, the glycogen accumulation observed in differentiated cells is the result of the glycogen synthase activity whose expression and activity are both upregulated by the synergetic action of dexamethasone and insulin (Fleig et al., 1985; Huang et al., 2000).

The late induction of the major circulating serine protease inhibitor *α-1-antitrypsin* from day 12 onwards suggests an effect of the third cytokine cocktail containing OSM, described to induce its expression through signal transducer and activator of transcription 3 (STAT3) activity and binding to an OSM responsive element in a 3' enhancer of *α1AT* gene (Morgan et al., 2002). In addition, OSM is also described to induce the expression of *TDO2* (Teratani et al., 2005). Indeed, STAT3 would potentiate the transcriptional activity of HNF1α for the expression of liver specific transcripts such as *α1AT* but also *TDO2* (Leu et al., 2001). The *TDO2* transcript encodes for an enzyme involved in the early steps of the Kynurenine pathway and thus in tryptophan catabolism (Jones et al., 2013). The strong increase in differentiating cells, up to day 12, is expected but the brutal decrease is not explained. Nonetheless, the *TDO2* transcript levels remain higher in differentiating cells than in undifferentiated cells at the end of the process, supporting an efficient differentiation process. *TDO2* expression is essentially restricted to the liver and normally increases at the end of hepatogenic differentiation process and during hepatic maturation (Banas et al., 2007). Insulin signaling is also described to be involved in the induction of both *α1AT* and *TDO2* through induction of both *HNF1α* and *HNF4α*, two known master regulators of numerous hepatic genes (Magner et al., 2013). HGF, FGF and dexamethasone, mainly, are also upstream regulators controlling *HNF4* transcription factors expression (Michalopoulos et al., 2003).

The transcription factor TBX3 is a known regulator of several developmental processes such as limb formation, heart, liver and mammary gland development (Washkowitz et al., 2012; Weidgang et al., 2013). During embryonic development, TBX3 is first involved in the autoregulatory-loop leading to definitive endoderm formation through the Wnt-mediated enhancement of Nodal signaling

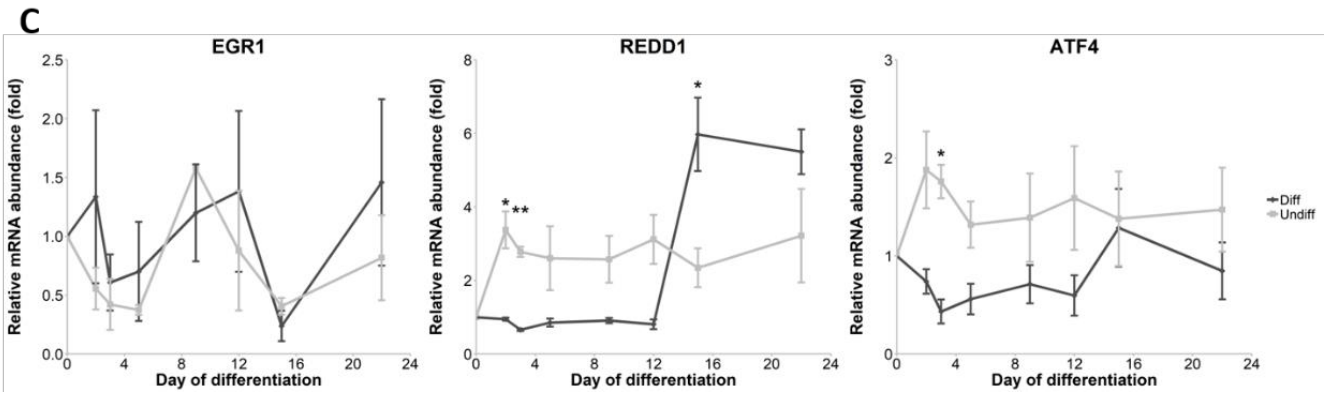

Figure 19 (following). Proposed mechanistic hypothesis for 4EBP1 expression profile during the hepatogenic differentiation. (C) Expression of *EGR1*, *REDD1* and *ATF4* in Diff and Undiff cells along the differentiation process, assessed by Real-Time PCR. mRNA abundance of each gene is normalized to PPIE (Peptidyl-prolyl cis-trans isomerase E) and then expressed relatively to day 0 ratio. Data are presented as mean ± SEM (n = 3). Unpaired two-tailed t-test were performed for each timepoint, comparing Diff with Undiff conditions.

(Weidgang et al., 2013). During liver development (**Figure 3**), TBX3 directs hepatocyte and cholangiocyte differentiation. It is thus expressed in hepatoblasts and disappear after lineage commitment (Gordillo et al., 2015) as it is illustrated by its increased expression during the hepatic differentiation step and subsequent reduced expression during hepatic maturation. In addition, TBX3 is a known downstream effector of both Wnt and FGF signaling (Washkowitz et al., 2012), the latter being present from day 2 to day 12, correlating with *TBX3* increased expression in differentiating cells. Thus, the used *in vitro* differentiation protocol does induce hepatic differentiation and subsequent maturation with the triggering of master regulators involved in cell fate commitment and cell differentiation at the appropriate time.

The significantly reduced *SOX9* expression in differentiated cells at the end of the process further confirms previous observations (Wanet et al., 2014) and confirms the occurrence of a differentiation process. *SOX9* is involved in the maintenance of the cells in an undifferentiated state (Kawaguchi, 2013). Its expression is indeed comparable between undifferentiated cells and expanding cells but also between differentiated and expanding cells, which is not expected. Despite the absence of significant differences between differentiated cells and expanding cells, previously described, a significant decrease is observed compared to day 0 showing reduced pluripotency compared to the cells just prior entry in differentiation program. This absence of significant difference between expanding cells and differentiated cells could be explained by the variability between donors for the EXP condition at least. In addition, *SOX9* is a master regulator of testis determination (Bhandari et al., 2012), marker of pancreas and liver (cholangiocytes) duct cells (Kawaguchi, 2013) and a marker of chondrogenic differentiation (Siegel et al., 2013), thus confirming the specificity of the used hepatogenic differentiation protocol. Interestingly, following results of the transcriptomic analysis performed on this model, the expression of the cholangiocyte marker *Keratin 7* (*KRT7*) is strongly downregulated at days 3 and 5 in differentiating cells compared with expanding and undifferentiated cells (**Table 1**), confirming, with *SOX9* downregulation, hepatic specification and underlying activity of TBX3.

Altogether these results confirm that a differentiation process was indeed initiated in the three donors, despite variability in differentiation efficiency due to donor-dependent responsiveness to the differentiation process. The used protocol mimics the molecular mechanisms observed during *in vivo* liver development with a first acquirement of hepatoblast-like cells directed to hepatocyte differentiation, followed by incomplete maturation.

Before addressing the question of translational regulation, we wanted to verify that a mitochondrial remodeling does occur during the differentiation process. The nuclear-encoded ATP5A and ATP5B abundance normally correlates with mitochondrial abundance and was described to increase during the differentiation process, associated with the mitochondrial remodeling (Wanet et al., 2014). Therefore, the results observed for ATP5A and ATP5B abundance with no differences between differentiating and undifferentiated cells were not expected. NDUFS6, a mitochondrial protein necessary for complex I assembly, is a known target translationally upregulated by mTORC1 (Morita et al., 2013; Stroud et al., 2016). Thus, the increase in NDUFS6 abundance but not in the abundance of the two other mitochondrial proteins, could underline that a translational regulation involving mTORC1 axis indeed occurs. Although no significant differences could be detected for NDUFS6 abundance between differentiating and undifferentiated cells, a consistent increase of NDUFS6 abundance is observed in differentiating cells in each donor cells, suggesting that the analysis of additional replicates would probably allow to reach significance.

In addition, the analysis of mtDNA content, used as a marker of mitochondria biomass, reveals an increase in differentiating cells, although this increase does not occur at the same time-point for the two donors, highlighting donor-dependent variability. The correlated increase observed in mtDNA and NDUFS6 abundance strengthen the hypothesis of mTORC1 activity, known to ensure mitochondrial biogenesis through the regulation of 4EBP1 activity. mTORC1 indeed promotes mitochondrial global translation and selective translation of some nuclear-encoded mitochondrial

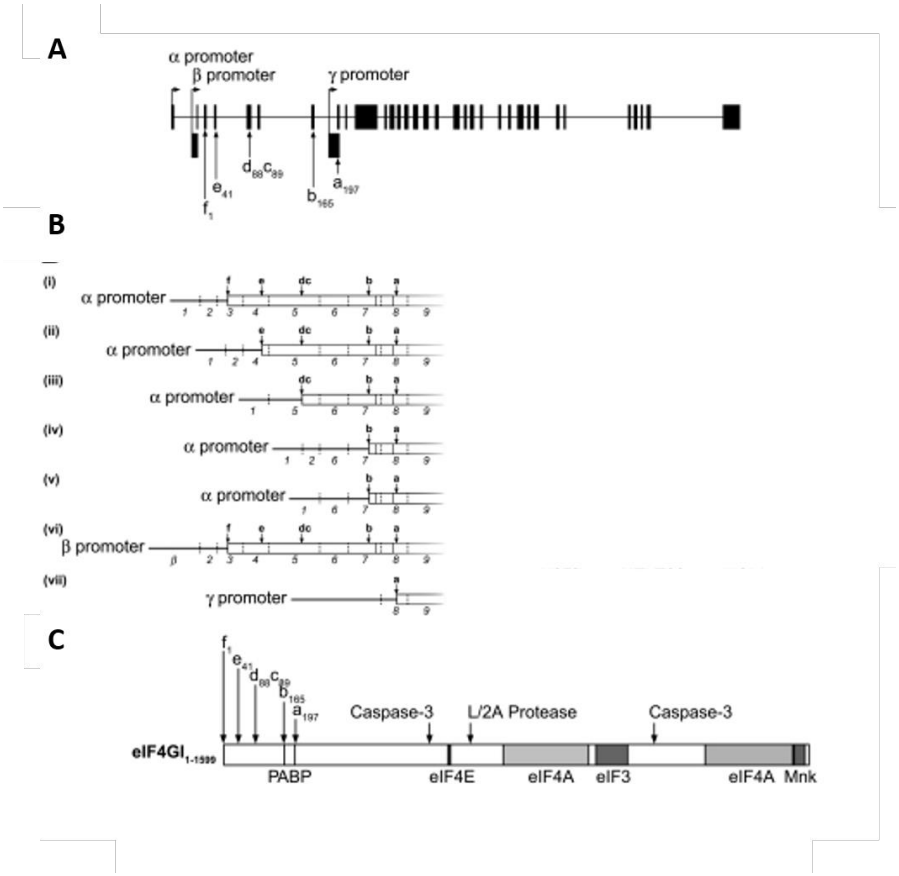

Figure 20. *eIF4GI* encodes different isoforms (adapted from, Coldwell & Morley, 2006). (A) Diagrammatic representation of the *eIF4GI* gene locus, showing the locations of the three promoters, designated α, β, and γ. Coding exons are shown in gray, and noncoding exons are shown in black. (B) Diagrammatic representation of the *eIF4GI* mRNAs showing alternative splice variants generated from the different promoters. (C) Schematic representation of the eIF4G1 protein. This figure shows the sites of alternative translation initiation, binding sites of other components of the translation initiation machinery. The site of cleavage by the picornaviral (L/2A) protease is indicated (Coldwell & Morley, 2006).

transcripts like NDUFS6 (Morita et al., 2013, reviewed in, Morita et al., 2015). In addition, mTORC1 would also promotes mtDNA replication as the inhibition of its activity results in a 40% decrease of mtDNA content in MEF (Morita et al., 2013). The putative involvement of mTORC1 in the regulation of the eIF4E-4EBP1 axis during the hepatogenic differentiation process is further supported by the strong upregulation of *PPARγ* in the early stages of the process (**Table 1**), as mTORC1 has been described to drive adipogenesis through the induction of *PPARγ* (H. H. Zhang et al., 2009). Moreover, mTOR-dependent 4E-BP1 hyperphosphorylation is involved in the increased protein synthesis associated with murine embryonic stem cell differentiation (Sampath et al., 2008). Interestingly, insulin, contained in the second and third cytokine cocktails, is a known activator of PI3K-mTORC1 pathway and could explain a potential activation of this pathway leading to mitochondrial biogenesis (Roux & Topisirovic, 2012; Showkat et al., 2014).

Altogether, these results globally support that a mitochondrial remodeling occurs during the differentiation process, as it has been previously characterized in this model of hepatogenic differentiation (Wanet et al., 2014). Indeed, despite variability between donors, the increased abundance of some mitochondrial proteins (NDUFS6 mainly) and of mtDNA content confirm a mitochondrial biogenesis. The question of the involvement of a translational regulation as part of the mitochondrial remodeling regulation can thus be addressed as the increase in NDUFS6 abundance suggests mTORC1 involvement.

2. Variable activity of the eIF4F complex regulating global protein synthesis

a) eIF4G

In order to characterize a putative translational regulation, the abundance of several eIF4F components and actors of the eIF4E-4EBP1 axis has been first addressed. Regarding the abundance of the scaffold protein eIF4G1, its decreased abundance in differentiating cells would suggest a reduced canonical cap-dependent translation as less eIF4G1 molecules are available for eIF4E association, whose abundance is maintained constant during the differentiation. However, three different isoforms of eIF4G exist, eIF4G1 being the most studied and the sole isoform investigated in this work (Bradley et al., 2002). Additionally, several short isoforms of eIF4G1 exist, as illustrated in **Figure 20** (Bradley et al., 2002; Coldwell & Morley, 2006; Jackson et al., 2010). Indeed, through the activity of three different promoters (α, β and γ), alternative splicing and alternative translation initiation sites, the eIF4GI gene encodes seven different eIF4G1 transcripts (Byrd et al., 2002; Coldwell & Morley, 2006). Five transcripts are produced through alternative splicing from the α promoter whereas two others are produced by the β and γ promoters activity. The transcripts deriving from the α and β promoters ensure the production of five polypeptides showing different N-terminal sequence length but presenting similar translational activity, with higher potency for the longest form. The two longer isoforms are the most abundant ones in human and can be observed on **Figure 14A** for some experimental conditions but not for all of them because of poor resolution. A sixth and shorter polypeptide is produced by the γ promoter and show differential activity due to the absence of the PABP binding domain in its N-terminal domain, reducing its ability to promote efficient translation initiation (Coldwell & Morley, 2006). An additional layer of regulation for *eIF4G1* expression corresponds to the presence of IRES in the transcript and of one uORF in the 5'UTR of the transcript, reducing the translation of the downstream ORF (Byrd et al., 2002). Thus, *eIF4G1* expression control shows a complex regulation at both the transcriptional and translational levels. Additionally, a cleaved form of eIF4G1, called p100 and resulting from viral proteinase activity, is also able to ensure translation even if unable to bind to eIF4E. Indeed, p100 is known to specifically ensure the translation of a subset of mRNAs by delivering the 40S ribosomal subunit to the 5'UTR of these mRNAs (Ali et al., 2001). Caspase activity can also result in the subsequent cleavage of

eIF4G1 leading to the formation of shorter fragments lacking PABP binding domain but still able to bind to eIF4E, therefore acting as translational inhibitors (Marissen et al., 2000; Marissen & Lloyd, 1998).

Two other eIF4G isoforms also exist and could be involved in translation initiation during the differentiation process. The ubiquitous isoform eIF4G2 (also known as Death Associated Protein 5 (DAP5), NAT1 or p97) could be a good candidate as it is known to be involved in the translational regulation driving megakaryocyte differentiation, this isoform being selectively recruited for eIF4F complex assembly in the early stage of the differentiation process (Caron et al., 2004). This specific recruitment of eIF4G2 follows thrombopoietin signaling and leads to eIF4E S209 phosphorylation by the associated MNK1 (Caron et al., 2004; Jackson et al., 2010). In addition, ERK 1/2 and p38 MAPK pathways synergic activation is necessary to achieve this phosphorylation associated with reduced eIF4E-4EBP1 association and thus increased protein synthesis (Caron et al., 2004). Interestingly, no modifications of *eIF4G1* and *eIF4G2* expression is observed with this selective association of eIF4G2 with eIF4E, as observed in our case (**Table 1**). Nonetheless, eIF4G2 doesn't contain an eIF4E binding domain as well as a PABP binding domain while containing a MNK1, eIF4A and eIF3 interacting domains. It has been first proposed to act as a negative regulator of the eIF4F complex assembly, which can bind eIF4A and eIF3 and could sequester MNK1 and the 43S complex, preventing eIF4E-dependent cap translation (Pyronnet et al., 1999). Indeed, eIF4G2 seems to essentially ensure cap-independent translation with the specific translation of IRES-containing mRNA, in association with eIF2β and eIF4A1 (Liberman et al., 2015). Among the targeted mRNA, the anti-apoptotic protein *Bcl2* was the first specific eIF4G2-target described. Among other targets, the scaffold protein also ensures its own IRES-dependent translation, providing an auto-regulatory loop supporting continuous cap-independent translation in contexts of impaired cap-dependent translation (Liberman et al., 2015; Yoffe et al., 2016). Given this and the results obtained by Caron et al., where a specific pull-down of eIF4E and subsequent revelation of eIF4G2 revealed the association of these two proteins, the question of a potential indirect interaction between eIF4E and eIF4G2 is the more probable hypothesis and still need to be addressed.

Finally, the third eIF4G paralog, eIF4G3, is less known and has been described, in mouse, to be involved in the translational regulation of the chaperone HSPA2 necessary for cyclin-dependent kinase 1 (CDK1) activity involved in meiotic prophase regulation. This isoform would ensure translational regulation in testis necessary for spermatogenesis and its deficiency is linked to male infertility in mouse (Sun et al., 2010). Although eIF4G3 isoform is less relevant in our case, eIF4G2 is a good candidate for a possible involvement in the putative and suspected translational regulation occurring during this model of differentiation.

b) 4EBP1

The mRNA and protein levels of 4EBP1, the main regulator of the eIF4F complex, were addressed. The robust downregulation of *4EBP1* expression, in differentiating compared with undifferentiated cells, initially revealed by the transcriptomic analysis performed in the early stage of the differentiation process (**Table 1**), was confirmed by qPCR analysis, despite the absence of significant differences (**Figure 14A**). This decreased expression is verified at the protein level and thus could suggest a decrease in 4EBP1 binding activity and relieve of the eIF4F complex repression, supporting increased cap-dependent translation. Further on, the upregulation of 4EBP1 observed during the hepatic maturation step, suggests that the reverse phenomenon happens in the end of the differentiation process. Due to its role in translational regulation and promotion of mitochondrial and ribosomal-associated transcript translation (Morita et al., 2013; Tahmasebi et al., 2016), the putative involvement of the eIF4E-4EBP1 axis in the mitochondrial remodeling is supported by this data. In addition, 4EBP1 is also involved in the control of YY2 specific translation, ensuring pluripotency markers expression repression and involved in the upregulation of several mitochondrial genes (Tahmasebi et al., 2016). Thus, regarding the involvement of the eIF4E-4EBP1 axis in the

translational control of the balance between stemness maintenance and differentiation on one hand and in the control of mitochondria abundance and activity on the other hand, it would not be surprising to find an involvement of this axis in the mitochondrial remodeling occurring during this differentiation process.

The unchanged abundance of eIF4E, correlated with the fluctuant profile of 4EBP1, supports an early increase in cap-dependent translation during the first steps of the differentiation process while the opposite interpretation can be drawn for the end of the process with reduced eIF4F complex assembly and thus translation. However, before drawing any conclusions, the functional regulation of the eIF4E-4EBP1 axis by post-translational modifications needed to be addressed.

3. Another purpose for the mTORC1-dependent regulation of the eIF4E-4EBP1 axis

The unchanged phosphorylated state of eIF4E all along the differentiation process, despite a decrease in eIF4G1 abundance is unexpected since eIF4G1 is necessary for the recruitment of MNK1 responsible for the phosphorylation of the eIF4E bound to the same eIF4G1 molecule (Jackson et al., 2010; Pyronnet et al., 1999). However, the two other eIF4G1 isoforms, namely eIF4G2 and eIF4G3, also possess an MNK1 binding domain and could thus ensure MNK1-dependent phosphorylation of eIF4E on S209 (Pyronnet et al., 1999). Whereas, eIF4G3 is a functional homolog of eIF4G1 able to ensure cap-dependent translation in case of viral- dependent cleavage of eIF4G1 (Gradi et al., 1998), eIF4G2 does not directly bind eIF4E and would thus not be involved in its phosphorylation (Pyronnet et al., 1999). However, as discussed above, a yet unidentified intermediate interactor could be involved in the bridge between eIF4E and eIF4G2, thereby ensuring MNK1-dependent eIF4E phosphorylation (Caron et al., 2004). As a consequence, the maintained phosphorylation state of eIF4E suggests a maintained translational function as it is required for UBC9-dependent sumoylation and enhancement of eIF4E binding to eIF4G, at the expense of 4EBP1 binding (Xu et al., 2010). However, the cap-binding assay (**Figure 16A**) reveals that eIF4E association with 4EBP1 is not decreased in differentiating cells, and is even slightly increased, which suggests reduced eIF4F complex assembly. However, the question of a potential eIF4G3 binding could be addressed to check if the eIF4F complex assembly is maintained, in agreement with only slight differences in global protein synthesis rate observed in differentiating cells all along the process.

Nonetheless, S209 phosphorylation is also associated with increased eIF4E affinity for the cap-moiety, in synergy with Chip-dependent mono-ubiquitination of eIF4E on the K159 residue. This mono-ubiquitination is involved in the proteasome-dependent degradation of eIF4E which is reduced upon 4EBP1 binding to eIF4E. This would suggest that 4EBP1 binding could protect eIF4E from degradation and could remain associated in ternary complexes with eIF4E and bound mRNAs under low levels of mTOR-induced phosphorylation an inhibition of 4EBP1 (Murata & Shimotohno, 2006), as observed in differentiating cells during the first part of the differentiation process. This poised translational status of the cells allows for a rapid increase in translation upon increased phosphorylation of 4EBP1, as observed during the hepatic maturation step, where the eIF4E-bound mRNAs can be rapidly translated. Due to their mTORC1-sensitivity, TOP-containing mRNAs, such as several mitochondrial transcripts, would be the first translated through the targeted and spatially restricted 4EBP1 phosphorylation, targeting 4EBP1 removal from these eIF4E-associated TOP mRNAs (Hong et al., 2017). However, in order to confirm this hypothesis, the maintenance and increased assembly of the eIF4F complex at the end of the process, when increased phosphorylation of 4EBP1 is observed, should first be verified by addressing the question of eIF4G3 binding to eIF4E.

As mentioned, a reduced phosphorylation of 4EBP1 is observed during the hepatic differentiation step suggesting a reduced activity of mTORC1 during the first part of the differentiation process (Showkat et al., 2014). However, in order to assess total mTORC1 activity the phosphorylation levels of both its targets has to be addressed (Carnevalli et al., 2010). Thus, in order to evaluate mTORC1

total activity, both the proportion of the phosphorylated form of its two main targets (S6K and 4EBP1) and the total phosphorylation of mTOR on S2448, associated with active mTORC1-containing mTOR, were addressed (**Figure 15**). Considering all three parameters, mTORC1 total activity seems to be globally reduced in differentiating cells during the first part of the differentiation process with the reduced phosphorylation of mTOR on S2448 correlating with reduced phosphorylation of its downstream targets. In addition, a reduced abundance of both targets is also observed in differentiating cells compared with undifferentiated cells, resulting, for S6K1, in a constant proportion of phosphorylated S6K1 (similar and constant phosphorylated/total form ratio between the two experimental conditions) all along the differentiation process.

Regarding mTORC1 activity toward 4EBP1, we hypothesize that the modification of 4EBP1 abundance is compensated by modifications in the phosphorylated fraction of this protein to maintain a constant number of active 4EBP1 molecules (i.e. a constant number of unphosphorylated 4EBP1 molecules) in differentiating cells. In order to maintain this constant pool of active 4EBP1, mTORC1 activity is reduced in the beginning of the process characterized by a low 4EBP1 abundance. Afterwards, the upregulation in 4EBP1 abundance requires an increased activity of mTORC1 to phosphorylate much more 4EBP1 molecules in order to maintain similar levels of active 4EBP1. Thus, together with the constant level of eIF4E during the differentiation process, this would suggest constant level of eIF4E-bound 4EBP1 complexes in differentiating cells all along the differentiation process, which is confirmed by the CBA (**Figure 16A**). Similarly, in undifferentiated cells, the abundance and phosphorylated state of 4EBP1 is maintained with a constant activation of mTORC1 leading to reduced levels of 4EBP1 bound to eIF4E compared with differentiating cells (**Figure 16A**). According to this hypothesis, this precise number of active 4EBP1 would ensure a fine tuning of the eIF4F complex assembly.

Altogether these results support a reduced activity of mTORC1 in differentiating cells, mainly in the beginning of the process. This was unexpected regarding the specific increased abundance, already in the beginning of the process, of the mitochondrial protein NDUFS6, one of the translationally upregulated targets of mTORC1 and the known role of mTORC1 connecting mitochondria biogenesis and translational regulation (Morita et al., 2013). Indeed, despite a low increase in mTORC1 activity toward 4EBP1 at the end of the process, the maintained binding of 4EBP1 to eIF4E and the absence of a clear difference in relative protein synthesis between differentiating and undifferentiated cells does not support a clear involvement of the mTORC1-eIF4E-4EBP1 axis in a putative translational regulation supporting the mitochondrial remodeling observed during the differentiation process.

Nonetheless, one major point remains unexplained. Regarding relative protein synthesis, while the main driver of protein synthesis in undifferentiated cells can be easily explained by the mTORC1-dependent phosphorylation of 4EBP1 and subsequent reduced binding of 4EBP1 to eIF4E which allows eIF4G binding and eIF4F complex formation, one question remains for differentiating cells: why is there a maintained translational rate in those cells where a constant inhibition of the eIF4F complex assembly seems to occur, suggesting a complete shutdown of translation during the differentiation process (**Figure 16**)? In addition, the dual association of eIF4E with both eIF4G and 4EBP1 in differentiating cells at day 5 is unexpected and would suggest a normally higher translational rate compared with these cells at day 15, where only 4EBP1 is detected in association with eIF4E at the expense of eIF4G, which abundance is additionally reduced. However, the opposite is observed.

A first explanation would be that the eIF4F complex could be formed by another isoform of eIF4G such as eIF4G3, as discussed previously. In addition, cleaved forms of eIF4G1, by viral proteinase but also by caspases can generate either translationally functional or inhibitory fragments of eIF4G1 (reviewed in, Prévôt et al., 2003) and this could correspond to the unidentified 135 kDa band pulled-down with eIF4E and observed in differentiating cells at day 5 and 15 (**Figure 16A**). Although no viral infections are supposed to have occurred in these cells and no sign of apoptosis is observed during

the differentiation process, preliminary data suggested a potential activation of caspase 3 in differentiating cells at day 5 compared with undifferentiated cells for which no such activation was observed (Wanet et al., 2017). The eIF4G1 fragments generated by caspase 3 present, for the longest of them, a size of 120 kDa (Marissen & Lloyd, 1998) which could then correspond to the uncharacterized band. Additionally, these fragments prevent translation initiation since they bind eIF4E but do not contain a PABP binding domain preventing eIF4F complex assembly (Marissen et al., 2000; Marissen & Lloyd, 1998).

Another hypothesis to explain these discrepancies could be that the eIF4E-4EBP1 axis would be regulated at the level of subcellular localization of both actors, targeting the export activity of eIF4E. However, following the immunofluorescence and fractionation results, it does not seem that this axis is specifically regulated in this case, as the export of two eIF4E-sensitive mRNAs does not seem to be modified in differentiating cells over the time and compared with undifferentiated cells. In addition, no clear differences in eIF4E and 4EBP1 localization can be observed between the two conditions: an increase in eIF4E and 4EBP1 nuclear localization is observed in both conditions upon confluency reaching (already at day 0), compared with expanding cells. This could be explained by the fact that expanding cells are actively dividing compared with confluent cells and thus present a higher protein synthesis rate, as observed in the SUnSET experiment, and thus eIF4E is more associated with the translational machinery in the cytoplasm and 4EBP1 is more inhibited, supported by the increased mTORC1 signaling observed in expanding cells. Although additional replicates are necessary to confirm these results as well as more functional assessment of eIF4E export activity, the regulation of the localization of both eIF4E and 4EBP1 would not be the main driver of eIF4E-4EBP1 axis regulation and can't help to explain by itself the unexpected results obtained so far. One way to more functionally address eIF4E function would be to assess its binding activity to target mRNAs in the nucleus of differentiating cells and during the differentiation, using RNA immunoprecipitation and subsequent RNA sequencing.

Still another hypothesis could involve the eIF2α axis as the main driver of the putative translational regulation, well-known to ensure translation initiation repression in case of several stresses (Holcik & Sonenberg, 2005). In addition this regulatory axis was one of the main candidate shown to be strongly and robustly downregulated following the transcriptomic analysis performed in the early stage of the differentiation process (Wanet et al., 2017). However, according to preliminary data, it does not appear that this axis plays a specific role in translation initiation regulation during the differentiation process (unshown data).

The last and most relevant hypothesis to our opinion would concern a transition, in differentiating cells, in the mode of translation. Indeed, upon differentiation induction, cells would change from a cap-dependent translation to a cap-independent and IRES-based translation. A first argument for this hypothesis, already mentioned, concerns the eIF4G2-dependent translational regulation observed during megakaryocyte differentiation (Caron et al., 2004). As explained before, eIF4G2 is preferentially recruited to eIF4E and would ensure its phosphorylation and enhancement of translation. However, subsequent studies showed that this isoform of eIF4G strictly ensures IRES-based translation in a rabbit reticulocyte lysate (Liberman et al., 2015). Interestingly, another experiment showed the requirement of IRES-dependent translation in megakaryocyte differentiation (Grech & von Lindern, 2012). This could suggest that the essential role of eIF4G2 during megakaryocyte differentiation determined by Caron et al. could be due in part to its IRES-based translational function in addition to a potential but not essential role in eIF4E-phosphorylation, but this needs experimental confirmation. In addition, eIF4G2 requires eIF2β and eIF4A1 association to further ensure its cap-independent translation where active helicase activity of eIF4A1 is required (Liberman et al., 2015).

Another argument comes from *in vivo* experiments: late gestational fetal rat hepatocytes are resistant to rapamycin treatment, whereas adult counterparts are sensitive to that treatment (Boylan et al., 2015; Gruppuso et al., 2008). Hepatocyte maturation would thus not be affected by mTORC1 signaling, which is supported by the absence of modification in the distribution of TOP-containing

mRNAs in the polysomal fraction upon mTORC1 inhibition by rapamycin in fetal hepatocytes (Gruppuso et al., 2008). Although the mechanism underlying this rapamycin resistance remains to be elucidated, it could depend on a specific modification of the eIF4F complex as eIF4A1 is highly abundant in polysomal fractions (Boylan et al., 2015; Gruppuso et al., 2008). Thus, this rapamycin resistance in fetal hepatocyte might be due to an eIF4G2-dependent/cap-independent translation (Boylan et al., 2015; Gruppuso et al., 2008).

Last but not least, a recent study showed the involvement of eIF4G2 in the differentiation regulation and priming of hESCs through the eIF4G2-based cap-independent translational regulation of pluripotency markers and mitochondrial transcripts (Yoffe et al., 2016). The previously shown lethality of eIF4G2 depletion in mouse would be explained by its essential role in the control of hESC differentiation which is impaired upon eIF4G2 depletion. The scaffold protein ensures the translational downregulation of pluripotency markers such as Nanog or Oct4 and promotes the translation of differentiation markers in response to extracellular stimuli. In addition, and most importantly, the differentiation impairment observed in hESC depleted from eIF4G2 would be due to impaired mitochondrial remodeling required for the metabolic transition naturally occurring upon ESC differentiation. Indeed, the loss of eIF4G2, which does not affect the translation of TOP-containing mRNA in MEF (Thoreen et al., 2012), leads to a shift of several mitochondrial transcripts (assembly factors, OXPHOS components,…) and translation-related transcripts (essentially ribosomal proteins) from polysomes to monosomes (Yoffe et al., 2016). Therefore, the role of eIF4G2 in the hepatogenic differentiation should be addressed regarding its essential developmental role and putative role in fetal hepatocytes.

Regarding the results presented here, a transition from a cap-dependent to cap-independent translation in differentiating cells could correlate with a decreased mTORC1 signaling which is no more necessary to support protein synthesis but would mainly control and maintain a constant level of active 4EBP1. This fine-tuning of eIF4F complex formation, based on the association of eIF4E with another scaffold protein, such as eIF4G3, could be necessary to prevent the sequestration of eIF3 and eIF4A1 by these eIF4F complex, therefore promoting the maintenance of their association with eIF4G2, ensuring the cap-independent translation of mitochondrial transcripts, among others. In addition, a caspase 3-dependent generation of cleaved inhibitory fragment of eIF4G1 could also be involved in the required eIF4F complex assembly inhibition. Nonetheless, the constant phosphorylation of eIF4E and the increased global protein synthesis observed in the differentiating cells during the hepatocyte maturation step could highlight a possible maintained formation of eIF4F complexes with an increase in their assembly at the end of the process. In order to address this question, cap-binding assays and revelation of eIF4G3 all along the differentiation process should be performed. To further check if a constant number of unphosphorylated 4EBP1 is indeed required to fine tune the differentiation process and check if thus mTORC1 activity is essential for the differentiation, 4EBP1 point mutation with replacement of mTORC1 target amino acid (mainly T37/46) by alanine could be done, rendering these mutants resistant to mTORC1-directed phosphorylation.

Nonetheless, the transition from a cap-dependent to cap-independent translation would result in specific modifications of the translatome whereas to functionally address such translational regulation, polysome-enriched transcripts in differentiating cells compared with undifferentiated ones should be analyzed using different unbiaised methods. Polysome profiling on the early stage of the hepatogenic differentiation is under investigation in the lab and will characterize the existence of the putative translational regulation of the mitochondrial remodeling. Other high-throughput methods could be performed in order to functionally characterize the cell translatome such as ribosome profiling or even puromycin-associated nascent chain proteomics (PUNCH-P) to have a protein resolution level (Aviner et al., 2014).

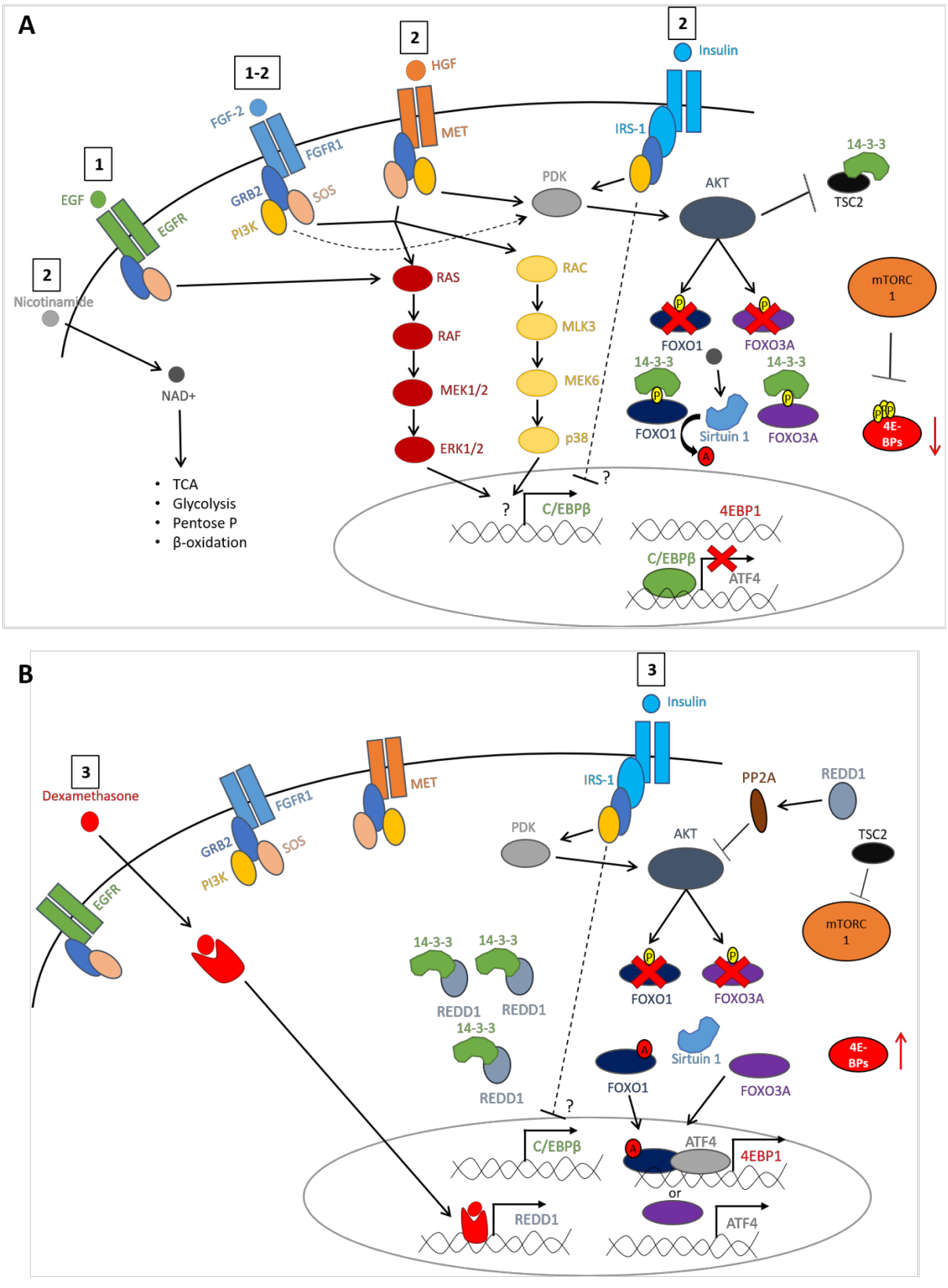

Figure 21. Proposed model for 4EBP1 transcriptional regulation. (A) Upon exposure to the first and second cytokine cocktails (the cytokines are numerated following their presence in the first (1), second (2) or third (3) cocktail), the same actors as those involved in the first hypothesis (**Figure**) are maintained with the sole difference concerning the downstream effector of the p38 and ERK MAPK pathways leading to the induction of C/EBPβ, a repressor of *ATF4* which normally drives *4EBP1* expression. Additionally, the EGFR activation due to EGF exposure, present in the first cytokine cocktail, also targets MAPK activation. Nicotinamide is converted into NAD^+ in the cells, promoting Sirtuin 1 activity which targets the deacetylation of FOXO1, associated with reduced transcriptional activity. (B) Following exposure to the third cytokine cocktail, the MAPK-dependent induction of C/EBPβ is lost, while the repressive signaling of insulin remains, leading to *ATF4* expression which, together with FOXO signaling, induces *4EBP1* expression.

4. Literature-driven model of 4EBP1 transcriptional regulation

In another context, the putative transcriptional network controlling *4EBP1* expression led to a first hypothesis was explored, and depicted in **Figure 19**. Although the experimental results obtained for *REDD1* expression are in accordance with the hypothesis explaining *4EBP1* upregulation, those obtained for *EGR1* expression did not confirm the proposed hypothesis for the downregulation of *4EBP1*. Therefore, we propose a second hypothesis with ATF4 as one of the transcription factors involved in the control of *4EBP1* profile during the differentiation (**Figure 21**). This transcription factor induces several genes involved in amino acid and nucleotide synthesis, among others. ATF4 is also an inducer of *4EBP1* expression under endoplasmic reticulum stress (Yamaguchi et al., 2008). Interestingly, *ATF4* expression is itself repressed by the hepatic transcription factor C/EBPβ (Dey et al., 2012), which expression is induced by EGF (Li et al., 2014), FGF-1 (Rajesh Raju et al., 2014) and HGF (Shen et al., 1997). At the opposite, the insulin repress *C/EBPβ* expression (Bosch et al., 1995). Thus, following the exposure to the first and second cytokine cocktails, *ATF4* expression is globally repressed by C/EBPβ (**Figure 21A**), while the absence of these inducers in the third cytokine cocktail but not of insulin, which represses C/EBPβ, leads to the repression of C/EBPβ and consequent restoration of *ATF4* expression (**Figure 21B**). The experimental data shows that *ATF4* expression does follow *4EBP1* expression and thus corroborates the proposed model. Additionally, *4E-BP1* expression is also induced by HIF1α (Azar et al., 2013), a transcription factor strongly downregulated in the differentiation process (**Table 1**) and a potent candidate linking mitochondrial remodeling and hepatogenic differentiation (Wanet et al., 2017).

In addition, the nicotinamide found in the second cytokine cocktail leads to the final production of NAD^+, an important cofactor for redox reaction, involved in several metabolic pathways such as the tricarboxylic acid cycle (TCA), glycolysis, pentose phosphate pathway, β-oxidation of fatty acids, among others. Interestingly, NAD^+ is also a co-substrate used by Sirtuins, a major family of deacetylase, involved in the regulation of numerous cell processes such as metabolic or epigenetic processes taking part to stem cell maintenance and differentiation (**Figure 2**) (reviewed in, Rodriguez et al., 2013; Lisowski et al., 2018). Sirtuin 1, the main cytoplasmic and nuclear sirtuin is known to deacetylate FOXO1, leading to its reduced transcriptional activity (Daitoku et al., 2011). The provided nicotinamide during the hepatic differentiation step would thus promote sirtuin activity and additional repression of FOXO1 function which is relieved upon exposure to the third cytokine cocktail which does not contain nicotinamide (**Figure 21**).

In order to further confirm the new hypothesis, the expression of CEBP/β during the differentiation process should be assessed. In another hand, to validate the proposed mechanism for REDD1-dependent upregulation of *4EBP1*, immunoprecipitation of FOXO1 and FOXO3A could be performed in order to check their association with 14-3-3 proteins. A colocalization study could also be performed to check the cytosolic versus nuclear localization of these factors and their associated inhibitor. In addition, functional study of FOXO1 and FOXO3A could also be performed in order to characterize their transcriptional activity such as chromatin immuno-precipitation experiment with subsequent sequencing.

The proposed model of transcriptional regulation for *4EBP1* expression thus involves master regulators of the hepatogenic differentiation program.

CONCLUSION

VI. CONCLUSION

The differentiation model used in this work can be handled and used to study developmental processes, that require further *in vivo* validations (Wanet et al., 2017). However, due to the intrinsic nature of the cells, and more precisely, of the MSC populations used, large inter- and intra-individual variability is observed, requiring a higher number of replicates to draw representative and relevant conclusions. Nonetheless, the transcriptomic analysis performed in the early stage of the differentiation process, highlighted a possible translational regulation involved in the regulation of the observed mitochondrial remodeling and driving the differentiation process. Following preliminary data and well described literature, the regulation of the eIF4E-4EBP1 axis by mTORC1 appeared as an interesting and relevant regulatory axis linking mitochondrial remodeling and hepatogenic differentiation. However, according to the results obtained, the regulation of the eIF4E-4EBP1 axis by mTORC1 would not have similar purpose than commonly described and expected in this case (enhancement of cell growth and global protein synthesis) and would have for objective to maintain a constant pool of active 4EBP1. A plausible hypothesis to explain these unexpected but interesting results is that this tight control of 4EBP1 could help to fine-tune the association of eIF4E with other eIF4F components in order to enhance eIF4G2 association with eIF3 and eIFA1 and promote cap-independent translational regulation of mitochondrial genes, supporting the mitochondrial remodeling and driving hepatogenic differentiation.

Altogether this hypothesis suggests that a potential translational regulation involving a transition from cap-dependent to cap-independent IRES-based translation does occur, this kind of regulation being already known to play a major role during the embryogenesis and thus to ensure developmental process (Yoffe et al., 2016). To confirm this hypothesis, characterization of the polysome-bound mRNAs in the early steps of the differentiation process will help to explore the putative translational regulation occurring during this cellular process and will allow for the identification of the main actors involved in this process.

Although hepatocyte-like cells obtained at the end of the differentiation process are really immature, the molecular mechanisms described in this model are based on *in vivo* liver development. Therefore, despite the limited potential of these cells for cellular therapy and regenerative medicine (Ullah et al., 2015), the *in vitro* hepatogenic differentiation model remains useful for fundamental research and better understanding of developmental processes.

REFERENCES

VII. REFERENCES

Agostini, M., Romeo, F., Inoue, S., Niklison-Chirou, M. V, Elia, A. J., Dinsdale, D., Morone, N., Knight, R. A., Mak, T. W., & Melino, G. (2016). Metabolic reprogramming during neuronal differentiation. *Cell Death & Differentiation*, *23*(9), 1502–1514. https://doi.org/10.1038/cdd.2016.36

Aviner, R., Geiger, T., & Elroy-Stein, O. (2014). Genome-wide identification and quantification of protein synthesis in cultured cells and whole tissues by puromycin-associated nascent chain proteomics (PUNCH-P). *Nature Protocols*, *9*(4), 751–760. https://doi.org/10.1038/nprot.2014.051

Ayatollahi, M., Soleimani, M., Tabei, S. Z., & Salmani, M. K. (2011). Hepatogenic differentiation of mesenchymal stem cells induced by insulin like growth factor-I. *World Journal of Stem Cells*, *3*(12), 113–121. https://doi.org/10.4252/wjsc.v3.i12.113

Azar, R., Lasfargues, C., Bousquet, C., & Pyronnet, S. (2013). Contribution of HIF-1α in 4E-BP1 gene expression. *Molecular Cancer Research : MCR*, *11*(1), 54–61. https://doi.org/10.1158/1541-7786.MCR-12-0095

Banas, A., Yamamoto, Y., Teratani, T., & Ochiya, T. (2007). Stem cell plasticity: Learning from hepatogenic differentiation strategies. *Developmental Dynamics*, *236*(12), 3228–3241. https://doi.org/10.1002/dvdy.21330

Bhandari, R. K., Haque, M. M., & Skinner, M. K. (2012). Global Genome Analysis of the Downstream Binding Targets of Testis Determining Factor SRY and SOX9. *PLoS ONE*, *7*(9), e43380. https://doi.org/10.1371/journal.pone.0043380

Birchmeier, W. (2016). Orchestrating Wnt signalling for metabolic liver zonation. *Nature Cell Biology*, *18*(5), 463–465. https://doi.org/10.1038/ncb3349

Blanco, G., & Blanco, A. (2017). *Medical biochemistry*. Retrieved from https://www.sciencedirect.com/book/9780128035504/medical-biochemistry

Bosch, F., Sabater, J., & Valera, A. (1995). Insulin inhibits liver expression of the CCAAT/enhancer-binding protein beta. *Diabetes*, *44*(3), 267–271. https://doi.org/10.2337/DIAB.44.3.267

Boylan, J. M., Sanders, J. A., Neretti, N., & Gruppuso, P. A. (2015). Profiling of the fetal and adult rat liver transcriptome and translatome reveals discordant regulation by the mechanistic target of rapamycin (mTOR). *American Journal of Physiology-Regulatory, Integrative and Comparative Physiology*, *309*(1), R22–R35. https://doi.org/10.1152/ajpregu.00114.2015

Bradley, C. A., Padovan, J. C., Thompson, T. L., Benoit, C. A., Chait, B. T., & Rhoads, R. E. (2002). Mass spectrometric analysis of the N terminus of translational initiation factor eIF4G-1 reveals novel isoforms. *The Journal of Biological Chemistry*, *277*(15), 12559–12571. https://doi.org/10.1074/jbc.M111134200

Burke, Z. D., Reed, K. R., Yeh, S.-W., Meniel, V., Sansom, O. J., Clarke, A. R., & Tosh, D. (2018). Spatiotemporal regulation of liver development by the Wnt/β-catenin pathway. *Scientific Reports*, *8*(1), 2735. https://doi.org/10.1038/s41598-018-20888-y

Buszczak, M., Signer, R. A. J., & Morrison, S. J. (2014). Cellular differences in protein synthesis regulate tissue homeostasis. *Cell*, *159*(2), 242–251. https://doi.org/10.1016/j.cell.2014.09.016

Byrd, M. P., Zamora, M., & Lloyd, R. E. (2002). Generation of multiple isoforms of eukaryotic

translation initiation factor 4GI by use of alternate translation initiation codons. *Molecular and Cellular Biology*, *22*(13), 4499–4511. https://doi.org/10.1128/MCB.22.13.4499-4511.2002

Cai, S.-L., Tee, A. R., Short, J. D., Bergeron, J. M., Kim, J., Shen, J., Guo, R., Johnson, C. L., Kiguchi, K., & Walker, C. L. (2006). Activity of TSC2 is inhibited by AKT-mediated phosphorylation and membrane partitioning. *The Journal of Cell Biology*, *173*(2), 279–289. https://doi.org/10.1083/jcb.200507119

Carnevalli, L. S., Masuda, K., Frigerio, F., Le Bacquer, O., Um, S. H., Gandin, V., Topisirovic, I., Sonenberg, N., Thomas, G., & Kozma, S. C. (2010). S6K1 plays a critical role in early adipocyte differentiation. *Developmental Cell*, *18*(5), 763–774. https://doi.org/10.1016/j.devcel.2010.02.018

Caron, S., Charon, M., Cramer, E., Sonenberg, N., & Dusanter-Fourt, I. (2004). Selective modification of eukaryotic initiation factor 4F (eIF4F) at the onset of cell differentiation: recruitment of eIF4GII and long-lasting phosphorylation of eIF4E. *Molecular and Cellular Biology*, *24*(11), 4920–4928. https://doi.org/10.1128/MCB.24.11.4920-4928.2004

Chen, C. C., Lee, J. C., & Chang, M. C. (2012). 4E-BP3 regulates eIF4E-mediated nuclear mRNA export and interacts with replication protein A2. *FEBS Letters*, *586*(16), 2260–2266. https://doi.org/10.1016/j.febslet.2012.05.059

Cohen, N., Sharma, M., Kentsis, A., Perez, J. M., Strudwick, S., & Borden, K. L. (2001). PML RING suppresses oncogenic transformation by reducing the affinity of eIF4E for mRNA. *The EMBO Journal*, *20*(16), 4547–4559. https://doi.org/10.1093/emboj/20.16.4547

Coldwell, M. J., & Morley, S. J. (2006). Specific isoforms of translation initiation factor 4GI show differences in translational activity. *Molecular and Cellular Biology*, *26*(22), 8448–8460. https://doi.org/10.1128/MCB.01248-06

Copp, J., Manning, G., & Hunter, T. (2009). TORC-specific phosphorylation of mammalian target of rapamycin (mTOR): phospho-Ser2481 is a marker for intact mTOR signaling complex 2. *Cancer Research*, *69*(5), 1821–1827. https://doi.org/10.1158/0008-5472.CAN-08-3014

Couvillion, M. T., Soto, I. C., Shipkovenska, G., & Churchman, L. S. (2016). Synchronized mitochondrial and cytosolic translation programs. *Nature*, *533*(7604), 499–503. https://doi.org/10.1038/nature18015

Culjkovic, B., Tan, K., Orolicki, S., Amri, A., Meloche, S., & Borden, K. L. B. (2008). The eIF4E RNA regulon promotes the Akt signaling pathway. *The Journal of Cell Biology*, *181*(1), 51–63. https://doi.org/10.1083/jcb.200707018

Culjkovic, B., Topisirovic, I., & Borden, K. L. B. (2007). Controlling Gene Expression through RNA Regulons The Role of the Eukaryotic Translation Initiation Factor eIF4E. *Cell Cycle*, *61*(1), 65–69. Retrieved from http://www.landesbioscience.com/journals/cc/abstract.php?id=3688

Culjkovic, B., Topisirovic, I., Skrabanek, L., Ruiz-Gutierrez, M., & Borden, K. L. B. (2005). eIF4E promotes nuclear export of cyclin D1 mRNAs via an element in the 3'UTR. *The Journal of Cell Biology*, *169*(2), 245–256. https://doi.org/10.1083/jcb.200501019

Culjkovic, B., Topisirovic, I., Skrabanek, L., Ruiz-Gutierrez, M., & Borden, K. L. B. (2006). eIF4E is a central node of an RNA regulon that governs cellular proliferation. *The Journal of Cell Biology*, *175*(3), 415–426. https://doi.org/10.1083/jcb.200607020

Cunningham, J. T., Rodgers, J. T., Arlow, D. H., Vazquez, F., Mootha, V. K., & Puigserver, P. (2007).

mTOR controls mitochondrial oxidative function through a YY1–PGC-1α transcriptional complex. *Nature*, *450*(7170), 736–740. https://doi.org/10.1038/nature06322

Daitoku, H., Sakamaki, J., & Fukamizu, A. (2011). Regulation of FoxO transcription factors by acetylation and protein–protein interactions. *Biochimica et Biophysica Acta (BBA) - Molecular Cell Research*, *1813*(11), 1954–1960. https://doi.org/10.1016/J.BBAMCR.2011.03.001

Dennis, M. D., Coleman, C. S., Berg, A., Jefferson, L. S., & Kimball, S. R. (2014). REDD1 enhances protein phosphatase 2A-mediated dephosphorylation of Akt to repress mTORC1 signaling. *Science Signaling*, *7*(335), ra68. https://doi.org/10.1126/scisignal.2005103

Dever, T. E., & Green, R. (2012). The elongation, termination, and recycling phases of translation in eukaryotes. *Cold Spring Harbor Perspectives in Biology*, *4*(7), a013706. https://doi.org/10.1101/cshperspect.a013706

Dey, S., Savant, S., Teske, B. F., Hatzoglou, M., Calkhoven, C. F., & Wek, R. C. (2012). Transcriptional repression of ATF4 gene by CCAAT/enhancer-binding protein β (C/EBPβ) differentially regulates integrated stress response. *The Journal of Biological Chemistry*, *287*(26), 21936–21949. https://doi.org/10.1074/jbc.M112.351783

DeYoung, M. P., Horak, P., Sofer, A., Sgroi, D., & Ellisen, L. W. (2008). Hypoxia regulates TSC1/2-mTOR signaling and tumor suppression through REDD1-mediated 14-3-3 shuttling. *Genes & Development*, *22*(2), 239–251. https://doi.org/10.1101/gad.1617608

Dobrikov, M. I., Shveygert, M., Brown, M. C., & Gromeier, M. (2014). Mitotic phosphorylation of eukaryotic initiation factor 4G1 (eIF4G1) at Ser1232 by Cdk1:cyclin B inhibits eIF4A helicase complex binding with RNA. *Molecular and Cellular Biology*, *34*(3), 439–451. https://doi.org/10.1128/MCB.01046-13

Dominici, M., Le Blanc, K., Mueller, I., Slaper-Cortenbach, I., Marini, F. ., Krause, D. S., Deans, R. J., Keating, A., Prockop, D. J., & Horwitz, E. M. (2006). Minimal criteria for defining multipotent mesenchymal stromal cells. The International Society for Cellular Therapy position statement. *Cytotherapy*, *8*(4), 315–317. https://doi.org/10.1080/14653240600855905

Esnault, S., Shen, Z.-J., & Malter, J. S. (2017). Protein Translation and Signaling in Human Eosinophils. *Frontiers in Medicine*, *4*, 150. https://doi.org/10.3389/fmed.2017.00150

Fernandez-Marcos, P. J., & Auwerx, J. (2011). Regulation of PGC-1α, a nodal regulator of mitochondrial biogenesis. *The American Journal of Clinical Nutrition*, *93*(4), 884S–90. https://doi.org/10.3945/ajcn.110.001917

Fleig, W. E., Nöther-Fleig, G., Steudter, S., Enderle, D., & Ditschuneit, H. (1985). Regulation of insulin binding and glycogenesis by insulin and dexamethasone in cultured rat hepatocytes. *Biochimica et Biophysica Acta*, *847*(3), 352–361. Retrieved from http://www.ncbi.nlm.nih.gov/pubmed/3933576

Fonseca, B. D., Zakaria, C., Jia, J.-J., Graber, T. E., Svitkin, Y., Tahmasebi, S., … Damgaard, C. K. (2015). La-related Protein 1 (LARP1) Represses Terminal Oligopyrimidine (TOP) mRNA Translation Downstream of mTOR Complex 1 (mTORC1). *The Journal of Biological Chemistry*, *290*(26), 15996–16020. https://doi.org/10.1074/jbc.M114.621730

Formosa, L. E., & Ryan, M. T. (2018). Mitochondrial OXPHOS complex assembly lines. *Nature Cell Biology*, *20*(5), 511–513. https://doi.org/10.1038/s41556-018-0098-z

Fortier, S., MacRae, T., Bilodeau, M., Sargeant, T., & Sauvageau, G. (2015). Derivation of

completely cell culture-derived mice from early-passage embryonic stem cells. *PNAS*, *90*(18), 8424–8428. https://doi.org/10.1073/pnas.90.18.8424

Fromm-Dornieden, C., von der Heyde, S., Lytovchenko, O., Salinas-Riester, G., Brenig, B., Beissbarth, T., & Baumgartner, B. G. (2012). Novel polysome messages and changes in translational activity appear after induction of adipogenesis in 3T3-L1 cells. *BMC Molecular Biology*, *13*(1), 9. https://doi.org/10.1186/1471-2199-13-9

Gandin, V., Masvidal, L., Hulea, L., Gravel, S.-P., Cargnello, M., McLaughlan, S., Cai, Y., Balanathan, P., Morita, M., Rajakumar, A., Furic, L., Pollak, M., Porco, J. A., St-Pierre, J., Pelletier, J., Larsson, O., & Topisirovic, I. (2016). nanoCAGE reveals 5' UTR features that define specific modes of translation of functionally related MTOR-sensitive mRNAs. *Genome Research*, *26*(5), 636–648. https://doi.org/10.1101/gr.197566.115

Ghosh, Z., Huang, M., Hu, S., Wilson, K. D., Dey, D., & Wu, J. C. (2011). Dissecting the oncogenic and tumorigenic potential of differentiated human induced pluripotent stem cells and human embryonic stem cells. *Cancer Research*, *71*(14), 5030–5039. https://doi.org/10.1158/0008-5472.CAN-10-4402

Gingras, A. C., Raught, B., Gygi, S. P., Niedzwiecka, A., Miron, M., Burley, S. K., Polakiewicz, R. D., Wyslouch-Cieszynska, A., Aebersold, R., & Sonenberg, N. (2001). Hierarchical phosphorylation of the translation inhibitor 4E-BP1. *Genes & Development*, *15*(21), 2852–2864. https://doi.org/10.1101/gad.912401

Goo, C. K., Lim, H. Y., Ho, Q. S., Too, H.-P., Clement, M.-V., & Wong, K. P. (2012). PTEN/Akt Signaling Controls Mitochondrial Respiratory Capacity through 4E-BP1. *PLoS ONE*, *7*(9), e45806. https://doi.org/10.1371/journal.pone.0045806

Gordillo, M., Evans, T., & Gouon-Evans, V. (2015). Orchestrating liver development. *Development (Cambridge, England)*, *142*(12), 2094–2108. https://doi.org/10.1242/dev.114215

Gradi, A., Imataka, H., Svitkin, Y. V., Rom, E., Raught, B., Morino, S., & Sonenberg, N. (1998). A Novel Functional Human Eukaryotic Translation Initiation Factor 4G. *Molecular and Cellular Biology*, *18*(1), 334–342. https://doi.org/10.1128/MCB.18.1.334

Grech, G., & von Lindern, M. (2012). The Role of Translation Initiation Regulation in Haematopoiesis. *Comparative and Functional Genomics*, *2012*, 1–10. https://doi.org/10.1155/2012/576540

Gruppuso, P. A., Tsai, S.-W., Boylan, J. M., & Sanders, J. A. (2008). Hepatic translation control in the late-gestation fetal rat. *American Journal of Physiology-Regulatory, Integrative and Comparative Physiology*, *295*(2), R558–R567. https://doi.org/10.1152/ajpregu.00091.2008

Hang, H., Yu, Y., Wu, N., Huang, Q., Xia, Q., & Bian, J. (2014). Induction of Highly Functional Hepatocytes from Human Umbilical Cord Mesenchymal Stem Cells by HNF4α Transduction. *PLoS ONE*, *9*(8), e104133. https://doi.org/10.1371/journal.pone.0104133

Hawkins, K. E., Joy, S., Delhove, J. M. K. M., Kotiadis, V. N., Fernandez, E., Fitzpatrick, L. M., Whiteford, J. R., King, P. J., Bolanos, J. P., Duchen, M. R., Waddington, S. N., & McKay, T. R. (2016). NRF2 Orchestrates the Metabolic Shift during Induced Pluripotent Stem Cell Reprogramming. *Cell Reports*, *14*(8), 1883–1891. https://doi.org/10.1016/j.celrep.2016.02.003

Hinnebusch, A. G., Ivanov, I. P., & Sonenberg, N. (2016). Translational control by 5'-untranslated regions of eukaryotic mRNAs. *Science (New York, N.Y.)*, *352*(6292), 1413–1416. https://doi.org/10.1126/science.aad9868

Holcik, M., & Sonenberg, N. (2005). Translational control in stress and apoptosis. *Nature Reviews Molecular Cell Biology*, *6*(4), 318–327. https://doi.org/10.1038/nrm1618

Hong, S., Freeberg, M. A., Han, T., Kamath, A., Yao, Y., Fukuda, T., Suzuki, T., Kim, J. K., & Inoki, K. (2017). LARP1 functions as a molecular switch for mTORC1-mediated translation of an essential class of mRNAs. *ELife*, *6*, e25237. https://doi.org/10.7554/eLife.25237

Horwitz, E. M., Le Blanc, K., Dominici, M., Mueller, I., Slaper-Cortenbach, I., Marini, F. C., Deans, R. J., Krause, D. S., Keating, A., & International Society for Cellular Therapy. (2005). Clarification of the nomenclature for MSC: The International Society for Cellular Therapy position statement. *Cytotherapy*, *7*(5), 393–395. https://doi.org/10.1080/14653240500319234

Hsu, Y.-C., Wu, Y.-T., Yu, T.-H., & Wei, Y.-H. (2016). Mitochondria in mesenchymal stem cell biology and cell therapy: From cellular differentiation to mitochondrial transfer. *Seminars in Cell & Developmental Biology*, *52*, 119–131. https://doi.org/10.1016/j.semcdb.2016.02.011

Huang, X., Vaag, A., Hansson, M., Weng, J., Laurila, E., & Groop, L. (2000). Impaired Insulin-Stimulated Expression of the Glycogen Synthase Gene in Skeletal Muscle of Type 2 Diabetic Patients Is Acquired Rather Than Inherited 1. *The Journal of Clinical Endocrinology & Metabolism*, *85*(4), 1584–1590. https://doi.org/10.1210/jcem.85.4.6535

Iacob, R., Rüdrich, U., Rothe, M., Kirsch, S., Maasoumy, B., Narain, N., Verfaillie, C. M., Sancho-Bru, P., Iken, M., Popescu, I., Schambach, A., Manns, M. P., & Bock, M. (2011). Induction of a mature hepatocyte phenotype in adult liver derived progenitor cells by ectopic expression of transcription factors. *Stem Cell Research*, *6*(3), 251–261. https://doi.org/10.1016/J.SCR.2011.02.002

Iansante, V., Chandrashekran, A., & Dhawan, A. (2018). Cell-based liver therapies: past, present and future. *Philosophical Transactions of the Royal Society of London. Series B, Biological Sciences*, *373*(1750), 20170229. https://doi.org/10.1098/rstb.2017.0229

Inoki, K., Li, Y., Zhu, T., Wu, J., & Guan, K.-L. (2002). TSC2 is phosphorylated and inhibited by Akt and suppresses mTOR signalling. *Nature Cell Biology*, *4*(9), 648–657. https://doi.org/10.1038/ncb839

Jackson, R. J., Hellen, C. U. T., & Pestova, T. V. (2010). The mechanism of eukaryotic translation initiation and principles of its regulation. *Nature Reviews Molecular Cell Biology*, *11*(2), 113–127. https://doi.org/10.1038/nrm2838

Jones, S. P., Guillemin, G. J., & Brew, B. J. (2013). The kynurenine pathway in stem cell biology. *International Journal of Tryptophan Research : IJTR*, *6*, 57–66. https://doi.org/10.4137/IJTR.S12626

Kapasi, P., Chaudhuri, S., Vyas, K., Baus, D., Komar, A. A., Fox, P. L., Merrick, W. C., & Mazumder, B. (2007). L13a blocks 48S assembly: role of a general initiation factor in mRNA-specific translational control. *Molecular Cell*, *25*(1), 113–126. https://doi.org/10.1016/j.molcel.2006.11.028

Kawaguchi, Y. (2013). Sox9 and programming of liver and pancreatic progenitors. *The Journal of Clinical Investigation*, *123*(5), 1881–1886. https://doi.org/10.1172/JCI66022

King, H. A., & Gerber, A. P. (2016). Translatome profiling: methods for genome-scale analysis of mRNA translation. *Briefings in Functional Genomics*, *15(1)*, 22–31. https://doi.org/10.1093/bfgp/elu045

Kleijn, M., Scheper, G. C., Wilson, M. L., Tee, A. R., & Proud, C. G. (2002). Localisation and regulation of the eIF4E-binding protein 4E-BP3. *FEBS Letters*, *532*(3), 319–323. https://doi.org/10.1016/S0014-5793(02)03694-3

Komar, A. A., & Hatzoglou, M. (2011). Cellular IRES-mediated translation: The war of ITAFs in pathophysiological states. *Cell Cycle*, *10*(2), 229–240. https://doi.org/10.4161/cc.10.2.14472

Koromilas, A. E., Lazaris-Karatzas, A., & Sonenberg, N. (1992). mRNAs containing extensive secondary structure in their 5' non-coding region translate efficiently in cells overexpressing initiation factor eIF-4E. *The EMBO Journal*, *11*(11), 4153–4158. Retrieved from http://www.ncbi.nlm.nih.gov/pubmed/1396596

Kristensen, A. R., Gsponer, J., & Foster, L. J. (2013). Protein synthesis rate is the predominant regulator of protein expression during differentiation. *Molecular Systems Biology*, *9*(1), 689. https://doi.org/10.1038/msb.2013.47

Kubacka, D., Miguel, R. N., Minshall, N., Darzynkiewicz, E., Standart, N., & Zuberek, J. (2015). Distinct features of cap binding by eIF4E1b proteins. *Journal of Molecular Biology*. https://doi.org/10.1016/j.jmb.2014.11.009

Lahr, R. M., Fonseca, B. D., Ciotti, G. E., Al-Ashtal, H. A., Jia, J.-J., Niklaus, M. R., Blagden, S. P., Alain, T., & Berman, A. J. (2017). La-related protein 1 (LARP1) binds the mRNA cap, blocking eIF4F assembly on TOP mRNAs. *ELife*, *6*. https://doi.org/10.7554/eLife.24146

Lallemand-Breitenbach, V., & de Thé, H. (2018). PML nuclear bodies: from architecture to function. *Current Opinion in Cell Biology*, *52*, 154–161. https://doi.org/10.1016/j.ceb.2018.03.011

Lee, K. H., Hyun, M. S., & Kim, J.-R. (2003). Growth factor-dependent activation of the MAPK pathway in human pancreatic cancer: MEK/ERK and p38 MAP kinase interaction in uPA synthesis. *Clinical & Experimental Metastasis*, *20*(6), 499–505. Retrieved from http://www.ncbi.nlm.nih.gov/pubmed/14598883

Lee, V. H. Y., Healy, T., Fonseca, B. D., Hayashi, A., & Proud, C. G. (2008). Analysis of the regulatory motifs in eukaryotic initiation factor 4E-binding protein 1. *FEBS Journal*, *275*(9), 2185–2199. https://doi.org/10.1111/j.1742-4658.2008.06372.x

Leu, J. I., Crissey, M. A. S., Leu, J. P., Ciliberto, G., & Taub, R. (2001). Interleukin-6-Induced STAT3 and AP-1 Amplify Hepatocyte Nuclear Factor 1-Mediated Transactivation of Hepatic Genes, an Adaptive Response to Liver Injury. *Molecular and Cellular Biology*, *21*(2), 414–424. https://doi.org/10.1128/MCB.21.2.414-424.2001

Li, J., Shan, F., Xiong, G., Chen, X., Guan, X., Wang, J.-M., Wang, W.-L., Xu, X., & Bai, Y. (2014). EGF-induced C/EBP participates in EMT by decreasing the expression of miR-203 in esophageal squamous cell carcinoma cells. *Journal of Cell Science*, *127*(17), 3735–3744. https://doi.org/10.1242/jcs.148759

Liao, Y., Zhuang, X., Huang, X., Peng, Y., Ma, X., Huang, Z.-X., Liu, F., Xu, J., Wang, Y., Chen, W.-M., Ye, W.-C., & Shi, L. (2018). A Bivalent Securinine Compound SN3-L6 Induces Neuronal Differentiation via Translational Upregulation of Neurogenic Transcription Factors. *Frontiers in Pharmacology*, *9*, 290. https://doi.org/10.3389/fphar.2018.00290

Liberman, N., Gandin, V., Svitkin, Y. V, David, M., Virgili, G., Jaramillo, M., Holcik, M., Nagar, B., Kimchi, A., & Sonenberg, N. (2015). DAP5 associates with eIF2β and eIF4AI to promote Internal Ribosome Entry Site driven translation. *Nucleic Acids Research*, *43*(7), 3764–3775. https://doi.org/10.1093/nar/gkv205

Lisowski, P., Kannan, P., Mlody, B., & Prigione, A. (2018). Mitochondria and the dynamic control of stem cell homeostasis. *EMBO Reports*, e45432. https://doi.org/10.15252/embr.201745432

Lysy, P. A., Campard, D., Smets, F., Malaise, J., Mourad, M., Najimi, M., & Sokal, E. M. (2008). Persistence of a chimerical phenotype after hepatocyte differentiation of human bone marrow mesenchymal stem cells. *Cell Proliferation*, *41*(1), 36–58. https://doi.org/10.1111/j.1365-2184.2007.00507.x

Mader, S., Lee, H., Pause, A., & Sonenberg, N. (1995). The Translation Initiation Factor eIF-4E Binds to a Common Motif Shared by the Translation Factor eIF-4 and the Translational Repressors 4E-Binding Proteins. *MOLECULAR AND CELLULAR BIOLOGY*, *15*(9), 4990–4997. Retrieved from http://mcb.asm.org/content/15/9/4990.full.pdf

Magner, N. L., Jung, Y., Wu, J., Nolta, J. A., Zern, M. A., & Zhou, P. (2013). Insulin and igfs enhance hepatocyte differentiation from human embryonic stem cells via the PI3K/AKT pathway. *STEM CELLS*, *31*(10), 2095–2103. https://doi.org/10.1002/stem.1478

Magnuson, B., Ekim, B., & Fingar, D. C. (2012). Regulation and function of ribosomal protein S6 kinase (S6K) within mTOR signalling networks. *Biochemical Journal*, *441*(1), 1–21. https://doi.org/10.1042/BJ20110892

Marissen, W. E., Gradi, A., Sonenberg, N., & Lloyd, R. E. (2000). Cleavage of eukaryotic translation initiation factor 4GII correlates with translation inhibition during apoptosis. *Cell Death & Differentiation*, *7*(12), 1234–1243. https://doi.org/10.1038/sj.cdd.4400750

Marissen, W. E., & Lloyd, R. E. (1998). Eukaryotic translation initiation factor 4G is targeted for proteolytic cleavage by caspase 3 during inhibition of translation in apoptotic cells. *Molecular and Cellular Biology*, *18*(12), 7565–7574. https://doi.org/10.1128/MCB.18.12.7565

Martin, F., Barends, S., Jaeger, S., Schaeffer, L., Prongidi-Fix, L., & Eriani, G. (2011). Cap-Assisted Internal Initiation of Translation of Histone H4. *Molecular Cell*, *41*(2), 197–209. https://doi.org/10.1016/J.MOLCEL.2010.12.019

Masvidal, L., Hulea, L., Furic, L., Topisirovic, I., & Larsson, O. (2017). mTOR-sensitive translation: Cleared fog reveals more trees. *RNA Biology*, *14*(10), 1299–1305. https://doi.org/10.1080/15476286.2017.1290041

Michalopoulos, G. K., Bowen, W. C., Mulè, K., & Luo, J. (2003). HGF-, EGF-, and dexamethasone-induced gene expression patterns during formation of tissue in hepatic organoid cultures. *Gene Expression*, *11*(2), 55–75. Retrieved from http://www.ncbi.nlm.nih.gov/pubmed/12837037

Mikkers, H., Pike-Overzet, K., & Staal, F. J. T. (2012). Induced pluripotent stem cells and severe combined immunodeficiency: merely disease modeling or potentially a novel cure? *Pediatric Research*, *71*(4–2), 427–432. https://doi.org/10.1038/pr.2011.65

Minshall, N., Reiter, M. H., Weil, D., & Standart, N. (2007). CPEB interacts with an ovary-specific eIF4E and 4E-T in early Xenopus oocytes. *The Journal of Biological Chemistry*, *282*(52), 37389–37401. https://doi.org/10.1074/jbc.M704629200

Mitani, S., Takayama, K., Nagamoto, Y., Imagawa, K., Sakurai, F., Tachibana, M., Sumazaki, R., & Mizuguchi, H. (2017). Human ESC/iPSC-Derived Hepatocyte-like Cells Achieve Zone-Specific Hepatic Properties by Modulation of WNT Signaling. *Molecular Therapy : The Journal of the American Society of Gene Therapy*, *25*(6), 1420–1433. https://doi.org/10.1016/j.ymthe.2017.04.006

Morgan, K., Marsters, P., Morley, S., van Gent, D., Hejazi, A., Backx, M., Thorpe, E. R. K., & Kalsheker, N. (2002). Oncostatin M induced alpha1-antitrypsin (AAT) gene expression in Hep G2 cells is mediated by a 3' enhancer. *The Biochemical Journal*, *365*(Pt 2), 555–560. https://doi.org/10.1042/BJ20011312

Morita, M., Gravel, S.-P., Chénard, V., Sikström, K., Zheng, L., Alain, T., … Sonenberg, N. (2013). mTORC1 controls mitochondrial activity and biogenesis through 4E-BP-dependent translational regulation. *Cell Metabolism*, *18*(5), 698–711. https://doi.org/10.1016/j.cmet.2013.10.001

Morita, M., Gravel, S.-P., Hulea, L., Larsson, O., Pollak, M., St-Pierre, J., & Topisirovic, I. (2015). mTOR coordinates protein synthesis, mitochondrial activity and proliferation. *Cell Cycle*, *14*(4), 473–480. https://doi.org/10.4161/15384101.2014.991572

Murata, T., & Shimotohno, K. (2006). Ubiquitination and proteasome-dependent degradation of human eukaryotic translation initiation factor 4E. *The Journal of Biological Chemistry*, *281*(30), 20788–20800. https://doi.org/10.1074/jbc.M600563200

Najar, M., Raicevic, G., Fayyad-Kazan, H., De Bruyn, C., Bron, D., Toungouz, M., & Lagneaux, L. (2013). Impact of different mesenchymal stromal cell types on T-cell activation, proliferation and migration. *International Immunopharmacology*, *15*(4), 693–702. https://doi.org/10.1016/J.INTIMP.2013.02.020

Osborne, M. J., & Borden, K. L. B. (2015). The eukaryotic translation initiation factor eIF4E in the nucleus: taking the road less traveled. *Immunological Reviews*, *263*(1), 210–223. https://doi.org/10.1111/imr.12240

Parent, R., & Beretta, L. (2008). Open Access Translational control plays a prominent role in the hepatocytic differentiation of HepaRG liver progenitor cells, *9*(1), R19. https://doi.org/10.1186/gb-2008-9-1-r19

Parent, R., Kolippakkam, D., Booth, G., & Beretta, L. (2007). Mammalian target of rapamycin activation impairs hepatocytic differentiation and targets genes moderating lipid homeostasis and hepatocellular growth. *Cancer Research*, *67*(9), 4337–4345. https://doi.org/10.1158/0008-5472.CAN-06-3640

Prévôt, D., Darlix, J.-L., & Ohlmann, T. (2003). Conducting the initiation of protein synthesis: the role of eIF4G. *Biology of the Cell*, *95*(3–4), 141–156. Retrieved from http://www.ncbi.nlm.nih.gov/pubmed/12867079

Proud, C. G. (2007). Signalling to translation: how signal transduction pathways control the protein synthetic machinery. *The Biochemical Journal*, *403*(2), 217–234. https://doi.org/10.1042/BJ20070024

Puig, O., Marr, M. T., Ruhf, M. L., & Tjian, R. (2003). Control of cell number by Drosophila FOXO: downstream and feedback regulation of the insulin receptor pathway. *Genes & Development*, *17*(16), 2006–2020. https://doi.org/10.1101/gad.1098703

Pyronnet, S., Imataka, H., Gingras, A. C., Fukunaga, R., Hunter, T., & Sonenberg, N. (1999). Human eukaryotic translation initiation factor 4G (eIF4G) recruits mnk1 to phosphorylate eIF4E. *The EMBO Journal*, *18*(1), 270–279. https://doi.org/10.1093/emboj/18.1.270

Qin, X., Jiang, B., & Zhang, Y. (2016). 4E-BP1, a multifactor regulated multifunctional protein. https://doi.org/10.1080/15384101.2016.1151581

Rafalski, V. A., Mancini, E., & Brunet, A. (2012). Energy metabolism and energy-sensing pathways

in mammalian embryonic and adult stem cell fate. *Journal of Cell Science*, *125*(23), 5597–5608. https://doi.org/10.1242/jcs.114827

Raju, R., Chau, D., Notelaers, T., Myers, C. L., Verfaillie, C. M., & Hu, W.-S. (2018). In Vitro Pluripotent Stem Cell Differentiation to Hepatocyte Ceases Further Maturation at an Equivalent Stage of E15 in Mouse Embryonic Liver Development. *Stem Cells and Development*, scd.2017.0270. https://doi.org/10.1089/scd.2017.0270

Raju, R., Palapetta, S. M., Sandhya, V. K., Sahu, A., Alipoor, A., Balakrishnan, L., Advani, J., George, B., Kini, K. R., Geetha, N. P., Prakash, H. S., Prasad, T. S. K., Chang, Y.-J., Chen, L., Pandey, A., & Gowda, H. (2014). A Network Map of FGF-1/FGFR Signaling System. *Journal of Signal Transduction*, *2014*, 962962. https://doi.org/10.1155/2014/962962

Raucci, A., Laplantine, E., Mansukhani, A., & Basilico, C. (2004). Activation of the ERK1/2 and p38 mitogen-activated protein kinase pathways mediates fibroblast growth factor-induced growth arrest of chondrocytes. *The Journal of Biological Chemistry*, *279*(3), 1747–1756. https://doi.org/10.1074/jbc.M310384200

Raught, B., & Gingras, A. C. (1999). eIF4E activity is regulated at multiple levels. *The International Journal of Biochemistry & Cell Biology*, *31*(1), 43–57. Retrieved from http://www.ncbi.nlm.nih.gov/pubmed/10216943

Richter, J. D. (2007). CPEB: a life in translation. *Trends in Biochemical Sciences*, *32*(6), 279–285. https://doi.org/10.1016/j.tibs.2007.04.004

Richter, J. D., & Sonenberg, N. (2005). Regulation of cap-dependent translation by eIF4E inhibitory proteins. *Nature*, *433*(7025), 477–480. https://doi.org/10.1038/nature03205

Rodrigues, M., Griffith, L. G., & Wells, A. (2010). Growth factor regulation of proliferation and survival of multipotential stromal cells. *Stem Cell Research & Therapy*, *1*(4), 32. https://doi.org/10.1186/scrt32

Rodriguez, R. M., Fernandez, A. F., & Fraga, M. F. (2013). Role of Sirtuins in Stem Cell Differentiation. *Genes & Cancer*, *4*(3–4), 105–111. https://doi.org/10.1177/1947601913479798

Rolli-Derkinderen, M., Machavoine, F., Baraban, J. M., Grolleau, A., Beretta, L., & Dy, M. (2003). ERK and p38 inhibit the expression of 4E-BP1 repressor of translation through induction of Egr-1. *The Journal of Biological Chemistry*, *278*(21), 18859–18867. https://doi.org/10.1074/jbc.M211696200

Rong, L., Livingstone, M., Sukarieh, R., Petroulakis, E., Gingras, A.-C., Crosby, K., Smith, B., Polakiewicz, R. D., Pelletier, J., Ferraiuolo, M. A., & Sonenberg, N. (2008). Control of eIF4E cellular localization by eIF4E-binding proteins, 4E-BPs. *RNA (New York, N.Y.)*, *14*(7), 1318–1327. https://doi.org/10.1261/rna.950608

Roux, P. P., & Topisirovic, I. (2012). Regulation of mRNA translation by signaling pathways. *Cold Spring Harbor Perspectives in Biology*, *4*(11), a012252. https://doi.org/10.1101/cshperspect.a012252

Sambathkumar, R., Akkerman, R., Dastidar, S., Roelandt, P., Kumar, M., Bajaj, M., Mestre Rosa, A. R., Helsen, N., Vanslembrouck, V., Kalo, E., Khurana, S., Laureys, J., Gysemans, C., Faas, M. M., de Vos, P., & Verfaillie, C. M. (2018). Generation of hepatocyte- and endocrine pancreatic-like cells from human induced endodermal progenitor cells. *PLOS ONE*, *13*(5), e0197046. https://doi.org/10.1371/journal.pone.0197046

Sampath, P., Pritchard, D. K., Pabon, L., Reinecke, H., Schwartz, S. M., Morris, D. R., & Murry, C. E. (2008). A Hierarchical Network Controls Protein Translation during Murine Embryonic Stem Cell Self-Renewal and Differentiation. *Cell Stem Cell*, *2*(5), 448–460. https://doi.org/10.1016/J.STEM.2008.03.013

Saulnier, N., Lattanzi, W., Puglisi, M. A., Pani, G., Barba, M., Piscaglia, A. C., Giachelia, M., Alfieri, S., Neri, G., Gasbarrini, G., & Gasbarrini, A. (2009). Mesenchymal stromal cells multipotency and plasticity: induction toward the hepatic lineage. *European Review for Medical and Pharmacological Sciences*, *13 Suppl 1*, 71–78. Retrieved from http://www.ncbi.nlm.nih.gov/pubmed/19530515

Schalm, S. S., & Blenis, J. (2002). Identification of a conserved motif required for mTOR signaling. *Current Biology : CB*, *12*(8), 632–639. https://doi.org/10.1016/S0960-9822(02)00762-5

Schalm, S. S., Fingar, D. C., Sabatini, D. M., & Blenis, J. (2003). TOS motif-mediated raptor binding regulates 4E-BP1 multisite phosphorylation and function. *Current Biology : CB*, *13*(10), 797–806. https://doi.org/10.1016/S0960-9822(03)00329-4

Schmidt, C., Beilsten-Edmands, V., & Robinson, C. V. (2016). Insights into Eukaryotic Translation Initiation from Mass Spectrometry of Macromolecular Protein Assemblies. *Journal of Molecular Biology*, *428*(2), 344–356. https://doi.org/10.1016/J.JMB.2015.10.011

Schmidt, E. K., Clavarino, G., Ceppi, M., & Pierre, P. (2009). SUnSET, a nonradioactive method to monitor protein synthesis. *Nature Methods*, *6*(4), 275–277. https://doi.org/10.1038/nmeth.1314

Segev, N., & Gerst, J. E. (2018). Specialized ribosomes and specific ribosomal protein paralogs control translation of mitochondrial proteins. *The Journal of Cell Biology*, *217*(1), 117–126. https://doi.org/10.1083/jcb.201706059

Shen, B.-J., Chang, C.-J., Lee, H.-S., Tsai, W.-H., Miau, L.-H., & Lee, S.-C. (1997). Transcriptional Induction of the agp/ebp (c/ebp β) Gene by Hepatocyte Growth Factor. *DNA and Cell Biology*, *16*(6), 703–711. https://doi.org/10.1089/dna.1997.16.703

Showkat, M., Beigh, M. A., & Andrabi, K. I. (2014). mTOR Signaling in Protein Translation Regulation: Implications in Cancer Genesis and Therapeutic Interventions. *Molecular Biology International*, *2014*, 686984. https://doi.org/10.1155/2014/686984

Siddiqui, N., Tempel, W., Nedyalkova, L., Volpon, L., Wernimont, A. K., Osborne, M. J., Park, H.-W., & Borden, K. L. B. (2012). Structural insights into the allosteric effects of 4EBP1 on the eukaryotic translation initiation factor eIF4E. *Journal of Molecular Biology*, *415*(5), 781–792. https://doi.org/10.1016/j.jmb.2011.12.002

Siegel, G., Kluba, T., Hermanutz-Klein, U., Bieback, K., Northoff, H., & Schäfer, R. (2013). Phenotype, donor age and gender affect function of human bone marrow-derived mesenchymal stromal cells. *BMC Medicine*, *11*(1), 146. https://doi.org/10.1186/1741-7015-11-146

Snykers, S., Vanhaecke, T., Papeleu, P., Luttun, A., Jiang, Y., Vander Heyden, Y., Verfaillie, C., & Rogiers, V. (2006). Sequential Exposure to Cytokines Reflecting Embryogenesis: The Key for in vitro Differentiation of Adult Bone Marrow Stem Cells into Functional Hepatocyte-like Cells. *Toxicological Sciences*, *94*(2), 330–341. https://doi.org/10.1093/toxsci/kfl058

Sonenberg, N., & Hinnebusch, A. G. (2009). Regulation of translation initiation in eukaryotes: mechanisms and biological targets. *Cell*, *136*(4), 731–745. https://doi.org/10.1016/j.cell.2009.01.042

Spangenberg, L., Shigunov, P., Abud, A. P. R., Cofré, A. R., Stimamiglio, M. A., Kuligovski, C., Zych, J., Schittini, A. V., Costa, A. D. T., Rebelatto, C. K., Brofman, P. R. S., Goldenberg, S., Correa, A., Naya, H., & Dallagiovanna, B. (2013). Polysome profiling shows extensive posttranscriptional regulation during human adipocyte stem cell differentiation into adipocytes. *Stem Cell Research*, *11*(2), 902–912. https://doi.org/10.1016/J.SCR.2013.06.002

Sperber, H., Mathieu, J., Wang, Y., Ferreccio, A., Hesson, J., Xu, Z., … Ruohola-Baker, H. (2015). The metabolome regulates the epigenetic landscape during naive-to-primed human embryonic stem cell transition. *Nature Cell Biology*, *17*(12), 1523–1535. https://doi.org/10.1038/ncb3264

Stock, P., Brückner, S., Winkler, S., Dollinger, M., Christ, B., Stock, P., Brückner, S., Winkler, S., Dollinger, M. M., & Christ, B. (2014). Human Bone Marrow Mesenchymal Stem Cell-Derived Hepatocytes Improve the Mouse Liver after Acute Acetaminophen Intoxication by Preventing Progress of Injury. *International Journal of Molecular Sciences*, *15*(4), 7004–7028. https://doi.org/10.3390/ijms15047004

Stroud, D. A., Surgenor, E. E., Formosa, L. E., Reljic, B., Frazier, A. E., Dibley, M. G., Osellame, L. D., Stait, T., Beilharz, T. H., Thorburn, D. R., Salim, A., & Ryan, M. T. (2016). Accessory subunits are integral for assembly and function of human mitochondrial complex I. *Nature*, *538*(7623), 123–126. https://doi.org/10.1038/nature19754

Sukarieh, R., Sonenberg, N., & Pelletier, J. (2009). The eIF4E-binding proteins are modifiers of cytoplasmic eIF4E relocalization during the heat shock response. *American Journal of Physiology-Cell Physiology*, *296*(5), C1207–C1217. https://doi.org/10.1152/ajpcell.00511.2008

Sun, F., Palmer, K., Handel, M. A., Poorman-Allen, P., Mori, C., Blizard, D. R., Brown, P. R., Goulding, E. H., Strong, B. D., & Eddy, E. M. (2010). Mutation of Eif4g3, encoding a eukaryotic translation initiation factor, causes male infertility and meiotic arrest of mouse spermatocytes. *Development (Cambridge, England)*, *137*(10), 1699–1707. https://doi.org/10.1242/dev.043125

Taanman, J.-W. (1999). The mitochondrial genome: structure, transcription, translation and replication. *Biochimica et Biophysica Acta (BBA) - Bioenergetics*, *1410*(2), 103–123. https://doi.org/10.1016/S0005-2728(98)00161-3

Tacheny, A., Michel, S., Dieu, M., Payen, L., Arnould, T., & Renard, P. (2012). Unbiased proteomic analysis of proteins interacting with the HIV-1 5'LTR sequence: role of the transcription factor Meis. *Nucleic Acids Research*, *40*(21), e168. https://doi.org/10.1093/nar/gks733

Tahmasebi, S., Jafarnejad, S. M., Tam, I. S., Gonatopoulos-Pournatzis, T., Matta-Camacho, E., Tsukumo, Y., … Sonenberg, N. (2016). Control of embryonic stem cell self-renewal and differentiation via coordinated alternative splicing and translation of YY2. *Proceedings of the National Academy of Sciences of the United States of America*, *113*(44), 12360–12367. https://doi.org/10.1073/pnas.1615540113

Takahashi, K., & Yamanaka, S. (2006). Induction of pluripotent stem cells from mouse embryonic and adult fibroblast cultures by defined factors. *Cell*, *126*(4), 663–676. https://doi.org/10.1016/j.cell.2006.07.024

Tapia, N., & Schö Ler, H. R. (2016). Cell Stem Cell Review Molecular Obstacles to Clinical Translation of iPSCs. *Stem Cell*, *19*, 298–309. https://doi.org/10.1016/j.stem.2016.06.017

Tcherkezian, J., Cargnello, M., Romeo, Y., Huttlin, E. L., Lavoie, G., Gygi, S. P., & Roux, P. P. (2014). Proteomic analysis of cap-dependent translation identifies LARP1 as a key regulator of 5'TOP mRNA translation. *Genes & Development*, *28*, 357–371. https://doi.org/10.1101/gad.231407.113

Teratani, T., Yamamoto, H., Aoyagi, K., Sasaki, H., Asari, A., Quinn, G., Sasaki, H., Terada, M., & Ochiya, T. (2005). Direct hepatic fate specification from mouse embryonic stem cells. *Hepatology*, *41*(4), 836–846. https://doi.org/10.1002/hep.20629

Terryn, J., Tricot, T., Gajjar, M., & Verfaillie, C. (2018). Recent advances in lineage differentiation from stem cells: hurdles and opportunities? *F1000Research*, *7*, 220. https://doi.org/10.12688/f1000research.12596.1

Theunissen, T. W., Friedli, M., He, Y., Planet, E., O'Neil, R. C., Markoulaki, S., … Jaenisch, R. (2016). Molecular Criteria for Defining the Naive Human Pluripotent State. *Cell Stem Cell*, *19*(4), 502–515. https://doi.org/10.1016/j.stem.2016.06.011

Theunissen, T. W., Powell, B. E., Wang, H., Mitalipova, M., Faddah, D. A., Reddy, J., … Jaenisch, R. (2014). Systematic identification of culture conditions for induction and maintenance of naive human pluripotency. *Cell Stem Cell*, *15*(4), 471–487. https://doi.org/10.1016/j.stem.2014.07.002

Thoreen, C. C., Chantranupong, L., Keys, H. R., Wang, T., Gray, N. S., & Sabatini, D. M. (2012). A unifying model for mTORC1-mediated regulation of mRNA translation. *Nature*, *485*(7396), 109–113. https://doi.org/10.1038/nature11083

Tian, Y., Gawlak, G., Shah, A. S., Higginbotham, K., Tian, X., Kawasaki, Y., Akiyama, T., Sacks, D. B., & Birukova, A. A. (2015). Hepatocyte growth factor-induced Asef-IQGAP1 complex controls cytoskeletal remodeling and endothelial barrier. *The Journal of Biological Chemistry*, *290*(7), 4097–4109. https://doi.org/10.1074/jbc.M114.620377

Topisirovic, I., Siddiqui, N., Leroux Lapointe, V., Trost, M., Thibault, P., Bangeranye, C., Pin˜ol-Roma, S., & Borden, K. L. B. (2009). Molecular dissection of the eukaryotic initiation factor 4E (eIF4E) export-competent RNP. *EMBO Journal*, *28*, 1087–1098. https://doi.org/10.1038/emboj.2009.53

Tzivion, G., Dobson, M., & Ramakrishnan, G. (2011). FoxO transcription factors; Regulation by AKT and 14-3-3 proteins. *Biochimica et Biophysica Acta (BBA) - Molecular Cell Research*, *1813*(11), 1938–1945. https://doi.org/10.1016/J.BBAMCR.2011.06.002

Ullah, I., Subbarao, R. B., & Rho, G. J. (2015). Human mesenchymal stem cells - current trends and future prospective. *Bioscience Reports*, *35*(2). https://doi.org/10.1042/BSR20150025

Vazquez-Martin, A., den Haute, C., Cufí, S., Faja, B., Cuyàs, E., Lopez-Bonet, E., Rodriguez-Gallego, E., Fernández-Arroyo, S., Joven, J., Baekelandt, V., & Menendez, J. (2016). Mitophagy-driven mitochondrial rejuvenation regulates stem cell fate. *Aging*, *8*(7), 1330–1352. https://doi.org/10.18632/aging.100976

Volpon, L., Culjkovic-Kraljacic, B., Sohn, H. S., Blanchet-Cohen, A., Osborne, M. J., & Borden, K. L. B. (2017). A biochemical framework for eIF4E-dependent mRNA export and nuclear recycling of the export machinery. *RNA (New York, N.Y.)*, *23*(6), 927–937. https://doi.org/10.1261/rna.060137.116

Wanet, A., Arnould, T., Najimi, M., & Renard, P. (2015). Connecting Mitochondria, Metabolism, and Stem Cell Fate. *Stem Cells and Development*, *24*(17), 1957–1971. https://doi.org/10.1089/scd.2015.0117

Wanet, A., Caruso, M., Domelevo Entfellner, J. B., Najar, M., Fattaccioli, A., Demazy, C., Evraerts, J., El-Kehdy, H., Pourcher, G., Sokal, E., Arnould, T., Tiffin, N., Najimi, M., & Renard, P. (2017). The Transcription Factor 7-Like 2–Peroxisome Proliferator-Activated Receptor Gamma Coactivator-1 Alpha Axis Connects Mitochondrial Biogenesis and Metabolic Shift with Stem

Cell Commitment to Hepatic Differentiation. *Stem Cells*, *35*(10), 2184–2197. https://doi.org/10.1002/stem.2688

Wanet, A., Remacle, N., Najar, M., Sokal, E., Arnould, T., Najimi, M., & Renard, P. (2014). Mitochondrial remodeling in hepatic differentiation and dedifferentiation. *The International Journal of Biochemistry & Cell Biology*, *54*, 174–185. https://doi.org/10.1016/j.biocel.2014.07.015

Wang, H., Kubica, N., Ellisen, L. W., Jefferson, L. S., & Kimball, S. R. (2006). Dexamethasone represses signaling through the mammalian target of rapamycin in muscle cells by enhancing expression of REDD1. *The Journal of Biological Chemistry*, *281*(51), 39128–39134. https://doi.org/10.1074/jbc.M610023200

Wang, L., Lawrence, J. C., Sturgill, T. W., & Harris, T. E. (2009). Mammalian target of rapamycin complex 1 (mTORC1) activity is associated with phosphorylation of raptor by mTOR. *The Journal of Biological Chemistry*, *284*(22), 14693–14697. https://doi.org/10.1074/jbc.C109.002907

Wang, X., Li, W., Parra, J.-L., Beugnet, A., & Proud, C. G. (2003). The C Terminus of Initiation Factor 4E-Binding Protein 1 Contains Multiple Regulatory Features That Influence Its Function and Phosphorylation. *MOLECULAR AND CELLULAR BIOLOGY*, *23*(5), 1546–1557. https://doi.org/10.1128/MCB.23.5.1546–1557.2003

Washkowitz, A. J., Gavrilov, S., Begum, S., & Papaioannou, V. E. (2012). Diverse functional networks of Tbx3 in development and disease. *Wiley Interdisciplinary Reviews. Systems Biology and Medicine*, *4*(3), 273–283. https://doi.org/10.1002/wsbm.1162

Weidgang, C. E., Russell, R., Tata, P. R., Kühl, S. J., Illing, A., Müller, M., … Kleger, A. (2013). TBX3 Directs Cell-Fate Decision toward Mesendoderm. *Stem Cell Reports*, *1*(3), 248–265. https://doi.org/10.1016/j.stemcr.2013.08.002

Wolfe, A. L., Singh, K., Zhong, Y., Drewe, P., Rajasekhar, V. K., Sanghvi, V. R., … Wendel, H.-G. (2014). RNA G-quadruplexes cause eIF4A-dependent oncogene translation in cancer. *Nature*, *513*(7516), 65–70. https://doi.org/10.1038/nature13485

Xie, K., & Sheppard, A. (2018). Dietary Micronutrients Promote Neuronal Differentiation by Modulating the Mitochondrial-Nuclear Dialogue. *BioEssays*, *40*(7), 1800051. https://doi.org/10.1002/bies.201800051

Xu, X., Vatsyayan, J., Gao, C., Bakkenist, C. J., & Hu, J. (2010). Sumoylation of eIF4E activates mRNA translation. *EMBO Reports*, *11*(4), 299–304. https://doi.org/10.1038/embor.2010.18

Xue, S., & Barna, M. (2012). Specialized ribosomes: a new frontier in gene regulation and organismal biology. *Nature Reviews Molecular Cell Biology*, *13*(6), 355–369. https://doi.org/10.1038/nrm3359

Yamaguchi, S., Ishihara, H., Yamada, T., Tamura, A., Usui, M., Tominaga, R., Munakata, Y., Satake, C., Katagiri, H., Tashiro, F., Aburatani, H., Tsukiyama-Kohara, K., Miyazaki, J., Sonenberg, N., & Oka, Y. (2008). ATF4-mediated induction of 4E-BP1 contributes to pancreatic beta cell survival under endoplasmic reticulum stress. *Cell Metabolism*, *7*(3), 269–276. https://doi.org/10.1016/j.cmet.2008.01.008

Yanagiya, A., Suyama, E., Adachi, H., Svitkin, Y. V., Aza-Blanc, P., Imataka, H., Mikami, S., Martineau, Y., Ronai, Z. A., & Sonenberg, N. (2012). Translational Homeostasis via the mRNA Cap-Binding Protein, eIF4E. *Molecular Cell*, *46*(6), 847–858.

https://doi.org/10.1016/J.MOLCEL.2012.04.004

Yang, Y., Liu, B., Xu, J., Wang, J., Wu, J., Shi, C., … Deng, H. (2017). Derivation of Pluripotent Stem Cells with In Vivo Embryonic and Extraembryonic Potency. *Cell*, *169*(2), 243–257.e25. https://doi.org/10.1016/j.cell.2017.02.005

Yoffe, Y., David, M., Kalaora, R., Povodovski, L., Friedlander, G., Feldmesser, E., Ainbinder, E., Saada, A., Bialik, S., & Kimchi, A. (2016). Cap-independent translation by DAP5 controls cell fate decisions in human embryonic stem cells. *Genes & Development*, *30*(17), 1991–2004. https://doi.org/10.1101/gad.285239.116

Zhang, H. H., Huang, J., Düvel, K., Boback, B., Wu, S., Squillace, R. M., Wu, C.-L., & Manning, B. D. (2009). Insulin Stimulates Adipogenesis through the Akt-TSC2-mTORC1 Pathway. *PLoS ONE*, *4*(7), e6189. https://doi.org/10.1371/journal.pone.0006189

Zhang, J., Nuebel, E., Daley, G. Q., Koehler, C. M., & Teitell, M. A. (2012). Metabolic regulation in pluripotent stem cells during reprogramming and self-renewal. *Cell Stem Cell*, *11*(5), 589–595. https://doi.org/10.1016/j.stem.2012.10.005

Zheng, X., Boyer, L., Jin, M., Mertens, J., Kim, Y., Ma, L., Ma, L., Hamm, M., Gage, F. H., & Hunter, T. (2016). Metabolic reprogramming during neuronal differentiation from aerobic glycolysis to neuronal oxidative phosphorylation. *ELife*, *5*. https://doi.org/10.7554/eLife.13374

ANNEXES

VIII. ANNEXE

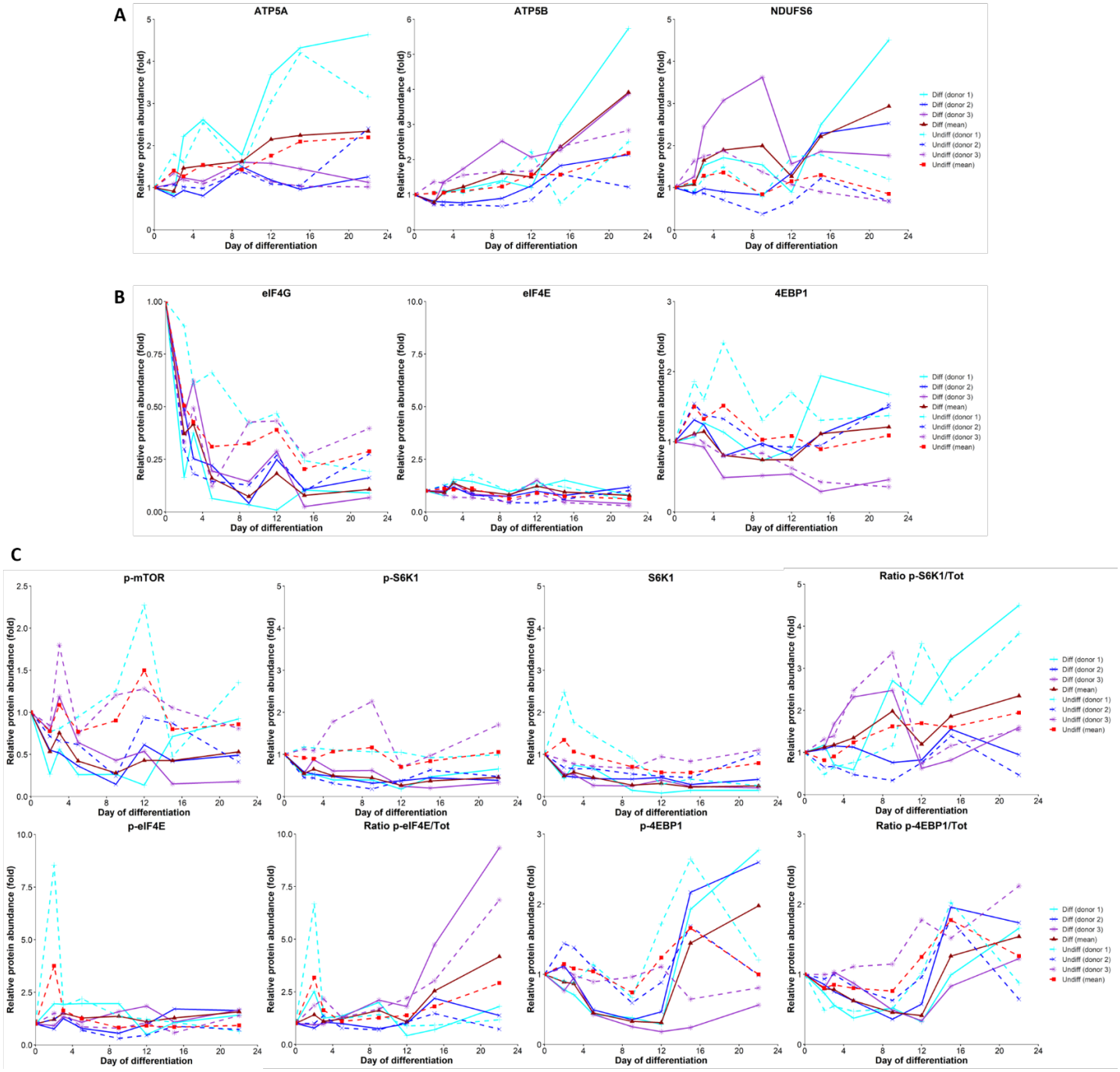

Supplementary figure 1. Detailed protein abundance of mitochondrial markers and of eIF4F-related actors per donor. Representation per donor of individual protein quantification of the blots shown in **Figure 13** (A), **Figure 14** (B) and **Figure 15** (C) and mean quantification of the three donors.

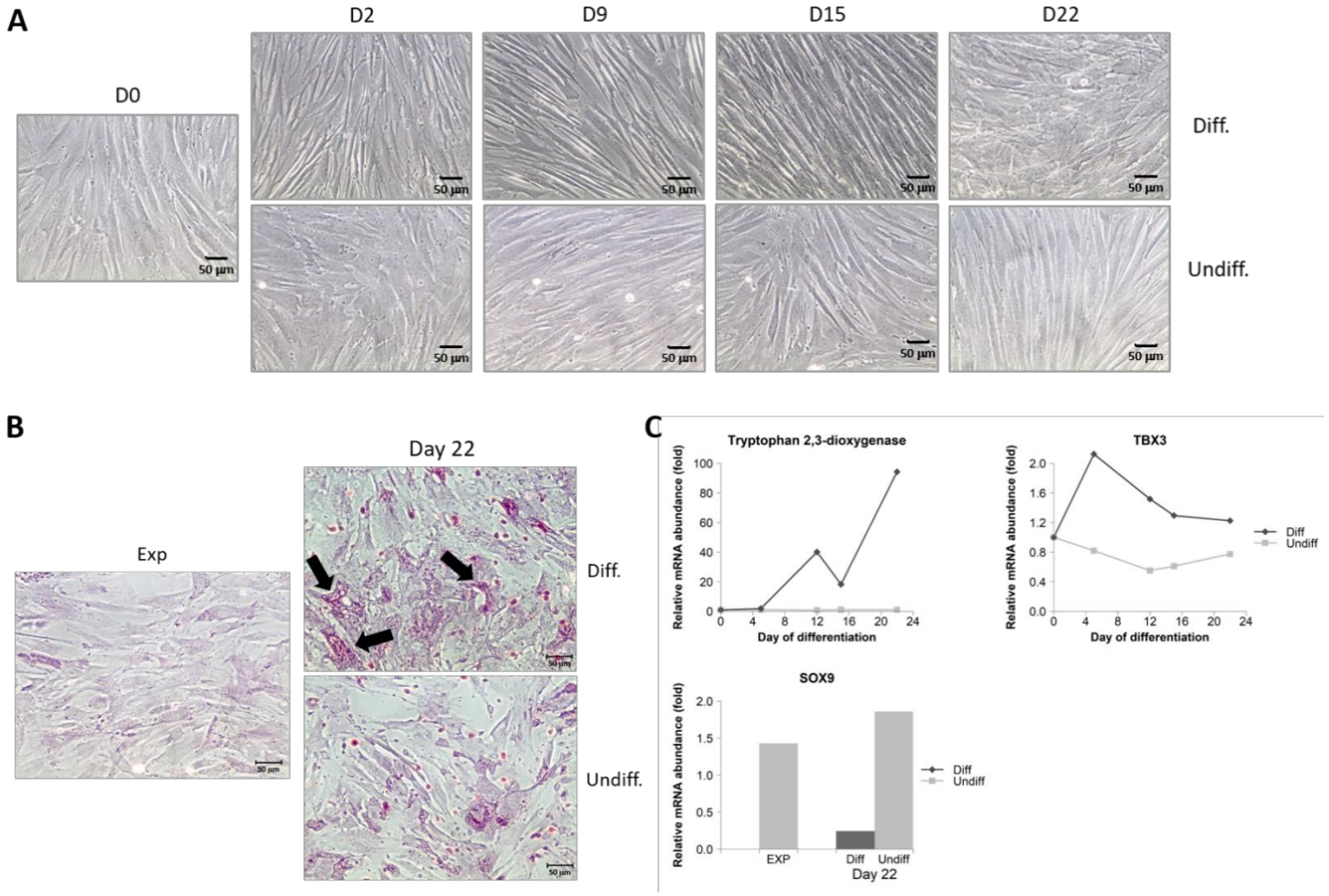

Supplementary figure 2. Differentiation efficiency control for the differentiation of donor 1 cells. Morphology assessment (A), PAS staining (B) and mRNA markers (hepatic with *TDO2*, developmental with *TBX3* and stemness marker with *SOX9*) (C) evaluation of donor 1 cells which underwent a differentiation process. The differentiation controlled here concern cells represented in **Figure 16A** and **Figure 17**.

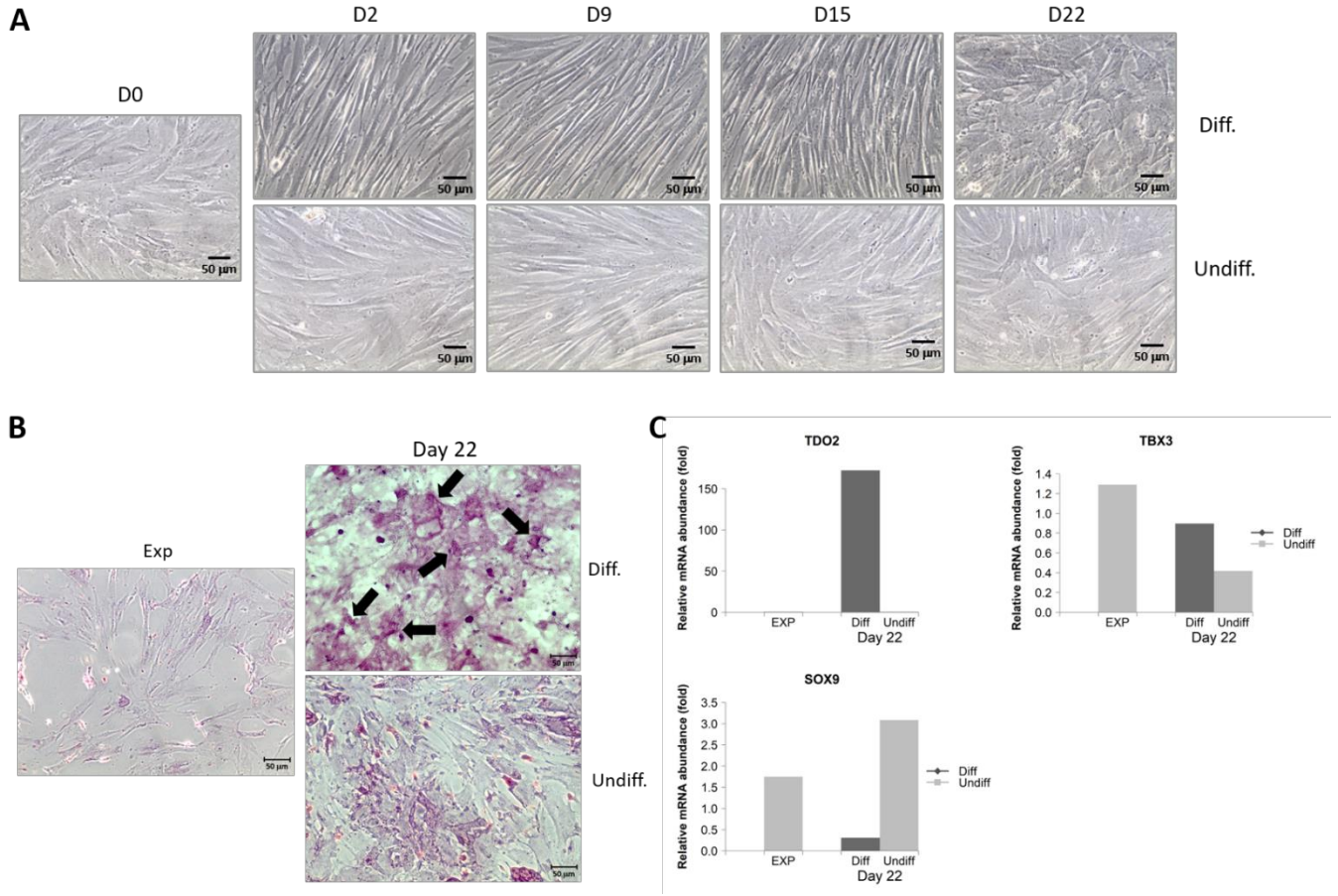

Supplementary figure 3. Differentiation efficiency control for the differentiation of donor 1 cells. Morphology assessment (A), PAS staining (B) and mRNA markers (hepatic with TDO2, developmental with TBX3 and stemness marker with SOX9) (C) evaluation of donor 1 cells which underwent a differentiation process. The differentiation controlled here concern cells represented in **Figure 16B**.

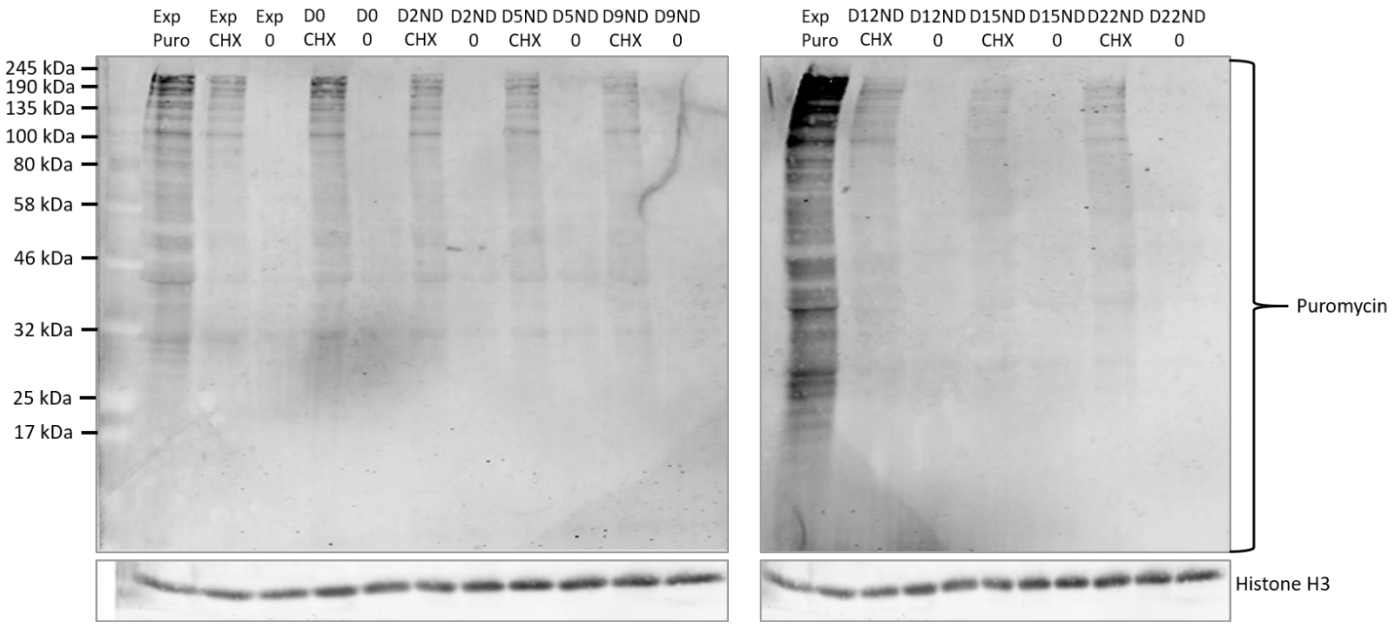

Supplementary figure 4. Negative controls for SUnSET experiment on donor 1 cells. Exp, Day 0 (D0) and Diff (D) and Undiff (ND) cells at day 2, 5, 9, 12, 15 and 22 were either exposed to 5 µg/mL puromycin (Puro) for 10 minutes (here Exp Puro was loaded on gel as a positive control), either to 20 µg/mL cycloheximide (CHX) for 30 minutes followed by exposition to puromycin + cycloheximide for 10 minutes or underwent medium replacement without puromycin. Cells were harvested and 10 µg of proteins were loaded on 10% acrylamide gel and puromycin and histone H3, the loading control, were revealed. Negative control linked to the experiment showed on **Figure 16B**.

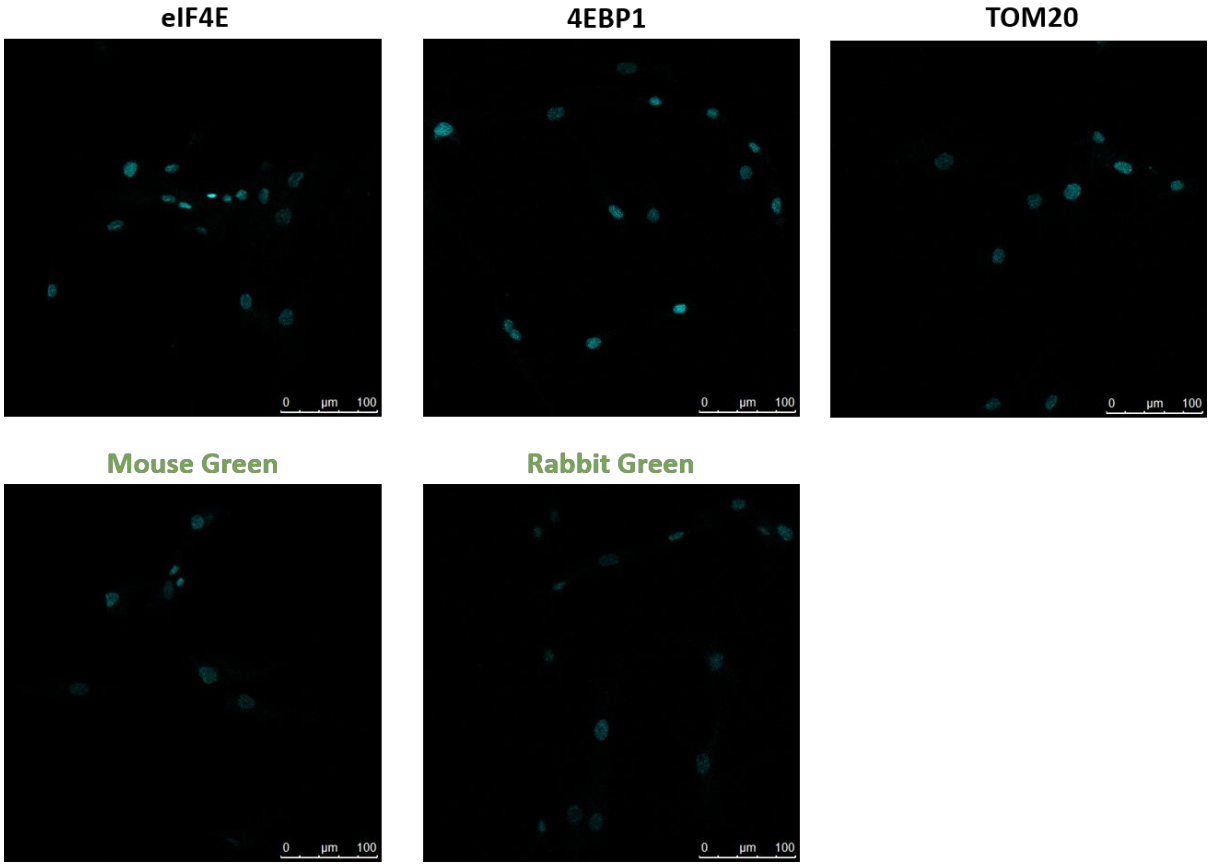

Supplementary figure 5. Primary and secondary antibodies controls for the immunofluorescence experiments on donor 1 cells. Exp cells were collected, seeded on coverslips and fixed. An immunofluorescence labelling was then performed with probing of eIF4E, 4EBP1 and TOM20 primary antibodies alone and of secondary antibodies mouse green (used for eIF4E marking) and rabbit green (used for 4EBP1 and TOM20 marking). Nuclei were stained with DAPI. Scale bar = 100 µm. Negative control linked to the experiment showed on **Figure 17**.